PECTIN METHYL ESTERIFICATION FUNCTIONS IN SEED DEVELOPMENT AND GERMINATION

by

Gabriel Levesque-Tremblay

B.Sc., Universite du Quebec a Montreal, 2005
M.Sc., University du Quebec a Montreal, 2009

A THESIS SUBMITTED IN PARTIAL FULFILLMENT OF
THE REQUIREMENTS FOR THE DEGREE OF

DOCTOR OF PHILOSOPHY

in

The Faculty of Graduate and Postdoctoral Studies
(Botany)

THE UNIVERSITY OF BRITISH COLUMBIA
(Vancouver)

April 2014

Abstract

Homogalacturonan pectin domains are synthesized in a highly methyl esterified form and can be de-methyl esterified by the cell wall enzyme Pectin Methyl Esterase (PME). The prevalent model for PME mode of action indicates that when PMEs act on a stretch of adjacent galacturonic acid glycosides, they may strengthen the cell wall but when PMEs act on non-adjacent galacturonic acid glycosides they may loosen the cell wall. PME activity can be regulated *in planta* by the proteinaceous inhibitor, PMEI.

I used PME and PMEI to study the importance of methyl esterification in seed development and germination. As a means to identify PMEs involved in seed coat mucilage I identified 7 PMEs expressed in the seed coat. The PME gene *HIGHLY METHYL ESTERIFIED SEED* (*HMS*) is highly expressed at 7 Day Post Anthesis (DPA) both in the seed coat and the embryo. Using a *hms-1* mutant, I showed that *HMS* is required for normal levels of PME activity and methyl esterification in the seed, mucilage extrusion and proper embryo cell expansion, rigidity and morphogenesis between 4 and 10 DPA. The mucilage extrusion defect is a secondary effect of the function of HMS in the embryo. I hypothesize that HMS is required for cell wall loosening in the embryo to allow for cell expansion during the accumulation of storage reserves.

To evaluate the importance of methyl esterification in germination my collaborators and I first showed that PME activity changed during the different stages of germination: it first increased before testa rupture and decreased during endosperm rupture. Treatment with the hormone abscisic acid (ABA) to increase dormancy prolonged PME activity in the seeds. Inversely when we negatively regulated PME activity in the *A. thaliana* seed with the overexpression of a PMEI (OE PMEI5), we generated larger seeds with bigger cells. These seeds germinated faster both in presence or absence of ABA. Therefore we hypothesize that the PME(s) inhibited by PMEI5 establishes stronger cell walls that restrict germination.

This thesis clearly demonstrates that PME activity is important in the regulation of seed cell wall methyl esterification impacting embryo growth and germination.

Preface

This thesis contains 4 chapters.

Chapter 1: Gabriel Levesque-Tremblay wrote Chapter 1 but used Figures that have been published elsewhere:
Figure 1.1 is a previously published image (Carbohydrate Research, 2009, by permission)
Figure 1.2 is a previously published image (Science, 1994, by permission)
Figure 1.3 is a previously published image (Journal of Experimental Botany, 2011, by permission)

Chapter 2: Gabriel Levesque-Tremblay designed and executed the research described in this chapter with the help of the principal investigators, Dr. George Haughn and Dr. Shawn Mansfield.

Chapter 3 has been published in the following manuscript.

Müller, K., Levesque-Tremblay, G., Bartels, S., Weitbrecht, K., Wormit, A., Usadel, B., Haughn, G., Kermode, A.R. (2013) Demethyl esterification of cell wall pectins in *Arabidopsis* plays a role in seed germination. Plant Physiol. 161(1), 305-316.

Gabriel Levesque-Tremblay designed part of the research project, performed part of the research and analyzed data and helped prepare the manuscript. This research was conducted in collaboration with the Kermode lab at the Simon Fraser University. Gabriel Levesque-Tremblay performed part of the PME activity assays (Figure 3.3B), the histological analysis and immunolabeling (Figure 3.5), the mucilage extrusion assays (Figure 3.8), and the SEM micrographs (Figure 3.9 (Müller et al., 2013). Sebastian Bartels generated the OE PMEI5 plants. Karin Weitbrecht obtained the environmental SEM (eSEM) micrographs and Alexandra Wormit analysed the cell wall composition in collaboration with Bjoern Usadel. Gabriel Levesque-Tremblay designed part of the

research and wrote part of the manuscript in collaboration with Kerstin Müller. Published data including figures and tables are reprinted with the permission of the American Society of Plant Biologist (ASPB).

Table of contents

List of tables

List of figures

List of abbreviations

35S	Promoter of cauliflower mosaic virus
βGlcY	Yariv phenylglycoside
ABA	Abscisic acid
ACT7	*Actin-7* gene
AG	Arabinogalactan
AGA	Apiogalacturonan
AGP	Arabinogalactan protein
ASPB	American Society of Plant Biologists
ATG	Adenosine, thymine, guanidine. Base triplet in DNA sequence that code for the amino acid methionine
BM1	Tetrapeptide domain Arginine-Lysine-Leucine-Leucine basic motif 1
BM2	Tetrapeptide domain Arginine-Lysine-Leucine-Leucine basic motif 2
Bp	Base pairs
BR	Hormone brassinosteroid
bri1-5	BR receptor mutant.
CAZy	Carbohydrate-active enzymes database
Col-0	Columbia-0
CSLA	glucomannan glycosyltransferase
Cys	Cysteine
det2	BR deficient mutants
DM	Degree of methyl esterification
DMA	Dynamic mechanical Analysis
DNA	Deoxyribonucleic acid
DPA	Days post-anthesis
EDTA	Ethylenediaminetetraacetic acid
EF1α	Elongation-factor-1 *alpha* gene
eSEM	Environmental scanning electron microscopy
ER	Endosperm rupture
EST	Expressed sequence tag

FLY1	FLYING SAUCER1
fus3-3	embryo-deficient mutants *fusca315*
GalA	Galacturonic Acid
GAPC	Glyceraldehyde-3-Phosphate Dehydrogenase
GAUT	GALactUronosylTransferase
GUS	β-glucuronidase
HCL	Hydrogen chloride
HG	Homoglacturonan
HMS	HIGHLY METHYL ESTERIFIED SEED
LP	Left Primer
mRNA	Messenger Ribonucleic acid
NaCL	Sodium chloride
NaOH	Sodium hydroxide
NCBI	National Center for Biotechnology Information
No-0	Nossen-0
NSERC	Natural Sciences and Engineering Research Council of Canada
OE	Overexpression
OE PMEI5	Overexpression Pectin Methyl Esterase Inhibitors-5
ORF	Open Reading Frame
PCR	Polymerase chain reaction
PG	Polygalacturonase
PhD	Doctor of Philosophy
PME	Pectin Methyl Esterase
PMEI	Pectin Methyl Esterase Inhibitors
PMT	Pectin Methyl Transferase
PP	Pre-Pro domain
PRO	Protein Precursor
(qRT)-PCR	Quantitative reverse transcription
QUA1	QUASIMODO1
RG I	Rhamnogalacturonan I
RG II	Rhamnogalacturonan II

Rha	Rhamnose
RIP	Ribosome-inactivating protein
RKLL	Tetrapeptide domain Arginine-Lysine-Leucine-Leucine
RP	Right Primer
RNA	Ribonucleic acid
RT-PCR	Reverse-transcription polymerase chain reaction
SAR	Systemic Acquired Resistance
SBT1	SUBTILISIN-LIKE SERINE PROTEASE 1
SE	Standard error
SEM	Scanning electron microscope
T-DNA	Transfer Deoxyribonucleic acid
TR	Testa rupture
UBC	University of British Columbia
UBQ1	Ubiquitin 1 promoter
UTR	Untranslated region of DNA
WT	Wild type
XG	Xyloglucan
XGA	Xylogalacturonan
YFP	Yellow Fluorescent Protein

Acknowledgements

I first want to thank my supervisors, Professors George Haughn and Shawn Mansfield, for the opportunity to be part of their laboratories and for the tremendous support and patience they showed throughout my PhD research. In addition, I am grateful for Professor Ljerka Kunst for her input as well as Professor Lacey Samuels for her support, training and collaboration. I would also like to express my enduring gratitude to my committee members, Professors Brian Ellis and Professor Carl Douglas for their insightful suggestions for improvement on my research and thesis. I gratefully acknowledge the support of my collaborator Dr. Kerstin Müller, my lab mates Elahe Esfandiari, Erin Gilchrist, Lifang Zhao, Lyn Shi, Catalin Volionic and Gillian Dean and my family. And finally, I would like to thank NSERC, NSERC CREATE, the UBC Faculty of Graduate Studies, Scott Paper Ltd. and Aide financiere au etudes Quebec for their funding.

Dedication

To my family, friends, Dr. George Haughn and Dr. Francois Ouellet.

Chapter 1: Introduction

1.1 Plant cell walls

1.1.1 Plant primary and secondary cell wall

The plant cell wall is a highly complex macromolecular structure located outside the plasma membrane that surrounds and protects the cells. Plant walls are intricate composites made of a variety of polysaccharides, proteins and aromatic or aliphatic substances (Caffall and Mohnen, 2009). Pectin is a major polysaccharide in the primary cell wall, forming a hydrated gel phase in which the other cell wall components are embedded. Pectin methyl esterification status appears to be a major factor influencing the function of pectin in the cell wall. This research investigates cell wall modification using the *Arabidopsis thaliana* (*A. thaliana*) seed as a model. The primary focus is on the modification of pectin methyl esterification and its involvement in the seed mucilage, seed development and seed germination. The broader goal for this thesis is to understand how specific pectin polysaccharide modification affects plant cell physiology.

The plant cell wall can be divided into two general types: the primary cell wall surrounding cells that are growing or capable of growth, and secondary walls synthesized inside of the primary wall following cessation of growth. The plant cell establishes a middle lamella and a primary cell wall at the time of division that may or may not later be thickened by a secondary cell wall. Differentiated cells contain cell walls with distinct compositions resulting in a spectrum of specialized primary and secondary cell walls (Keegstra et al., 2010).

The primary cell wall is a dynamic structure continually being modified during development and diverse environmental conditions. The current model describes the primary cell wall as a complex highly cross-linked framework, that provides strength and support to the plant cells (Somerville et al., 2004; Cosgrove et al., 2005). The composition of the average primary cell wall includes three classes of carbohydrates:

cellulose, hemicellulose and pectins. Cellulose represents the major polysaccharide in primary cell walls and is composed of β-1,4-linked glucan chains that hydrogen bond to form the microfibrils. Cellulose microfibrils represent the major structural component of the cell wall and are often referred to as the cell wall skeleton due to its rigidity and strength (Fry et al., 2004). Hemicelluloses are a class of heteropolymeric polysaccharides that include glucomannan, mannans, xylan and xyloglucans (Hayashi et al., 2011). Hemicellulose strengthens the cellulose network by cross-linking the cellulose microfibrils through hydrogen bonding, adding integrity to the cell wall (Hayashi, 2011; Cosgrove, 2005). The cellulose and hemicellulose network provides the strength and support necessary for the plant to withstand tension and compression. Pectins are acidic heteropolymers containing galacturonic acid (Willat et al., 2001). The three main types of pectin are homoglacturonan (HG), rhamnogalacturonan I (RG I) and rhamnogalacturonan II (RG II). Pectins are present throughout the primary cell wall and are the predominant carbohydrate in the middle lamella. The pectin polysaccharides form a hydrated gel in which the network of cellulose microfibrils and other cell wall components are embedded. The pectin network is partly responsible for the cell-cell adhesion, cell wall extension, cell wall hydration and some aspect of defense signaling. The primary cell wall is mainly polysaccharide, but the presence of structural and/or enzymatic proteins has been shown (Cosgrove et al., 2005). Structural proteins like extensins are non-enzymatic and they assemble into a scaffold that may act as template for negatively charged pectic polysaccharides (Cannon et al., 2008). Several types of enzymes that modify complex carbohydrates have been grouped in sequence-based families in the Carbohydrate-Active Enzymes (CAZy) database (http://www.cazy.org/).

The secondary cell wall is deposited after the cell expansion. The composition of the secondary wall is variable and relates to the role of the differentiated cell (Keegstra et al., 2010). The secondary cell wall can contain cellulose, hemicellulose, pectins and lignin. Some types of secondary cell walls have a reduced pectin component, resulting in a decrease in hydration (Cosgrove and Jarvis, 2012). The secondary cell wall is generally not as dynamic and malleable as the primary cell wall, and remains relatively static once deposited.

Walls of growing cells (primary cell wall) contain 30-50% pectic polysaccharides making pectin a major component of the cell wall (Cosgrove and Jarvis, 2012). The study of pectin modification and its importance in development is the primary focus of this thesis.

1.1.2 Pectins

Pectins are acidic heteropolymers containing galacturonic acid with a high degree of complexity (Willat et al., 2001). Pectins are thought to perform a variety of functions. They influence cell wall porosity, provide charged surfaces for modulating the wall pH, regulate cell adhesion, and serve as signalling molecules in pathogen recognition (Buchanan et al., 2000). The pectic polysaccharides contain a significant proportion of GalA, and are generally classified into homogalacturonan (HG), xylogalacturonan (XGA), apiogalacturonan (AGA), rhamnogalacturonan I (RG-I) and rhamnogalacturonan II (RG-II) (Ridley et al., 2001). HG is a polymer of α-1,4-linked-D-galacturonic acid and is usually the most abundant pectin in the primary plant cell wall (Ridley et al., 2001). The HG backbone can have xylose and apiose side chains, which form XGA and APA. RG-I has a backbone structure of $[\alpha\text{-D-GalpA-1,2-}\alpha\text{-L-Rhap-1,4}]_n$ repeating units that is frequently branched with side chains of arabinan, galactan or arabinogalactan at the C-4 position in the plant cell wall (Lau et al., 1985). RG-II has a highly complex structure with an HG backbone and four well-defined side chains with a total of 12 different types of glycosyl residues (Caffall and Mohnen, 2009). Despite the complexity of RG-II, its structure in the plant cell wall of higher and lower land plants varies little, suggesting that its function may be very important (O'Neill et al., 2004).

HG, RG-I and RG-II are thought to be covalently linked to each other (O'Neill et al., 2004). Studies have shown that the backbone of HG can not only be covalently cross-linked to RG-I and RG-II, but also cross-linked to the hemicellulose xyloglucan (XG) (Talmadge et al., 1973; Keegstra et al., 1973; York et al., 1996; Nakamura et al., 2002; Tan and al., 2013). HG can also be covalently attached to arabinogalactan proteins

(AGPs) with RGI/HG linked to the rhamnosyl residue in the arabinogalactan (AG) of the AGP (Tan and al., 2013).

Pectin is synthesized in the Golgi apparatus and later secreted to the cell wall. Nucleotide sugars are transported from the cytosol to the Golgi where glycosyl transferases assemble monosaccharides into polysaccharides. It has been postulated that a large number of glycosyl transferases are required to synthesize the pectin polysaccharides (reviewed in Ridley et al, 2001; Caffall and Mohnen, 2009). To date, HG synthesis is the best described: S-adenosyl methionine and UDP-GalA, precursors for pectin synthesis, are believed to be imported into the Golgi apparatus by specific transporters (Wolf et al., 2009). Subsequently, the HG galacturonosyl transferase (GAUT) and pectin methyl transferase (PMT) are thought to work together in a complex facilitating polymerization and methyl-esterification of HGs (Wolf et al., 2009). QUASIMODO1 (QUA1) was first suggested to be a galacturonic acid transferase responsible for the synthesis of HG (Bouton et al., 2002). However, to date, GAUT1 is the only galacturonic acid transferase that has been confirmed biochemically (Sterling et al., 2006). Two polypeptides of GAUT1 bind to one polypeptide of GAUT7, and this union is responsible for retaining GAUT1 in the Golgi membranes (Atmodjo et al., 2011). Evidence indicates that HG is synthesized in the *cis*-Golgi, methyl-esterified in the medial Golgi, and finally substituted in the *trans*-Golgi before being secreted in a methyl-esterified state to the plant cell wall (Sterling et al., 2001; Zhang et al., 1992; Staehelin et al., 1995). HG methyl esterification status is well studied and represents the most important factor influencing the gelling property of pectins. The focus of this thesis is on the modification of pectin methyl esterification.

1.1.3 The methyl esterification of HG pectin

HG GalpA residues may be methyl-esterified at the C-6 carboxyl group or acetylated at the O-2 or O-3 positions, and the pattern and extent to which methylation and acetylation occurs can vary considerably (Ridley et al., 2001). As much as 80% of the GalA residues are usually methyl-esterified before secretion (Mohnen, 1999). The

highly methyl esterified HGs are thought to be partially de-methyl esterified once secreted in the apoplastic space. The methyl esterification of pectin might be regulated in a tissue-specific manner during the development (Willats et al., 2001). Once demethyl esterified, C-6 of HG GalA residues are negatively charged and can have ionic interactions with Ca^{2+} forming a stable gel-like structure with other molecules of pectin if at least ten consecutive GalA residues are un-methylated (Liners et al., 1989). This is referred to as the 'egg-box' model (Figure 1.1).

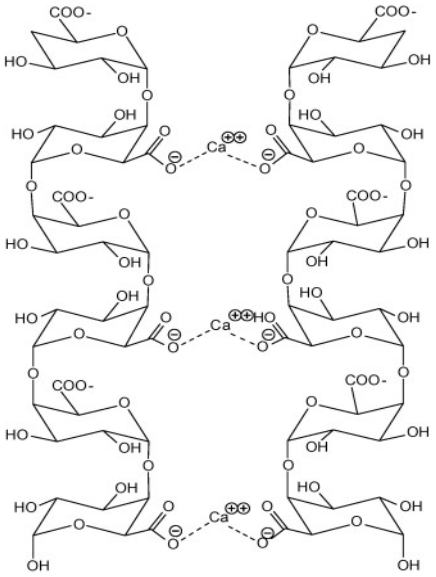

Figure 1.1: The egg-box model of calcium crosslinking in HG polysaccharides (Caffall and Mohen, 2009)

It is has been shown that GAUT or PMT activities are not involved in the modulation of the degree of methyl esterification of HG (Mouille et al., 2007). The pool size of S-adenosyl-methionine may affect the pattern of methyl-esterification, but it is widely accepted that it is primarily pectin methyl esterases (PMEs) that regulate the methylation status of pectin (Wolf et al., 2009). PMEs are responsible for remodelling the degree and pattern of pectin methyl esterification, and thus affecting its susceptibility to hydrolytic enzymes and gelling properties. Therefore, PME and its inhibitors have a major influence on the properties of the cell wall and are of interest to cell wall biologists.

1.2 Pectin methyl esterases

HG is thought to be modified locally in the cell wall, where the enzyme PME catalyzes the reaction by which the methyl group is removed from the chain, resulting in a free carboxyl group and the release of a proton and methanol (Wolf et al., 2009).

1.2.1 PME structures and functions

There are two types of PMEs, and these are distinguished by the presence or absence of an N-terminal PRO region as defined by the primary gene sequence. The PRO region has a high sequence similarity to PME inhibitors proteins (PMEI; see below). For this reason, it has been hypothesized that the PRO region auto-inhibits PME activity before secretion (Micheli, 2001). Group one/type II PMEs have either a very short N-terminal PRO region or lack it entirely, whereas the group two/type 1 PMEs possess one to three long N-terminal PMEI domains (Micheli, 2001). The PRO region was shown to mediate retention of at least one unprocessed type I PME (VGD1) in the Golgi (Wolf and al., 2009). The proteolytic removal of the N-terminal PRO region has been shown to depend on one to two conserved basic tetrad motifs (…RKLL…) named BM1 and BM2. In *A. thaliana* 35 out of 43 type I PME possess at least one RKLL-like cleavage site (Wolf et al., 2009). The PME VGD1 proteins, which possesses a mutated version of these motifs were shown not to be secreted to the cell wall and remained in the Golgi (Wolf et al., 2009). Therefore, the cleavage of the PRO region of VGD1 occurs before the secretion of the mature PME in the plant cell wall (Wolf and al., 2009). It was observed that PMEs extracted from the cell walls of other plants do not have a PRO region, which supports the hypothesis that the cleavage of PRO regions before secretion is a general phenomenon (Micheli, 2001; Bordenave et al., 1993). If the PRO region is always cleaved before secretion, it must have a function prior to secretion. Suggested functions for the PRO region before cleavage include aiding in correct folding of the PME, targeting of the PME to the cell wall, or inhibiting PME activity before secretion (Micheli, 2001). The PRO region of PMEs may also have a biological function in the Golgi after cleavage, although no such function has yet been discovered.

PMEs may remove methyl groups from individual non-adjacent galacturonic acid residues in HG (individually-randomly) or from a stretch of adjacent galacturonic acid molecules (linearly-blockwise; Pelloux et al., 2007; Jolie et al., 2010). These two modes of action have opposing consequences on the plant cell wall. If the PMEs act individually-randomly, the de-esterification of HGs frees protons, which promote the activity of polygalacturonases (PG) (acidic PMEs). The action of these polygalacturonases will, in turn, contribute to the cell wall loosening and extension (Moustacas et al., 1991). In contrast, when the PMEs act linearly-blockwise on HGs, long stretches of free carboxyl groups (on at least 10 consecutive GalA) are created that can interact with Ca^{2+}, creating a pectic gel (Figure 1.1; Al-Qsous et al., 2004; Goldberg et al, 1996). In addition, the action of endopolygalacturonase is greatly reduced in such gel-like environments, which further contributes to cell wall stiffening. The cell wall loosening or stiffening induced by PMEs plays an important function in cellular adhesion, separation, elongation and maturation (Pelloux et al., 2007; Jolie et al., 2010).

At first, acidic PMEs were thought to originate only from fungi and individual-random demethyl esterification was associated with acidic PMEs, whereas linear-blockwise demethyl esterification was related to the alkaline PMEs (Micheli, 2001). However, the individual-random attack mechanism is now known to occur in both fungi and plants (Catoire et al., 1998; Denes et al., 2000: Goldberg et al., 2001). To this date, there is no information about what determines the specificity in the mode of action of different PME isoenzymes. Recent studies have shown that PME action is dependent on the pH and the initial degree of pectin methyl esterification. Some PMEs have been shown to act individually-randomly at acidic pH levels and linearly at alkaline pH levels. At different pHs, some PME isoforms are more effective on highly esterified pectin (Catoire et al, 1998; Denes et al., 2000). PME activity is also enhanced by the presence of cations and both the type and concentration of cations in the cell wall affects the activity of PMEs. Trivalent cations are more effective than bivalent cations, which in turn, are more effective than monovalent cations on its activity (Schmohl et al., 2000).

There is a lack of data showing activity of higher plant PMEs expressed in heterologous systems. Therefore, it has been suggested that plant PME isoenzymes undergo organism-specific post-transcriptional processing necessary for their structural and functional integrity during the export to the cell wall. Studies have revealed the 3-D crystallographic structures of PMEs obtained from both bacterial (Jenkins et al., 2001) and plant species (Johansson et al., 2002). Plant PMEs were prepared from carrot (*Daucus carota*) roots and the structure was determined by molecular replacement methods using the bacterial enzyme from *E. chrysanthemi* as the search model (Johansson et al. 2002). The carrot PME structure consisting of three parallel β-sheets organized in a prism-like fashion. The structure shows a long cleft along the surface of the protein, which is thought to be the pectin-binding site.

Through gene duplication, the family of PMEs rapidly expanded in land plants, likely driven by their functional specialization in cell wall formation (Wang et al., 2013). Genome and EST sequencing projects have shown that PMEs are encoded by large multigene families in all plant species examined to date (CAZy, TIGR and TAIR). In *Populous trichocarpa*, 89 open reading frames (ORFs) have been annotated as putative full-length PMEs compared to 35 ORFs in *Oryza sativa*. *A. thaliana* has 66 ORFs annotated as PMEs, corresponding to 6.81% of all carbohydrate-active enzymes (CAZymes) in that species (Coutinho et al., 2003). The finding that HG is less abundant in grasses compared to dicotyledonous plants is consistent with the number of PME genes in rice relative to *A. thaliana* and *Populus* (Pelloux et al., 2007).

The PME-induced cellular changes impact physiological processes relevant to both vegetative and reproductive plant development. Endogenous plant PMEs are involved in seed germination, pollen tube elongation, root tip elongation, stem internode growth, and leaf growth (Micheli, 2001; Pelloux et al., 2007; Jolie et al., 2010). PMEs are also involved in decreasing the rate of fruit ripening by strengthening the cell wall and sometimes increasing the early stage of ripening when loosening the cell wall (Phan et al., 2007: Brummell et al., 2004). In wood development, PMEs strengthen the pectin rich middle lamella, which in turn regulates the fiber width and length in wood of aspen trees

(Siedlecka et al., 2008). *PME* genes are also highly expressed in xylem at different developmental stages, and it has been suggested that they play an important role in the development of xylem and cambial cells (Micheli et al., 2000). Plant PMEs are associated with plant defense responses against biotic and abiotic stresses, and may interact directly with virulence factors like the movement proteins of viruses, thus facilitating cell-to-cell and systemic infection (Dorokhov et al., 2006; Chen et al., 2000; Chen et al., 2003). Finally, PMEs may be indirectly involved in plant defense through the production of substances that are involved in plant defenses such as methanol, protons and oligogalacturonides (Pelloux et al., 2007; Jolie et al., 2010).

1.2.2 *A. thaliana* PMEs

As mentioned previously, genome sequence analysis has revealed that *A. thaliana* has 66 ORFs annotated as PMEs (Coutinho et al., 2003). These genes include basic PME isoforms active only at alkaline pH (i.e. AtPME31 and AtPME3; Dedeurwaerder et al., 2009; Guenin et al., 2011). Other *A. thaliana* PMEs are active at neutral pH (Klavons & Bennett, 1986), while still others, like PME-RIP, are known to be active at a broad range of pH values from pH 2-9 (see below; De-la-Pena et al., 2008). Finally, some *A. thaliana* PMEs are active primarily in acidic pH, which is not surprising due to the general acidic nature of the cell wall (Bourgault and Bewley, 2002; Downie et al., 1998; Tian et al., 2006). To date, only one protein annotated as a PME had another biochemical activity. Using chromatographic separation coupled with enzymology, a PME was identified as having ribosome-inactivating activity (De-la-Pena et al., 2008). Ribosome-inactivating proteins (RIPs) are enzymes that inhibit the translation process by removing a single adenine residue of a large rRNA (Nielsen et al., 2001). It has been suggested that a conformational change in different cellular locations could be responsible for its dual enzymatic activity.

In *A. thaliana*, groups of genes encoding PMEs are expressed in different tissues during development including xylem tissues (Zhao et al., 2005; Pelloux et al., 2007), stem (Minic et al., 2009), shoot apex (Wolf et al., 2009), hypocotyl (Pelletier et al., 2010)

flower buds (Louvet et al., 2006), pollen (Pina et al., 2005; Wolf et al., 2009), siliques (Louvet et al., 2006) and seed (seed coat, micropylar region, endosperm, and chalazal region) (Wolf et al., 2009). *A. thaliana* PME spatial and temporal expression patterns cluster into several distinct groups (Pelloux et al., 2007), suggesting some level of functional redundancy.

Several *A. thaliana* PMEs have been characterized functionally (Table 1.1), including pollen separation, pollen tube growth, phyllotaxis, internode elongation, hypocotyl growth, adventitious root primordia formation and stem mechanical strength. The PME QRT1 is required for pollen separation during floral development. The liberation of methyl groups from HG is believed to stimulate QRT3, encoding a PG, which in turn cleaves HG in the primary cell wall of pollen mother cell, contributing to its loosening. Other pollen-specific PMEs like AtVGD1, AtVGDH1 and AtPPME1 are required for the modification of the cell wall necessary for determination of the shape and elongation of the growing pollen tube (Jiang et al., 2005). Their specific PME activity in the pollen tube is suggested to stiffen the cell wall, thus adding the rigidity necessary for pollen tube growth and integrity (Tian et al., 2006).

Changes in rigidity associated with PME activity in the cell wall have also been shown to be involved in morphogenesis. *A. thaliana* organ initiation is dependent on PME-induced cell wall loosening and extensibility necessary to support organ development (Peaucelle et al., 2008; Peaucelle et al., 2011). Other *A. thaliana PME* genes may be involved in restricting organ development, such as AtPME3, which plays a role in restricting formation of adventitious root primordia (Guenin et al., 2011). The cell wall loosening and extensibility induced by PME5 is responsible for allowing stem cell expansion and internode elongation (Peaucelle et al., 2011). Recently, another *A. thaliana* PME (PME35) was shown to contribute to the mechanical strength of the stem by helping stiffen the primary cell wall (Hongo et al., 2012).

A. thaliana PMEs have also been shown to be involved in abiotic and biotic stresses. The hormone brassinosteroid (BR) plays an important role in plant growth and

development (Clouse & Sasse, 1998). BR acts through the activation of cell surface receptors, which in turn activate transcription factors controlling a large number of BR-responsive genes including *PMEs* genes (Sun et al., 2010; Yu et al., 2011). AtPME41 is a PME regulated by the BR-dependent response to chilling stress. This PME enhances the stiffness of cell walls resulting in an increase in cold and freezing tolerance (Qu et al. 2011). Other PMEs have negative effects for the plant during infection. *AtPME3* is required for the successful colonization of the pathogens *Pectobacterium* and *Botrytis* (Raiola et al., 2011). When *Pectobacterium* and *Botrytis* infects *A. thaliana*, the induction of *AtPME3* by the plant enhances pathogen invasion. It was suggested that AtPME3 decrease the HG methyl esterification necessary for these microorganism to metabolize or use the pectin (Raiola et al., 2011).

Table 1.1: PMEs characterized in *A. thaliana*.

Name	AGI code	Related Function in *A. thaliana*	References
ATPME1	*At1g53840*	-	Richard et al., 1996
ATPME2	*At1g53830*	-	Richard et al., 1996
ATPMEPCRA	*At1g11580*	-	Micheli et al., 1998
ATPMEPCRB, PME-RIP	*At4g02330*	Exhibit both PME and RIP activity	Micheli et al., 1998; Qu et al., 2011; De-la-Pena et al., 2007
ATPMEPCRC	*At3g14300*	-	Micheli et al., 1998
ATPMEPCRD	*At2g43050*	-	Micheli et al., 1998
ATPMEPCRF	*At5g53370*	-	Micheli et al., 1998
VGD1	*At2g47040*	Pollen tube growth	Jiang et al., 2005
VGDH1	*At2g47030*	Pollen tube growth	Jiang et al., 2005
VGDH2	*At3g62170*	-	Jiang et al., 2005
QRT1	*At5g55590*	Pollen separation	Francis et al., 2006
AtPPME1	*At1g69940*	Pollen tube shape and elongation	Rockel et al., 2008; Tian et al., 2006
PME5	*At5g47500*	Phyllotaxis	Peaucelle et al., 2008, 2011
ATPME3	*At3g14310*	Enhance plant-pathogen interactions	Micheli et al., 1998; Hewezi et al., 2008; Raiola et al., 2011; Guenin et al., 2011

Name	AGI code	Related Function in *A. thaliana*	References
-	*At3g49220*	Expressed in Dark-growth hypocotyl	Pelletier et al., 2010
ATPME35	*AT3G59010*	Stem support	Hongo et al., 2012
Name	AGI code	Related Function in *A. thaliana*	References
ATPME31	*At3G29090*	-	Dedeurwaerder et al., 2009
AtPME41	*At4G02330*	Freezing tolerance	Qu et al., 2011

1.3 Pectin methyl esterase inhibitors

The PMEI, a proteinaceous inhibitor capable of inhibiting PME activity, was first discovered in kiwi fruit *Actinidia deliciosa* (Balestrieri et al., 1990). Little is known about PMEI as compared to PME. However, PMEI activity should always be taken into account when studying PME related cell wall modification (Pelloux et al., 2007).

1.3.1 PMEI structure and function

Kiwi and *A. thaliana* PMEI are small proteins shown to inhibit PMEs from various sources and do not display inhibition of other cell wall degrading and loosening enzymes (Balestrieri et al., 1990; Wolf et al., 2003; Raiola et al., 2004). Plant PMEIs generally have five conserved Cys residues, the first four forming two disulfide bridges that function in maintaining the protein structure (Raiola et al., 2004). PMEI generally have N-terminal signal peptide required for the extracellular targeting of the protein (Giovane et al., 2004; Irifune et al, 2004). PMEI also shares amino acid sequence similarity with the invertase inhibitors, but both inhibitors have exclusive target specificity (Scognamiglio et al., 2003).

The mode of action of PMEI is still unclear, but there is growing evidence that PMEIs contribute to the regulation of PME activity (Juge, 2006). The PRO-sequence of type 1 PMEs show high homology with PMEIs (Giovane et al., 2004). The three dimensional structure of *A. thaliana* and kiwi PMEIs interacting with purified PMEs

from tomatoes has been determined, and shown that PMEI covers the PME cleft preventing access of the substrate. (Hothorn et al., 2004; Di Matteo et al., 2005).

Recently, database searches have indicated that PMEIs are present in many plants (cf. http://services.uniprot.org, 2010). Homology searches revealed similarity of the kiwi PMEI with a huge number of sequences in different plants including *Nicotiana tabacum*, *Lycopersicon esculentum*, *Ipomoea batatas* and *A. thaliana* (Giovane et al., 2004). The PMEI gene family was recently well described in flax (*Linum usitassimum*), where 95 putative *LuPMEI* genes were revealed (Pinzon-Latorre &Deyholos, 2013). The *LuPMEI* transcript was abundant in 12 different tissues and stages of development.

The role of PMEIs *in planta* is not as well defined as the protein it inhibits. PMEI was suggested to function in the modulation of PME activity through plant development and growth (Jolie et al., 2010). Therefore, the PMEIs may potentially be involved in all PME related roles and functions (see section on PME above). PMEIs were also shown to play a function in plant defense (Lionetti et al., 2007). PMEI may be involved in various abiotic and biotic stresses as shown by the modulation of the transcription of pepper *PMEI* genes during fungal infection, basal disease resistance and abiotic stress tolerance (An et al., 2008)

1.3.2 *A. thaliana* PMEIs

Initially, based on amino-acid identity, two genes, *AtPMEI1* and *AtPMEI2,* were shown to encode PMEIs in *A. thaliana* (Raiola et al., 2004). AtPMEI1 and AtPMEI2 share 38% amino acid identity with the protein sequence of the kiwi PMEI (Wolf et al., 2003; Raiola et al., 2004). Further database analysis has shown that *PMEIs*, like *PMEs,* belong to a large multigene family (64 genes in *A. thaliana*; Giovane et al., 2004; Pelloux et al. 2007). To date, very little is known of the biochemistry of *A. thaliana* PMEIs. This is in part due to the fact that only a few *A. thaliana PMEI* genes have been characterized (Table 1.2).

To date six *A. thaliana PMEI* genes have been characterized (*AtPMEI1* to *AtPMEI6*; see Table 1.2). The functions of the PMEIs described reflect the processes that the PME they inhibit are involved including pollen tube growth, cell extension and elongation, organ formation, BR pathway and plant defense.

AtPMEI1 and *ATPMEI2* are highly expressed in pollen suggesting an important role in this tissue (Wolf et al., 2003). Other studies used *AtPMEI1* and *ATPMEI2* to show the importance of pectin methyl esterification in pathogen interaction with *A. thaliana*. For example, constitutive expression of *AtPMEI1* and *AtPMEI2* resulted in a decrease in PME activity ultimately conferring higher resistance to the pathogen *Botrytis cinerae* (Lionetti et al., 2007).

PME activity in the meristem leads to cell wall extensibility necessary for the formation of organs. Experimental perturbation of the methyl-esterification status of pectin, using the alcohol inducible PMEI3, suppressed organ formation in the meristem (Peaucelle et al., 2008). PMEI may inhibit PME-induced cell wall loosening necessary for organ formation in the meristem. AtPMEI4 is also involved in inhibiting PME cell wall loosening impacting cell elongation in hypocotyls (Pelletier et al., 2010).

Over expression of *PMEI5* caused morphological defects such as root waving and organ fusion (Wolf et al., 2012) that could be explained by defects in the cell wall. These defects were suppressed by a mutation in the BR receptor protein (Wolf et al., 2012) suggesting that the morphological changes observed in the over expression line were due, in part, to the activation of the BR pathway. The BR receptor protein was shown to be perceiving the inhibition of PME activity in the cell wall, and activating the transcription factor BZR1. This pathway itself results in the transcription of a battery of cell wall modifying enzymes, including *PMEs,* as a mechanism to compensate for inhibition of PME activity (Wolf et al., 2012).

Recently, *PMEI6* was shown to be essential for seed mucilage release (Saez-Aguayo et al., 2013). The *pmei6* mutant results in an increase in PME activity and a

decrease in cell wall methyl esterification whereas wild type, transformed with *35S:PMEI6,* results in a decrease of PME activity (Saez-Aguayo et al., 2013). This result is consistent with the hypothesis that PME-PMEI induces changes in the methyl esterification status of seed coat cell walls.

Table 1.2: PMEIs characterized in *A. thaliana*.

Name	AGI code	Function	References
AtPMEI1	*At1g48020*	Pollen? Plant defense	Wolf et al. 2003; Raiola et al., 2004, 2011; and Lionetti et al., 2007
AtPMEI2	*At3g17220*	Plant defense	Wolf et al. 2003, Raiola et al., 2004, 2011; Lionetti et al., 2007, 2010
AtPMEI3	*At5g20740*	Organ formation	Peaucelle et al. 2008
AtPMEI4	*At4g25250*	Hypocotyls growth	Pelletier et al., 2010
AtPMEI5	*At2g31430*	BR pathway	**Müller** et al., 2013; Wolf et al., 2012
AtPMEI6	*At2g47670*	Seed mucilage release	Saez-Aguayo et al., 2013

1.4 *A. thaliana* seed

1.4.1 *A. thaliana* seed development

1.4.1.1 *A. thaliana* embryo development

Fertilization of the ovule initiates seed development (Gillaspy ibid.). In flowering plants two fertilization events occur (Essau, 1977). First, one sperm fuses with the egg cell to produce a zygote. A second sperm fuses with the central cell producing the triploid endosperm that later provides nutrients for the development of the embryo and germinating seedling (Lopes, ibid.). Plant embryogenesis can be divided in three general phases: 1) Post fertilization-proembryo, 2) globular-heart transition, and 3) organ expansion and maturation (Figure 1.2; Goldberg and al., 1994). During the post fertilization-proembryo phase the embryo first divides to form two asymmetric cells forming the suspensor and embryo proper with distinct developmental fates. During the globular-heart transition phase the embryonic organs and tissues form. The shoot and

root meristem differentiate. The embryo proper becomes bilaterally symmetrical and develops visible shoot-root structures (Goldberg and al., 1994). During organ expansion and maturation the cotyledon and axis enlarge considerably by cell division and cell expansion. Lipid and proteins bodies accumulate as a form of energy storage. Vacuolization of cotyledon and axis cells and cessation of RNA and protein synthesis precede dehydration and dormancy.

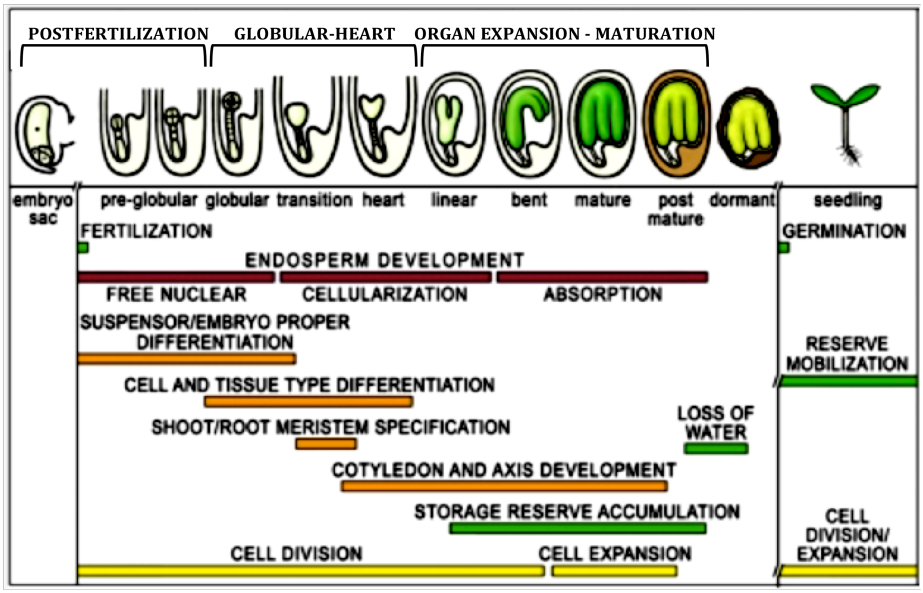

Figure 1.2: Schematic representation of *A.thaliana* seed development and stages of the life cycle. Seed cartoons were adapted from Le and al., 2010. Reprinted with the permission of Science.

A major shift in gene expression including genes encoding cell wall related enzymes is observed as the embryo progresses through the different phases of development (Ruuska et al., 2002). Modifications of cell wall structure have been shown to interfere with normal embryo development. For example, a mutant in glucomannan glycosyltransferase (*csla-7*) or a plant transformed with *p35S:CSLA* were shown to influence the progression of embryogenesis (Goubet et al., 2009). Blocking the function of cell wall AGPs during seed development using Yariv phenylglycoside (βGlcY) resulted in the formation of an abnormal embryo (Zhong et al., 2011). To date, little is known about how changes in embryo cell wall mechanical and biochemical properties

lead to proper embryo development. Further research concerning a role for enzymatic cell wall modification is needed to elucidate how embryo development is influenced.

1.4.1.2 *A. thaliana* seed coat development

The *A. thaliana* seed coat consists of five layers of specialized cells that act as a protective interface between the external world and the embryo. In *A. thaliana*, fertilization gives rise to the formation of a seed coat from the 5 layers of cells of the ovule integument. After pollination the seed coat cells grow rapidly to a length of 500 μm, roughly the length of a mature seed (Western et al., 2000). By 5 days after pollination the seed coat ceases growth, while the embryo has reached the heart stage. During differentiation, cells of the innermost layer synthesize condensed tannins that will eventually oxidize and impregnate other cell layers giving the seed coat its brown colour (Haughn and Chaudhury, 2005). Cells of the other two inner integument cell layers undergo programmed cell death. The two cell layers of the outer integuments accumulate starch during the growth phase and go through specific dramatic changes in their content and morphology. The palisade (subepidermal) layer produces a thickened cell wall on the inner tangential side of the cells. Cells of the epidermal layer secrete mucilage, initiating the formation of an apoplastic pocket. This pocket is filled with large quantities of mucilage consisting mainly of pectin (Haughn and Chaudhury, 2005). Late in development, the surviving layers of seed coat cells die. Upon hydration of mature seeds, the mucilage swells to create a gel like capsule around the seed that contributes to seed hydration and/or dispersal.

1.4.2 *A. thaliana* germination

For many plants, germination begins with imbibition and the perception of a germination-inducing signal by a dormant seed. The germination is said to have ended when the radicle has protruded through all covering layers (Bewley, 1997a). Water uptake by germinating seeds can be divided into three phases: phase I, II and III. These

phases in *A. thaliana* are shown in Figure 1.3. In Phase I, the imbibition, is characterized by rapid water uptake by the dry seed. During this phase, the embryo cells swell due to rehydration and damage to the membrane and cellular compartment causes massive leakage of cellular solute (Weitbrecht et al., 2011). In order to cope with the cellular damage, the seeds reactivate a number of mechanisms including respiration, energy production and translation of stored mRNA. Phase II is associated with a lag, during which water uptake slows considerably and several metabolic changes take place (Bewley, 1997a; Weitbrecht et al., 2011). Respiration and energy production is now activated, new *de novo* mRNAs are synthesized and translated, and damaged DNA and mitochondria are repaired. The awakening and activation of metabolic activity in the embryo requires the mobilization of energy storage reserves including starch, sucrose, oil bodies, protein bodies and phytin (Weitbrecht et al., 2011; Bewley, 1997). There are differences in the structure, composition and relative amounts of these storage compounds in different species (Obroucheva and Antipova, 1997; Linkies et al., 2010). *A. thaliana* seeds contain a significant portion of the stored carbon and energy as triacylglycerols (seed oil) along with small amounts of sucrose within the cotyledons of the mature embryo (Focks and Benning, 1998; Baud et al., 2002). During Phase III, there is further water uptake associated with the onset of seedling growth (Bewley, 1997a; Weitbrecht et al., 2011). During phase III the embryo cells expand considerably.

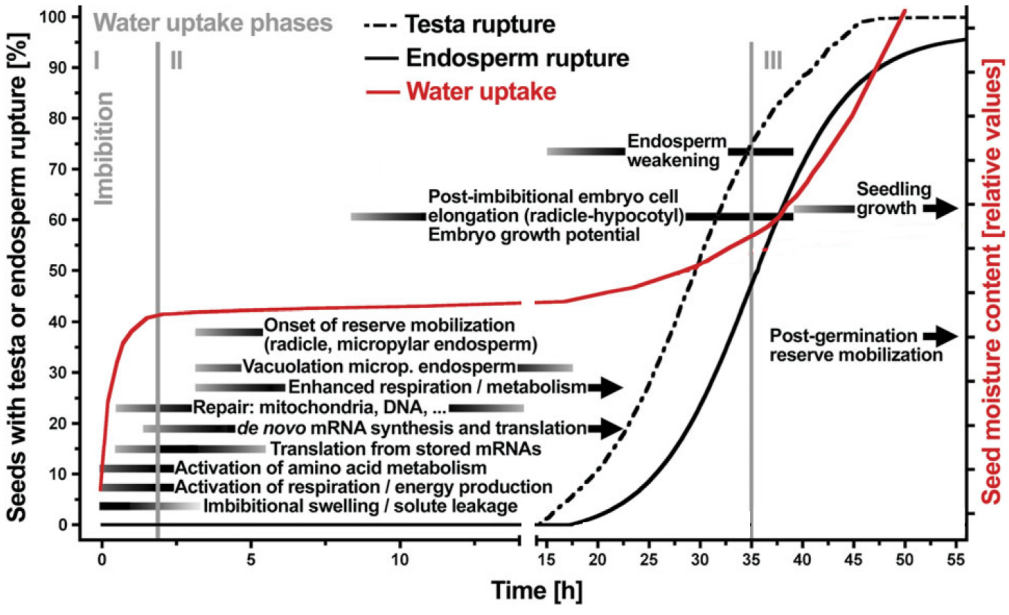

Figure 1.3: A diagram showing the key biophysical, biochemical, and cellular events during the three phases of water uptake occurring in *A. thaliana* seed germination. The time courses for testa and endosperm rupture are depicted in the diagram. This is a simplified version of the diagram published in (Weitbrecht et al., 2011). Reprinted with the permission of Oxford Journal.

A. thaliana embryo cells expand during the germination process, but cell division is not evident (Barroco et al., 2005; Gimeno-Gilles et al., 2009; Sliwinska et al., 2009). After the initial cell swelling, due to rehydration, all changes in seed size and shape are caused by cell expansion. The wall is in a state of tensile stress produced by water uptake generating increased turgor pressure. This stress is release by changes in mechanical properties of the wall material: cell wall loosening. Relaxation induced by cell wall loosening allows turgor pressure to produces irreversible cell enlargement through a mechano-hydraulic process, (cell expansion) resulting in overall growth (Schopfer, 2006). This cell wall loosening occurs through remodelling of the cell wall components including cellulose microfibrils, hemicellulose and the pectin matrix (Weitbrecht et al., 2011).

In general, mature angiosperm eudicot seed, including that of *A. thaliana,* consists of an embryo encompassed by a triploid endosperm surrounded by the maternal seed coat. In *A. thaliana* and related endospermic species, such as cress (*Lepidium sativum*) and tobacco, the completion of germination requires seed coat rupture (part of phase II) followed by endosperm rupture (Figure 1.3; Liu et al., 2005; Manz et al., 2005; Müller et al., 2006). Little is known about the changes in seed coat mechanical and biochemical properties leading to endosperm and seed coat rupture in *A. thaliana*. Further research concerning a potential enzymatic weakening of the cell wall and endosperm is required to elucidate how endosperm and seed coat rupture is accomplished.

1.5 Evidence for PME and PMEI function in *A. thaliana* seeds

Evidence for the action of PME and PMEI in seed development is mainly related to the identification of transcripts in the seed tissues. Approximately 20 *PMEs* were found to be expressed during silique development (Louvet et al., 2006). Real-time PCR data and promoter-GUS fusion in this study showed 2 *PME* genes expressed early in the developing seeds tissues (Louvet et al., 2006). Another study identified genes, annotated to encode *PME* and *PMEI* proteins, specifically expressed in the seed coat, endosperm, chalazal or embryo during development (Wolf et al., 2010).

A. thaliana seed coat mucilage has different relative amounts of cell wall components as compared to other cell walls. Several lines of evidence indicate that HG, the substrate of PME is present in seed coat mucilage. Monosaccharide analysis of *A. thaliana* seed coat mucilage suggests a small proportion of HG (Macquet et al., 2007; Dean et al., 2007). When an HG biosynthetic enzyme is mutated (mutant *gaut11-2*), the mucilage quantity decreases supporting the presence of HG in the seeds mucilage (Caffall et al., 2009). Finally, seed mucilage is bound by HG-specific antibodies JIM5, JIM7, PAM1 and 2F4 (Willats et al., 2001; Macquet et al., 2007; Voiniciuc et al., 2013). The domain specific labelling of mucilage by these antibodies revealed different degrees of methyl esterification in mucilage.

Mutants displaying defective seed mucilage revealed the potential presence of PME and its inhibitor in the seed coat. These mutated genes responsible for the phenotype were identified and the corresponding genes were characterized. FLYING SAUCER1 (FLY1), a transmembrane ring E3 Ubiquitin Ligase, was shown to regulate the degree of pectin methyl esterification in *A. thaliana* seeds mucilage (Voiniciuc et al., 2013). It was proposed that FLY1 regulates the degree of methyl esterification of pectin in mucilage by recycling PME enzymes from the apoplast of seed coat epidermal cells. The SUBTILISIN-LIKE SERINE PROTEASE 1 (SBT1) was shown to be a protease essential for the seed mucilage release (Rautengarten et al., 2008). The mutant *atsbt1.7* has increased PME activity in the seed suggesting it acts as a repressor of PME in the seeds. Recently, PMEI6 was shown to promote *A. thaliana* seed mucilage release by limiting methyl esterification of homogalacturonan in seed coat epidermal cells (Saez-

Aguayo, 2013). Its presence in the seeds was the first direct proof of an active PMEI in the seed. Because PMEI is believed to function with PME, the presence of PMEI indirectly supports the hypothesis that PME is present in the seed.

One study has characterized the role of PME in dormancy breakage and germination of gymnosperm (Ren and Kermode, 1999). Very little is known about the role of PME in the germination of angiosperm seeds in general. Interestingly, a battery of cell wall degrading and cell wall loosening enzymes were shown to be involved in plant germination including cell wall hydrolases (Bewley, 1997b), xyloglucan endotransglycosylase (Wu et al., 1994; Chen et al., 2002), expansins (Chen and Bradford, 2000), β-1,3-glucanase (Leubner-Metzger et al., 1995), endo-β-mannanase (Nonogaki et al., 2000) and β-mannosidase (Sanchez and de Miguel, 1997). In *A. thaliana*, a large number of genes encoding pectin-modifying enzymes and associated regulators showed significant differential regulation during the first 24 h of seed germination (Nakabayashi et al., 2005; Narsai et al., 2011; Dekkers et al., 2013). It is likely that members of the 2 large families of genes encoding PME and PMEI are involved in the germination process.

1.6 Research Outline and Goals

Pectin methyl esterification clearly impacts many different physiological processes. It is accepted that HG is secreted in the cell wall highly methyl esterified and later can be modified by the action of PME in the cell wall. PMEs are thought to play major roles in the gelling state or loosening of pectin and in interactions with other cell wall components. By inhibition of PME activity, the inhibitor PMEI is an important regulator of PME activity. Despite the importance of the PMEs and PMEIs in the cell wall structure, only a few genes of these large families have been characterized.

I am interested in elucidating the role of these proteins in seed biology. For my PhD research, I studied methyl esterification in two general phases of the seed developmental program using PME and PMEI. The following were my main objectives:

1. Identify and characterize a PME involved in seed mucilage structure and function by screening T-DNA and transposon insertional mutants for mucilage defects. Characterize the function of the *PME* gene(s) related to the phenotype(s) using cytological and biochemical methods.
2. Verify if the degree of pectin methyl esterification affects germination by manipulating the amount of PMEI in the seed.

Chapter 2: *HIGHLY METHYL ESTERIFIED SEEDS* is a PME involved in embryo development

2.1 Introduction

The primary plant cell wall is a highly complex mixture of cellulose, hemicellulose, pectin and both enzymes and structural proteins. Pectins include the HG (Ridley et al., 2001), which are a polymer of α-1,4-linked-d-galacturonic acid and is usually the most abundant pectin in the plant cell wall (Ridley et al., 2001). HG is synthetized in a highly methyl esterified form and can be demethyl esterified following secretion to the apoplast (Sterling et al., 2001; Zhang et al., 1992; Staehelin et al., 1995). Demethyl esterification of HG is catalyzed by PME in either a blockwise or non-blockwise fashion, which leads to the stiffening or loosening of the cell wall (Wakabayashi et al., 2003). PMEs have been shown to be involved in diverse physiological processes including cell wall elongation and fruit ripening (Jolie et al., 2010; Pelloux et al., 2007; Wolf and al., 2009; Micheli et al., 2001). Putative PME genes identified by bioinformatic analysis of the *A. thaliana* genome form a large family of 66 genes as shown by CAZy (http://www.cazy.org/CE8_eukaryota.html).

The epidermal cell layer of *A. thaliana* seed coat undergoes complex cell differentiation during which large quantities of pectinaceous mucilage is secreted in between the plasma membrane and the primary cell wall (Haughn et al. 2005). Upon exposure of the mature dry seed to water, this mucilage is extruded from the epidermal cells to encapsulate the seed. Recently, genes impacting the DM of mucilage were shown to be involved in seed mucilage extrusion (Saez-Aguayo et al, 2013; Voiniciuc et al., 2013).

2.1.1 Objectives

I sought to identify PMEs that function in the demethyl esterification of seed mucilage by screening for PME mutants with defective extrusion or adherence. I report

here the identification of *At1g23200,* which encodes a PME required for normal embryo development and, indirectly, mucilage extrusion.

2.2 Materials and methods

2.2.1 Plant material and growth conditions

Both *A. thaliana* Columbia-0 (Col-0) and Nossen-0 (No-0) were used as Wt in this study. Plants were grown as described by Dean et al. (2007), and flowers were staged as per Western et al. (2000). Briefly, seed were germinated on AT plate with 7% (w/v) agar, and seedlings were transferred to soil (Sunshine Mix; SunGro, Kelowna, British Columbia) after 7 days. Plants were grown in chambers with continuous fluorescent illumination (80-140 $\mu Em^{-2}s^{-1}$) at 20-22°C. The *A. thaliana* transposon-tagged line 15-4955-1 in the genes coding *At1g23200* and rename *hms-1* was ordered from Riken Genomic Science Center (Ito et al., 2002; Kuromori et al., 2006).

2.2.2 PCR and cloning

All DNA were amplified from Col-0 DNA using a two-step PCR protocol with very long primers and Phusion High Fidelity DNA Polymerase (New England Biolabs). The modification of the *pCAMBIA2300* vector by cloning the 780 bp Citrine YFP including spacers from pAD (Debono, 2011) by restriction enzymes PstI-XbaI was used to generate the construct *pro_{HMS}:PP::YFP::HMS* that was renamed pCAMBIA-YFPc. The use a LP (cattgcaagAAGCTTatttctttctctttgagttttagtatcaaatatttgta) and a RP (cattgcaagAAGCTTTTCCAGTAGTTTACGGTCGGAAAGAGGGAACCACGA) primers was use to amplify the HMS promoter (*pHMS*) including the Pre-Pro domain (*PP*) resulting in a pHMS:pp amplicon. Each of these two primers includes a *HindIII* site for use in cloning pHMS:pp into the pCAMBIA-YFPc vector. Secondly, a LP (cattgcaagTCTAGAGATTCCAAAACTACGGCAAAAGCCGATCTTGTGGTGG) including a *XbaI* site and a RP (cattgcaagGGTACCcaaagctacaataagaaaggtagaaagatacataaa) including a *KpnI* site were

used for in the cloning of HMS in pCAMBIA-YFPc. The cloned p*HMS:pp* amplicon starts 2372 bp upstream of the ATG of HMS and includes 723 bp in the coding region. The second HMS amplicon starts 723 bp downstream of the ATG of HMS and ends 300 bp downstream from the stop codon. pGreenII 0029 was used to generate the construct pHMS:HMS. A LP (cattgcaagGGATCCacaaaaaacctcgaatcgatggaagacaaactccca) that included a BamHI site and a RP (cattgcaagAAGCTTcaaagctacaataagaaaggtagaaagatacataa) that included a HindIII site were used to amplify *pHMS:HMS*. The *pHMS:HMS* amplicon starts 2000 bp upstream of the ATG to 300 bp downstream the stop codon. A modified *pCAMBIA2300* vector including the *UBQ1* promoter from Chris Ambrose, University of British Columbia, was use for the cloning of *UBQ1:HMS*. A LP (cattgcaagGGATCCaatatcccacatctctactcatccacattagtcaaaga) that included a BamHI site and a RP (cattgcaagGGTACCaaatcttccaagagcgagtcaatcggtttgctattata) that include a KpnI site were use to amplify the HMS genomic sequence including both the 5′ and the 3′ UTRs. The HMS amplicon starts 58 bp upstream of the 5′ UTR to 182 bp downstream of the 3′ UTR.

2.2.3 RT-PCR transcript analysis

The RNA used in this study was extracted from Col-0 and No-0 tissues using PureLink® RNA Mini Kit (Ambion®) according to the manufacturer's instructions. RNA quantification was performed using a NanoDrop 8000 (Thermo Scientific). Five hundred ng of total RNA treated with DNase I amplification grade (Invitrogen) were used for first-strand cDNA synthesis along with SuperScript™ II Reverse Transcriptase (Invitrogen). RT-PCR was conducted using a typical PCR reaction containing Taq polymerase (Genescript) and gene-specific pairs of intron-spanning primers for *At1g23200*, *At1g11590*, *At4g03930*, *At1g44980*, *At5g49180*, *At4g33220*, *At2g43050* and *GAPC* (Table 3). Amplicons of ~200 bp were expected after intron splicing. Transcript levels were analyzed after 23 amplification cycles, and GAPC was used as a loading control.

Table 2.1: Primers used for RT-PCR for 7 PMEs isolated in the screen.

Genes	LP	RP
At1g23200	GCAAGTGTCTCCGGTAGAGTTAAG	TCAAAGTCCATCGTTGACCGGTAC
At1g11590	AATAGCCCTTCTTGGTTATTCCAT	ATCATAAATGCCTGTCTTTATATAGATGA
At4g03930	AGACCTCATTTCTAAGGCAAAGGTA	ATTGGGTTTCGTATTCTCAATGG
At1g44980	GACCTCACTTCTAGGGCAAGAGA	GACGAATCTCTTTTGGCTGTGT
At5g49180	GGAAGAATTGACGATGAGAATGG	TTGACGTCACCAAGAAAATGACT
At4g33220	AAGCGAGTTTGTGAGCTCCATA	CAGCGACAAGGGATTTTACGA
At2g43050	TTATGTTAGTTGGTGACGGGAAG	GGTGCCGGTGATATCCGTC
GAPC	GATTCGGAAGAATTGGTCGTTT	CTTCAAGTGAGCTGCAGCCTT
Actin	TCAGATGCCCAGAAGTGTGTT	CCGTACAGATCCTTCCTGATA

2.2.4 Mucilage extrusion and staining

Whole mature seeds were hydrated and rotated in water for 45 min. Water was subsequently removed and replaced by 0.01% (w/v) ruthenium red (Sigma-Aldrich) for 30 min before a final wash in water. Hydrated seed samples were viewed using a light microscope.

2.2.5 High-pressure freezing, freeze substitution and immunolabeling

Developing seeds at 4, 7, 10 DPA were first high pressure frozen, resin embedded and sectioned according to a previously published method (Rensing et al., 2002; Young and al., 2008). Developing seeds at 4, 7 and 10 DPA were dissected and pierced with an insect pin before being frozen in the presence of hexadecene using Leica EM HPM 100 High Pressure Freezer (Leica; Germany). *A. thaliana* Nossen-0 (No-0) was used as Wt. Freeze substitution base with 8% (v/v) dimethoxypropane in acetone including 2% (w/v) osmium tetroxide as a general stain and 0.25% (v/v) glutaraldehyde with 2% (w/v) uranyl acetate was employed for immunollabeling assays. Freeze substitution was performed at -

80^{o}C using acetone with an increasing amount of resin. The samples were slowly infiltrated with Spurr's (Spurr, 1969) resin for morphological assays and LR white (London resin Company) for immunological studies. Thin sections (0.5uM) were used for both staining and immunollabeling. Sections were transferred and dried on Hydrophobic Printed Well Slides ER202W (Thermo Scientific). Slides were blotted in the presence of JIM5 and JIM7 antibodies in specific buffer as shown in (www.plantprobes.net).

2.2.6 Wax embedding, sectioning and mucilage extrusion

Seeds were embedded as per Dean et al., 2007. Briefly seeds were spread on the bottom of the Petri dish (Thermoscientific) and molten paraplast (Sigma-Aldrich) was added before incubation at 60°C for 2h before hardening at room temperature. Sections of ~20μm thick were prepared and hydrated with 0.001% (W/v) ruthenium red and imaged as described above.

2.2.7 Seed oil content analysis

The seed oil content analysis was performed as described by Li et al., 2006 with minor modifications. Briefly, ~ 2 mg of dry seeds for each line were transferred into a 1 × 10 cm glass tubes and 1 ml of 5% v/v sulfuric acid in methanol was added with 300 μl of 0.1 μg l^{-1} triheptadecanoin in toluene as an internal standard. Samples were incubated at 90°C for 1.5h and cooled on ice. Later, 1.5 ml of 0.9% NaCl were added before the fatty acid methyl esters were extracted with 2 ml hexane, followed by evaporation under nitrogen gas. Fatty acid methyl esters were analyzed by gas chromatography with flame ionization detection (GC-FID) as described previously (Kunst et al., 1992).

2.2.8 PME activity

Pectin Methyl Esterase activity was assayed using a modified version of a previously published method (Grsic-Rausch and Rausch, 2004). Briefly, ~1 mg of

developing seeds were dissected from the silique and immediately frozen with liquid nitrogen. After grinding in liquid nitrogen, 100 uL of protein extraction buffer (100 mM Tris-HCL pH 7.5, 500 mM NaCl and cOmplete, Mini, EDTA-free (Roche)) was added to the samples. The samples were rotated 15 min at 4 ^{o}C before centrifugation at 10,000 g for 5 min at 4 ^{o}C. 10 uL of supernatant was added to 100 ul (2U of formaldehyde dehydrogenase in presence of 5% W/V 80% Methyl Esterified Pectin (Sigma P9135) in a 0.4 mM NAD+ 50 mM phosphate buffer pH 7.5) using 96-well plate assay read with Synergy HT plate reader (BioTek). The protein concentration for each sample was measured using a Protein Assay Kit I 500-0001 (Bio-Rad), with a standard curve made of Albumin standard 23209 (PIERCE).

2.2.9 Biochemical determination of the DM

The methyl ester content was determined using a modified version of the protocol for DM in Lionetti and al. 2007. Approximately ~5 mg of developing seeds were frozen in the liquid nitrogen and ground to a fine powder. The ground seeds were washed twice with 70% ethanol, once with methanol:chloroform (1:1) and three times with acetone. Samples were dried under nitrogen gas at 60^{o}C between each wash. Afterward, the final dried, samples were saponified in 0.25 M NaOH for 60 min and neutralized with 0.25 M HCL. Following a quick centrifugation, fifty microliters of the supernatant was used in a 96-well plate for methanol assessment (Lionetti et al., 2007).

The galacturonic acid content was determined using a previously described protocol (van den Hoogen et al., 1998; Voiniciuc et al., 2012). The whole seed carbohydrates remaining following saponification were precipitated in 100% ethanol by centrifugation. The pellets were dried under nitrogen gas at 60^{o}C before being resuspended in distilled water. Samples were sonicated for 20 s with a Branson Sonifier 150 (Branson Ultrasonics) to create a homogenous suspension. Twenty microliters of each sample was used for the 96-well plate uronic acid assay (van den Hoogen et al., 1998).

2.2.10 Scanning electron microscopy

Dried *A. thaliana* seeds were mounted on stubs and coated with gold-palladium alloy using the Hummer VI sputtering system (Anatech). The prepared samples were observed with a Hitachi S-800 scanning electron microscope and images were captured with Evex Nano Analysis digital imaging system.

2.2.11 Confocal microscopy

Developing *pHMS:pp:YFP::HMS* and WT seeds were mounted with water between a glass slide and a coverslip. Images were captured in darkness immediately after being exposed to Propidium Iodide (SIGMA) or FM 4-64 (Invitrogen) for 5 and 10 min, respectively. Imaging was performed on an Olympus FV1000 laser scanning confocal microscope using a 63× numerical aperture oil-immersion objective. All image processing was performed using Olympus Fluoview software and Velocity. All confocal micrographs were processed and measured using ImageJ (Albramoff et al., 2004).

2.2.12 Dynamic mechanical analysis

For mechanical tests, 5 seeds were divided equally and placed between two specimen disks 15 mm in diameter (Electron Microscopy Sciences). The position of samples was consistent for each analysis. The samples were mounted on a QSeries Q800-0174 DMA (TA instruments), which was held in controlled force mode with the clamp compression applying a ramp force of 18 N/min at room temperature. Specific deformations were recorded at 0, 1.8, 3.6, 5.4, 7.2, 9 and 10.8 N force before the plateau was reached. The percentage of total seed deformation was calculated using the position measured by the clamp.

2.3 Results

2.3.1 Identification of *PME* genes expressed in the seed coat during mucilage secretion

I hypothesized that a *PME* gene involved in mucilage modification would be expressed between 4 and 9 DPA with a peak at approximate 7 DPA, the time of greatest mucilage secretion. Using the eFP browser (http://bar.utoronto.ca/efp) and a seed coat specific microarray (http://bar.utoronto.ca/efp_seedcoat/), I identified 7 *PMEs* expressed in the seed coat (Figure 2.1). Two studies previously identified *A. thaliana PMEs* with gene expression specifically up-regulated in the silique (Louvet et al., 2006) and seed coat (Wolf et al., 2009). In these studies, as well the current, the annotated genes *At5g49180*, *At1g11590*, *At4g03930* and *At4g33220* were identified as being expressed in the seed in agreement with my results. I verified the *in silico* results for all seven genes using RT-PCR (Figure 2.1).

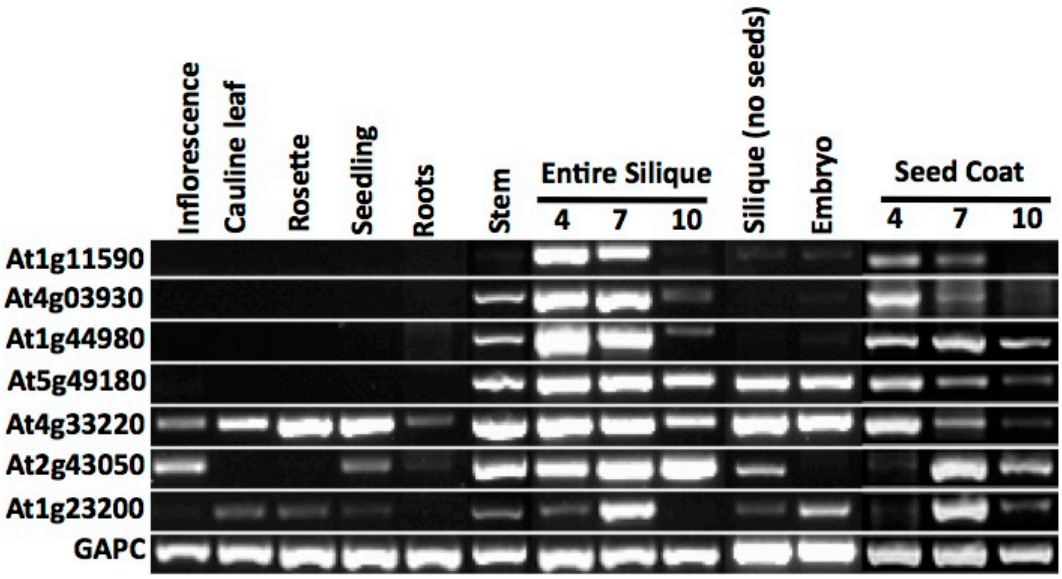

Figure 2.1: The expression of putative PME genes at different times and in various tissues of *A. thaliana*.

RT-PCR was used to identify the presence of transcripts from 7 *PME* genes in different plant tissues. GAPC mRNA was used as an internal positive control.

Two genes, *At1g23200* and *At2g43050,* were specifically up-regulated in the seed coat at 7 DPA (increase significantly from 4 to 7 DPA and decrease between 7 to 10 DPA). The expression of either gene is relatively low in other plant tissues, except the embryo (*At1g23200*) and stem (*At2g43050*) (Figure 2.1).

2.3.2 Insertion lines with a seed mucilage phenotype

I screened *A. thaliana* insertional mutant lines available from Arabidopsis Biological Resource Center (ARBC), Nottingham Arabidopsis Stock Center (NASC) and Riken Bioresource Center (BRC) for all 7 annotated *PME* genes. Only one insertional mutant line (15-4955-1; transposon-tagged line from RIKEN Genomic Sciences Center"; Ito et al., 2002; Kuromori et al., 2004), gave a mucilage phenotype. This line has an insert in the second exon of *At1g23200* (Figure 2.2A) encoding a pectin methyl esterase, which I designate as *HIGHLY METHYL ESTERIFIED SEED* (*HMS*; the 15-4955-1 allele is *hms-1*); as the mutant phenotype includes an increase in methyl esterification of seed tissue (see below). When the *hms-1* mutant was exposed to water, the mucilage extrudes less extensively than WT (Figure 2.2CD). The *hms-1* mutant completely lacks HMS WT transcript, as shown by RT-PCR (Figure 2.2B). Analysis of a F_2 population of 141 individuals from a cross between the WT and the *hms-1* mutant showed a segregation pattern of 107 WT:34 mutant plants, consistent with a single nuclear mutation (X_2= 0.167, $p > 0.05$). Using PCR-genotyping on the same population, I obtained a 29:78:34 ratio between WT:heterozygote:homozygote respectively, with a $X_2 = 0.548$, $p < 0.05$ again consistent with a single nuclear mutation. Moreover, the *hms-1* insertion segregates with the seed phenotype 100% of the time. This supports the hypothesis that the phenotype is due to the insertion of the transposon. To further confirm that *hms-1* is responsible for the phenotype I performed a molecular complementation. The *hms-1* mutant was transformed with a genomic DNA fragment spanning 1.935 kb upstream of the ATG to 0.300 kb downstream of the *HMS* stop codon. From 36 independent lines transformed, 24 showed complete rescue of the *A. thaliana* transposon-tagged line phenotype and transcript abundance was restored (Figure 2.2B, 2.3E, 2.4D).

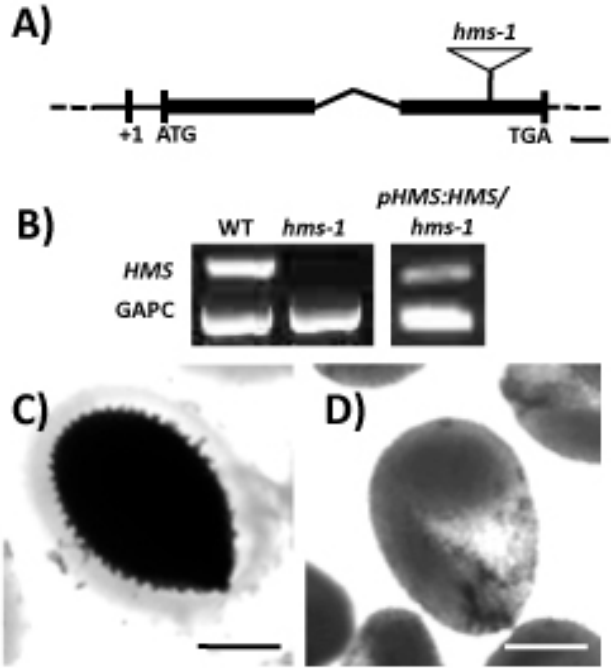

Figure 2.2: The position of insertion, level of transcript and mucilage phenotype of the *hms-1* mutant.

(A) *HMS* gene structure and mutation including the position of the transposon insertion in *hms-1*. The two exons are represented by black boxes and the intron by the connecting line. (B) *HMS* transcript accumulation in whole seeds at 7 DPA for WT, *hms-1* and *pHMS:HMS* transformed *hms-1* plants. RNA was extracted and mRNA was detected by RT-PCR. GAPC mRNA was used as an internal control. (C) and (D) Seeds following shaking in water and subsequent staining with ruthenium red . The photographs of Wt in (C) and *hms-1* in (D) were taken with illumination from below. Bar = 100 μm

2.3.3 The morphology of *hms-1* seed coat and embryo is affected

The mature *hms-1* seed morphology was altered when compared to *WT*. The *hms1-1* seeds appeared smaller in size and were irregular in shape (Figure 2.3A-B). When mature hydrated seed was illuminated from underneath and observed with a light microscope, the *hms-1* mutant seed appeared translucent while the WT were opaque, and the mutant embryo appeared smaller and underdeveloped (Figure 2.2C-D), a conclusion

supported by dissection of the embryos from the seed (Figure 2.3C-D). The weight of *hms-1* seeds was found to be less than WT (Figure 2.4E).

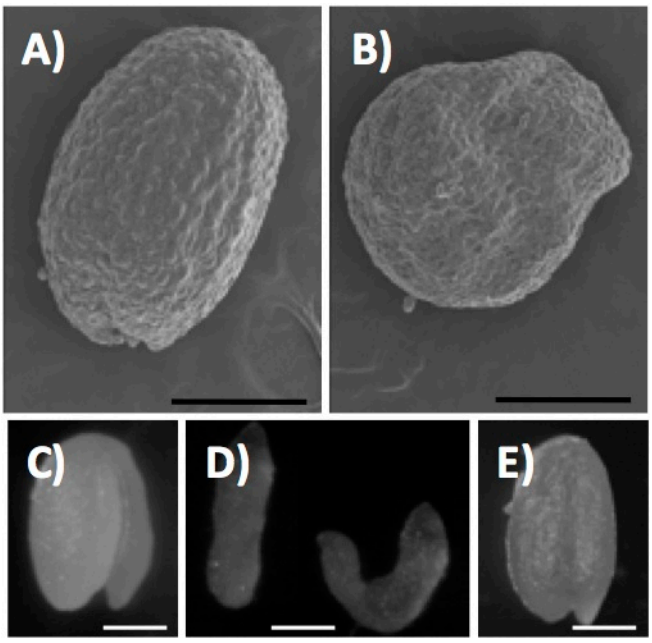

Figure 2.3: Morphological phenotype of the *hms-1* mutant seed.
(A) and (B) Scanning Electron Microscope imaging showing Wt in (A) and *hms-1* in (B). (C) to (E) Image of re-hydrated embryo showing Wt in (C), *hms-1* in (D) and *pHMS:HMS* transformed *hms-1* in (E). Bar = 100 μm

2.3.4 The *hms-1* mucilage phenotype is a consequence of an embryo defect

Since the *hms-1* phenotype includes defects to both seed coat and embryo, I investigated whether the phenotype was due to the genotype of the seed coat, the embryo or both. The *hms-1* mutant was used as the female parent in a cross with WT. The F1 seeds have a seed coat that is homozygous for *hms-1* and an embryo that is heterozygous. The morphology, weight and mucilage extrusion of the F1 seeds was normal (Figure 2.4C-E). Differences in the degree of methyl esterification of mucilage were also depended on the genotype of the embryo (Appendix A). Thus, the *hms-1* seed phenotype, including the characteristics for mucilage extrusion and the seed coat is due to loss of HMS function in the embryo.

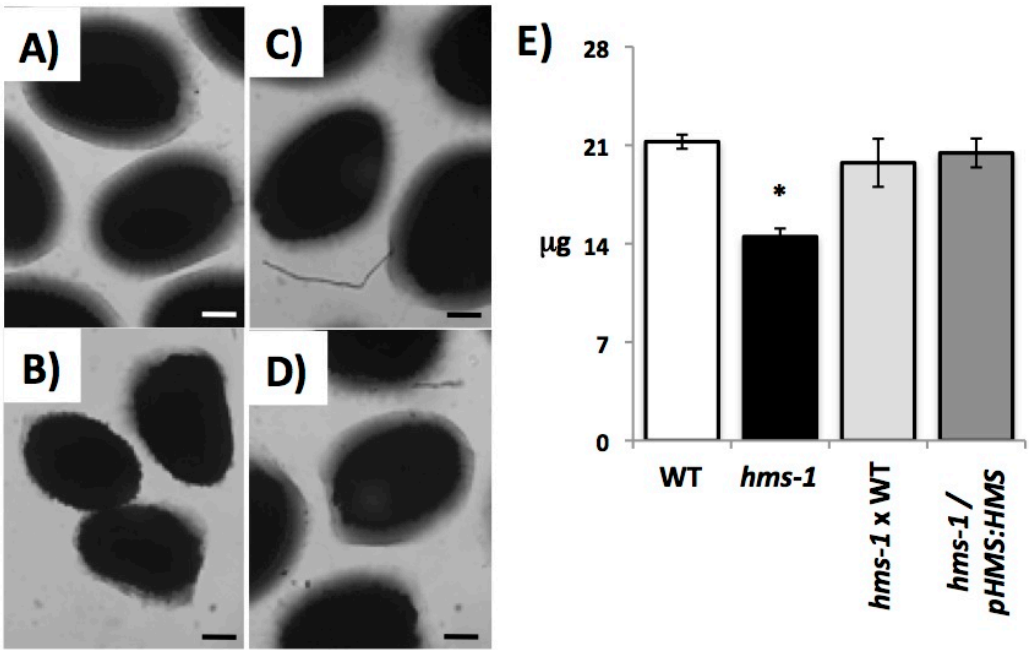

Figure 2.4: Seed mucilage and mature seed weight phenotype.
(A) to (D) Mature seeds after shaking in water and subsequently staining in ruthenium red. WT (A), *hms-1* (B), F1 progeny from the cross *hms-1* x WT (C) and *pHMS:HMS transformed hms-1* seeds (D). Bar = 50 µm (E) Average seed weight in µg per seeds for WT, *hms-1*, F1 progeny from the cross *hms-1* x WT and *pHMS:HMS* transformed *hms-1* seeds. Values represent the mean ± SE of 30 replicates. Asterisks indicate significant difference using a Students t-test with a Bonferroni correction ($P < 0.05$).

2.3.5 The *hms-1* seed mucilage properties are not affected

To determine whether the amount or hydration property of *hms-1* mucilage is impaired, I sectioned wax embedded *hms*-1 and WT mature seeds and exposed the sections to water with ruthenium red (Figure 2.5A-B). The mucilage expansion of *hms-1* is comparable to WT, suggesting that the defect in mucilage extrusion characteristic of *hms-1* seeds is not due to a large decrease in amount or a change in mucilage hydration properties. For this reason I investigated the embryo defects further.

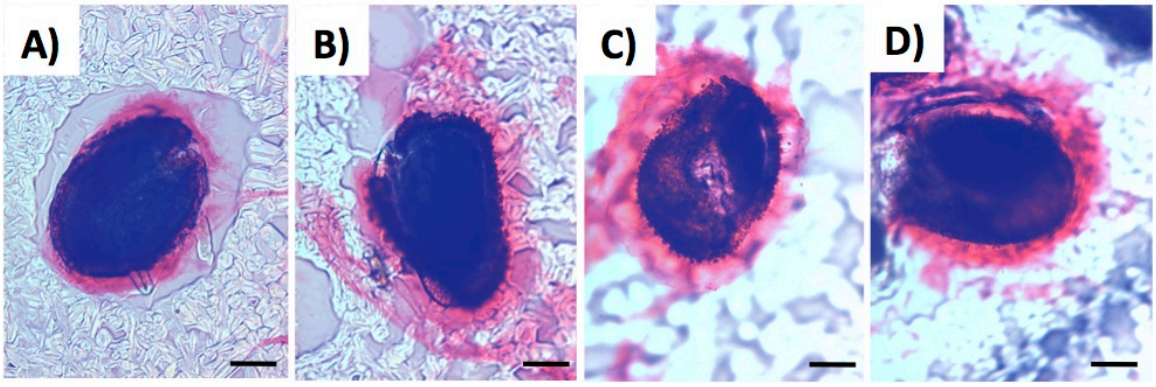

Figure 2.5: Mucilage extrusion of seeds sections.

(A) to (D) Wax embedded mature seeds sectioned and stained with ruthenium red showing WT in (A), *hms-1* in (B), F1 progeny from the cross *hms-1* x WT in (C) and *pHMS:HMS* transformed *hms-1* seeds in (D). Bar = 100 μm.

2.3.6 The *hms-1* embryo defect is first visible at 7 DPA

To investigate the development of *hms-1* seed, WT and *hms-1* seeds were sectioned at 4, 7 and 10 DPA. These times represent key stages in WT seed development. At 4 DPA, WT epidermal seed coat cells have finished growing but have not begun to synthesize mucilage (Figure 2.6A). The WT embryo at this time is at the heart stage with large vacuolated cells (Figure 2.7AC). By 7 DPA, mucilage secretion in the seed coat epidermal cells is almost complete (Figure 2.6C). The 7 DPA embryo has reached the bent cotyledon stage (Figure 2.7E), and its cells are expanding and beginning to accumulate storage reserves (Figure 2.7G). The seed coat epidermal cells of the 10 DPA seed have begun to synthesize a secondary cell wall (Figure 2.6E). Embryo morphogenesis and growth is almost complete and its cells contain considerable storage reserves (Figure 2.7I-K). Seed coat development of *hms-1* was similar to that of WT throughout development (Figure 2.6; Figure 2.7 compare A,E,I with B,F,J). The *hsm-1* embryo was similar to WT at 4 DPA (Figure 2.7AB), but very different from WT by 7 DPA (Figure 2.7EF). The 7 DPA *hms-1* embryo was significantly smaller than WT and appears to be at an earlier developmental stage (torpedo). These differences were more pronounced by 10 DPA (Figure 2.7IJ). Interestingly, the *hms-1* embryo defects (7 DPA) roughly coincide with *HMS* expression in WT seed (Figure 2.1).

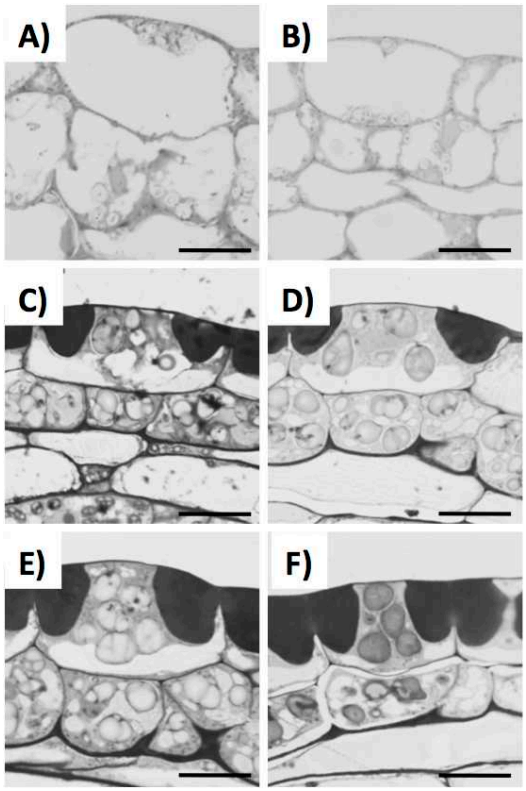

Figure 2.6: Seed coat differentiation.

(A) and (B) seeds at 4 day post anthesis. (C) and (D) seeds at 7 day post anthesis. (E) and (F) seeds at 10 day post anthesis. WT seed in (A), (C), (E) and *hms-1* seed in (B), (D), (F). Bar = 10 μm.

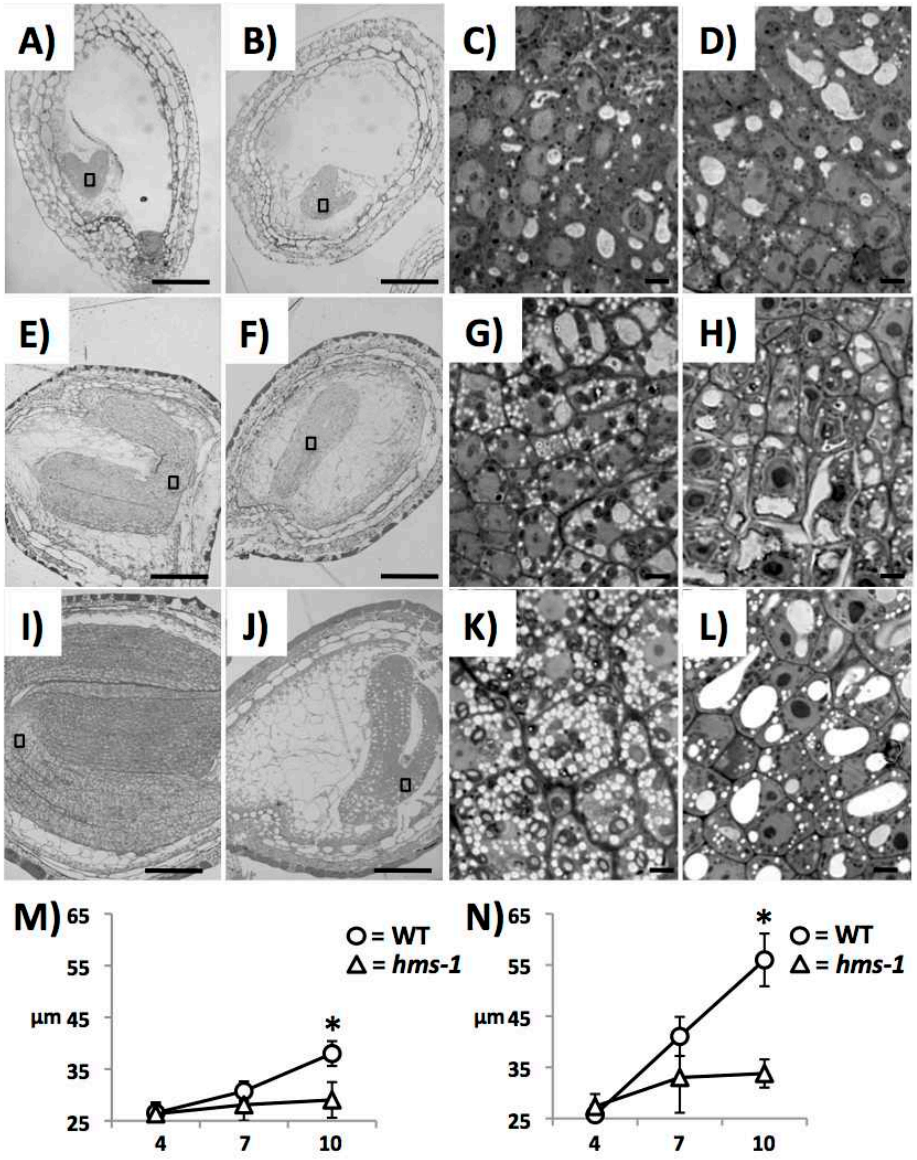

Figure 2.7: Seed anatomy and embryo cell sizes throughout development.

(A) to (D) seeds at 4 day post anthesis. (C) to (D) seeds at 7 day post anthesis. (E) to (F) seeds at 10 day post anthesis. WT seed in (A), (C), (E), (G), (I), (K) and *hms1-1* seed in (B), (D), (F), (H), (J), (L). Bar = 100 µm in (A), (B), (E), (F), (I), (J) and Bar = 6 µm in (C), (D), (G), (H), (K), (L). (M) and (N) Average perimeter length of embryo cells. Cotyledon cells in (M) and radicule cells in (N) both at 4, 7 and 10 days post anthesis. Asterisks indicate significant difference using a Students t-test with a Bonferroni correction ($P < 0.05$). Values represent the mean ± SE of 30 replicates.

2.3.7 The *hms-1* embryo cells size is decreased

I have shown that *hms-1* embryo grows more slowly than WT past 4 DPA. To determine the anatomical basis for this size change, I examined the anatomy of WT and *hms-1* seeds at 4, 7 and 10 DPA. Cells of the 4 and 7 DPA embryo were similar in structure to those of WT (Figure 2.7CD, GH). However, at 10 DPA, *hms-1* embryo cells appear smaller than WT, maintain their large vacuoles and appear to have fewer lipid bodies, a phenotype more closely resembling the linear cotyledon stage of embryogenesis (Figure 2.7KL). Because the oil bodies seemed smaller and less abundant, the oil content at maturity was quantified. The *hms-1* seeds had a lower oil content compared to WT (Figure 2.8). Measurement of the perimeter of the cells in sections was employed as a means to quantify the cell sizes. Embryo cell sizes were similar between *hms-1* and WT at 4-7 DPA, but were significantly different at 10 DPA where the *hms-1* radicals and cotyledons both had a reduced cell perimeter as compared to WT (Figure 2.7MN). This suggests that cell expansion in the embryo is reduced in *hms-1*.

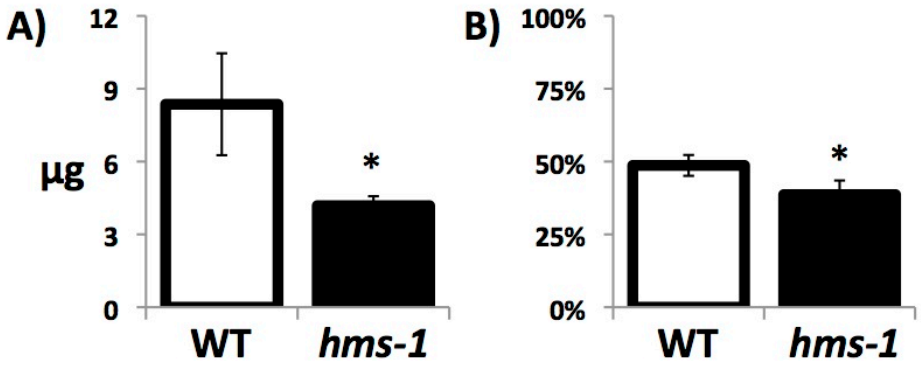

Figure 2.8: Oil content of mature seeds.
(A) Oil content in µg/seeds. (B) Oil content in % of fresh weight. Values represent the mean ± SE of 4 replicates. Asterisks indicate significant difference using a Students t-test with a Bonferroni correction ($P < 0.05$).

2.3.8 The YFP-HMS protein fusion is found in the seed coat and embryo cells

To investigate the localization of HMS, two constructs with Citrine YFP (Griesbeck et al., 2001) were generated, one with *YFP* fused in frame to the in C-terminus of *HMS* and a second with the *YFP* positioned after the putative pre-pro domain, respectively pro_{HMS}*:HMS::YFP* and pro_{HMS}*:PP::YFP::HMS*. Of the 64 pro_{HMS}*:HMS::YFP* and 28 pro_{HMS}*:PP::YFP::HMS* transformed lines, 9 and 6 lines respectively showed YFP fluorescence signal. None of the transformed lines carrying either construct showed complementation of the phenotype suggesting that the YFP domain interferes with function. Nevertheless, both protein fusions had similar temporal, spatial and intracellular localization patterns in the seed (Figure 2.9; Appendix B). Fluorescence was not observed in the pro_{HMS}*:HMS::YFP* and pro_{HMS}*:PP::YFP::HMS* plants at 4 DPA (Appendix B), while at 7 and 10 DPA showed localization in the epidermal cell layer of the seed coat as well as multiple cell layers of the embryo (Figure 2.9; Appendix B). The YFP signal in the epidermal cells of the seed coat co-localized with the cell wall stain propidium iodide supporting cell wall localization (Figure 2.9AC). The YFP signal in the epidermal seed coat cells did not co-localized with the membrane marker FM 4-64. It is visible in the cell compartment outside the FM 4-64 stained region consistent with cell wall localization (Figure 2.9DF). The YFP signal was present in the embryo cell wall and partly co-localized with the cell wall marker propidium iodide suggesting cell wall location (Figure 2.9GI). The YFP present in the embryo cells also partly co-localized with the membrane marker FM 4-64 (Figure 2.9JL). Looking closely at the merged images of the YFP and FM 4-64 of the embryo, the YFP was present in between the FM 4-64 signal suggesting a cell wall localization (Figure 2.9J-L).

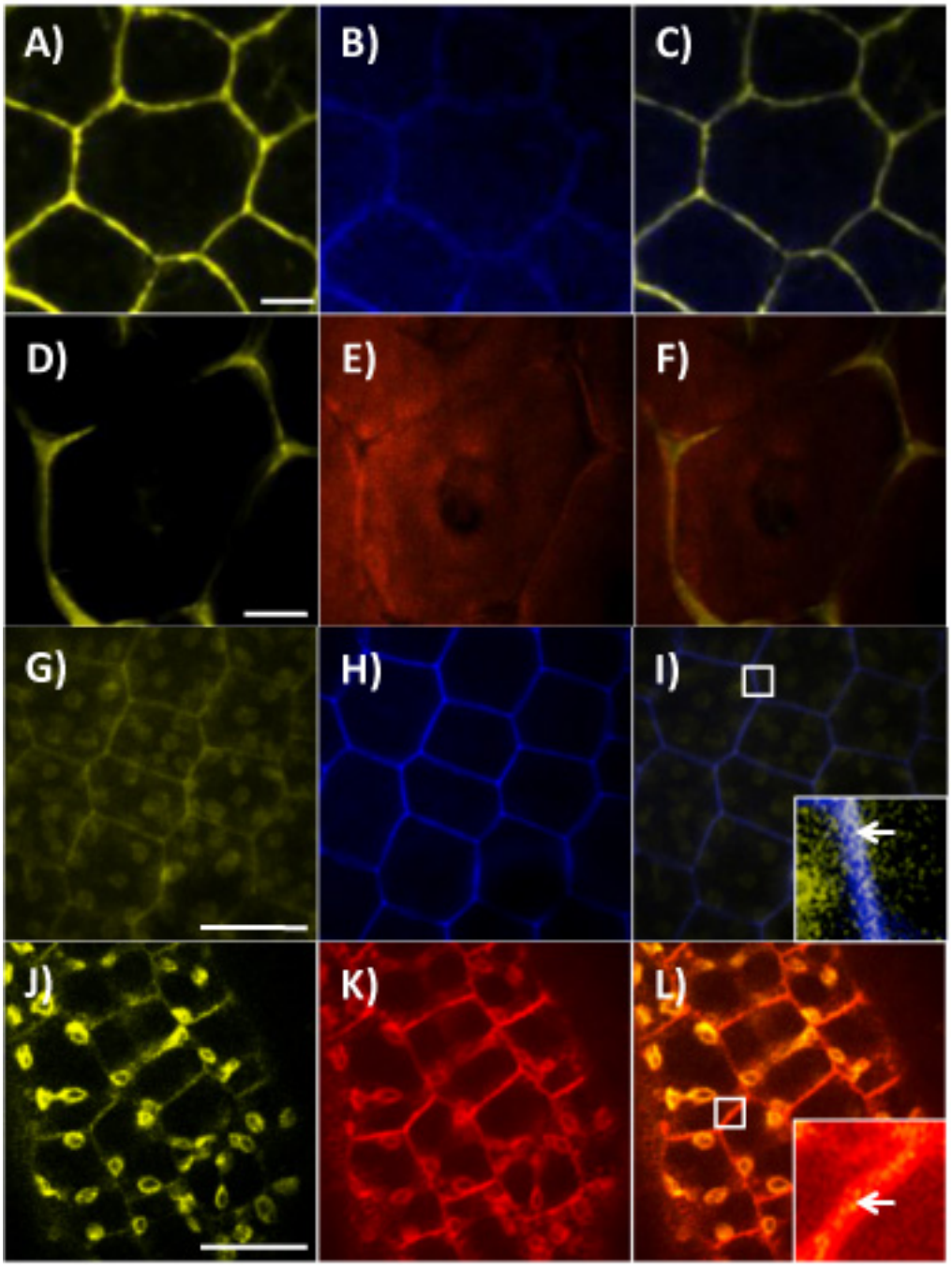

Figure 2.9: Localization of YFP-HMS in seed coat and embryo cells.

(A) to (F) 7 DPA seed coat epidermal cells showing YFP signal in (A) and (D), cell wall stained with Propidium iodide in (B) and membrane stain FM 4-64 in (E) as well as respective image composite in (C) and (F). (G) to (I) 7 DPA Embryo cells showing YFP signal in (G) and (J), cell wall stain with Propidium iodide in (H) and membrane stain FM 4-64 in (K) as well as respective image composite in (I) and in (L). To locate the

YFP signal in the embryo cell a section of the image composite is zoomed in (I) and in (L). Bar = 10 μm

2.3.9 The PME activity is decreased and the DM is increased in *hms-1* 7 DPA seeds

Heterologous expression failed to demonstrate that HMS has PME activity (Appendix C). As an alternative, measurement of the PME activity in protein extracts from developing 4, 7 and 10 DPA *hms-1* and WT seeds was used to test if the presence of HMS protein is correlated with the PME activity. PME activity from 4 DPA developing seed was similar in *hms-1* and WT (Figure 2.10A). By 7 DPA, PME activity was significantly lower in *hms-1* as compared with WT (Figure 2.10A). This decrease in activity was significantly less in F1 seeds of the *hms-1* × WT cross, and transformation with a *pHMS:HMS* construct was able to complement the loss of PME activity in *hms-1*. The 10 DPA seed protein extracts showed no PME activity in any sample (Figure 2.10A). Since a decrease in PME is expected to result in an increase in DM, the DM of the same extracts was quantified and showed a small but significant increase only at 7 DPA in the *hms1-1* mutant (Figure 2.10B). Interestingly, the difference in the DM was not conserved later in the development. This suggests the need for a decrease in DM specifically at 7 DPA for the embryo to develop properly.

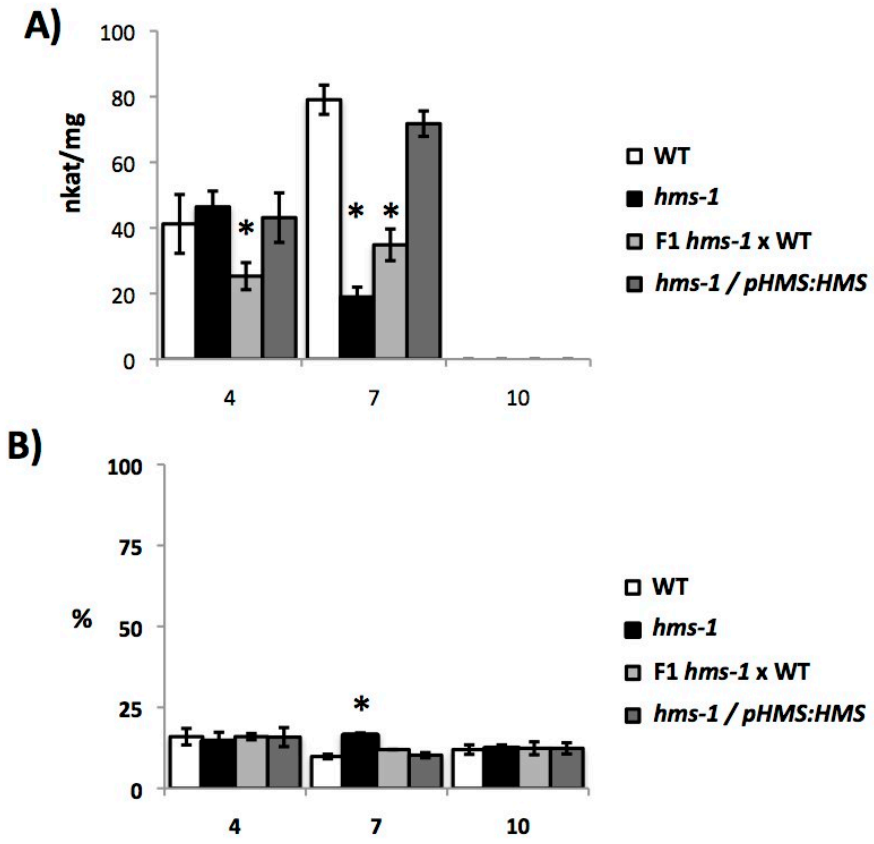

Figure 2.10: PME activity and DM in developing seed extracts.
(A) PME activity in nkat/mg of crude protein extracts from 4, 7 and 10 DPA developing seeds comparing WT, *hms-1*, F1 progeny from the cross *hms-1* x WT and *pHMS:HMS* transformed *hms-1* seeds. Values are means for n = 4. (B) Biochemical determination of the % methyl-esters of galacturonic acid in developing seeds comparing WT, *hms-1*, F1 progeny from the cross *hms-1* x WT and *pHMS:HMS* transformed *hms-1* seeds. Values represent the mean ± SE of 4 replicates. For (A) and (B) Asterisks indicate significant difference using a Students t-test with a Bonferroni correction ($P < 0.05$).

2.3.10 Ectopic *HMS* expression causes dwarfism and increases the PME activity

If the decrease in the DM at 7 DPA is caused by a lack of HMS PME activity, expressing HMS ectopically may increase the PME activity and decrease the DM in tissues other than the seed. I generated lines expressing the *HMS* gene under the control of the *UBIQUITIN1* (*UBQ1*) promoter. Of 14 transformed plants with the *pUBQ1:HMS*

construct, five lines expressed *HMS* in the leaves where *HMS* is not normally expressed (Figure 2.1; Figure 2.11B). Three lines, named U1, U2 and U3 respectively, were studied. Plants of these lines were smaller than WT and appeared highly infertile (Figure 2.11A, unpublished results). The PME activity in crude proteins extracts isolated from *U1, U2,* and *U3* leaves were increased relative to WT (Figure 2.11C). The PME activity in *hms1-1* leaves appeared the same as in WT most likely due to the low level of HMS in this tissue in both WT and *hms1-1*. This hypothesis is also supported by the lack of YFP tagged HMS signal seen in the leaves of transformants carrying pro_{HMS}*:PP::YFP::HMS* (data not shown). The DM in U1, U2, and U3 leaf extracts is decreased compared to WT (Figure 2.11D), while the DM of *hms-1* leaf extracts was similar to WT (Figure 2.11D). Because plants transformed with *pUBQ1:HMS* have a general decrease in plant size, I verified the cell size in leaves. The perimeter of leaves cells was significantly smaller in all plants tested as compared with WT (Figure 2.11E). This finding strongly suggests that HMS activity impacts cell elongation.

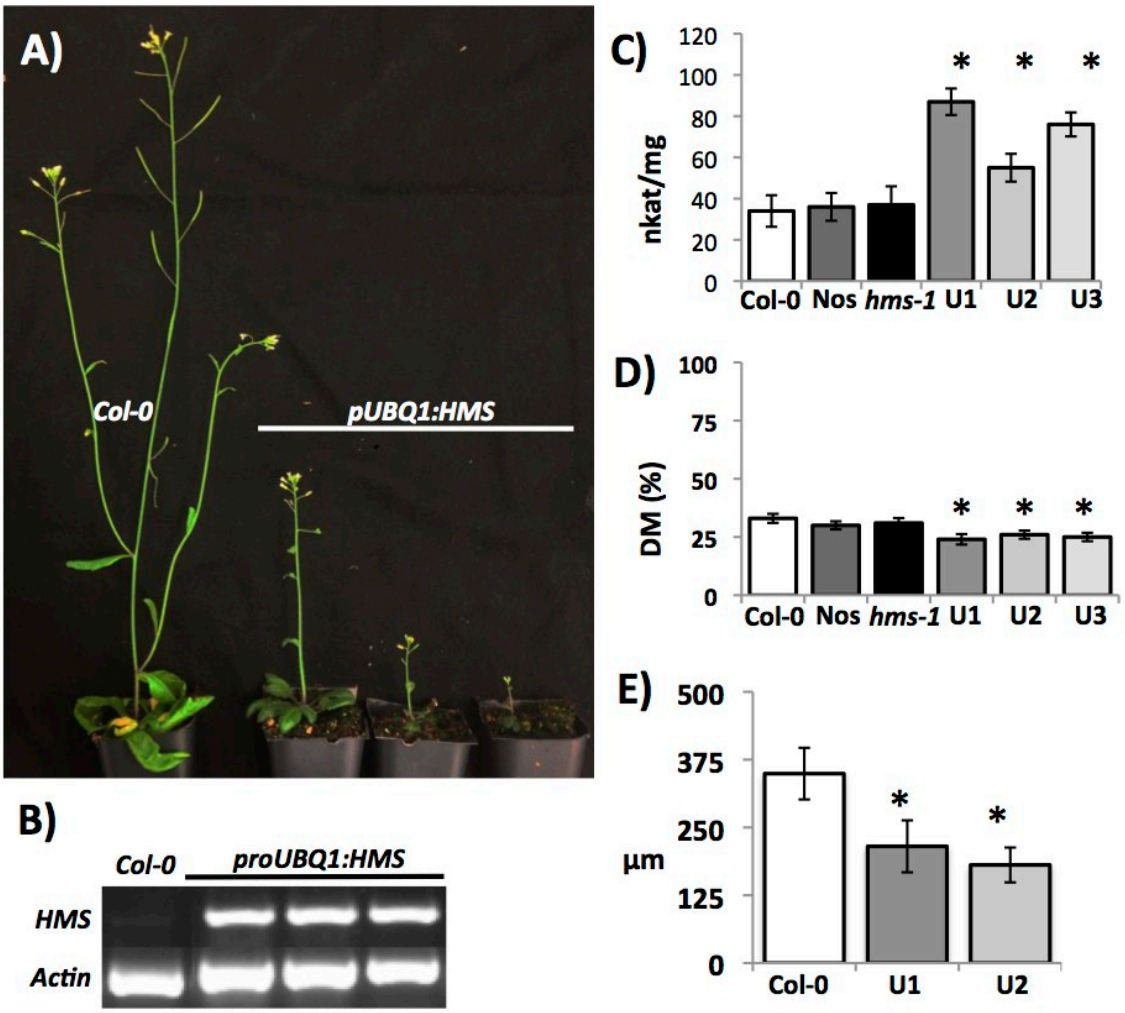

Figure 2.11: Plants transformed with *pUBQ1:HMS* physiological and biochemical phenotype.

(A) 26 day old WT and three plants transformed with *pUBQ1:HMS*, U1, U2 and U3. (B) *HMS* transcript accumulation in WT and *pUBQ1:HMS* transformed plants. RNA was extracted from leaves and mRNA was detected by RT-PCR. Actin mRNA was used as an internal control. (C) PME activity in Nkat/mg of crude protein extracts from leaves comparing WT col-0 and Nossen, *hms-1*, *U-1, U-2 and U-3.* Values represent the mean ± SE of 4 replicates. (D) Biochemical determination of DM comparing WT col-0 and Nossen, *hms-1*, *U-1, U-2 and U-3.* Values represent the mean ± SE of 4 replicates. (E) Average leaf epidermal cell perimeters comparing Col-0 WT with *U-1, U-2 and U-3*. Values represent the mean ± SE of 30 replicates. For (C) to (E) Asterisks indicate significant difference using a Students t-test with a Bonferroni correction ($P < 0.05$).

2.3.11 The 7 DPA *hms-1* embryos have increased labelling by HG specific antibodies

PME activity and DM of *hms-1* and *pUBQ1:HMS* leaves suggest that HMS is an active PME. Localizing pectin demethyl esterification in cross sections of seed can give additional information on the differences in DM between *hms1-1* embryo and WT. To examine the DM of HG pectin in seeds, I treated thin sections of developing seeds with JIM7 and JIM5 antibodies, where the epitope for JIM7 is HG with a high DM while that for JIM5 is HG with low DM (Willat et al., 2000, 2001). For the seed coat, no differences in the binding of either antibody were observed between *hms-1* and WT (Figure 2.12; Figure 2.13; Figure 2.14). A similar result was found for JIM5 and JIM7 signal in the embryo at 4 DPA (Figure 2.13). However, by 7 DPA, JIM7 signal in the *hms-1* embryo appeared higher compared to WT (Figure 2.13CD). JIM7 binding is distributed through both the radical and cotyledon while in the WT it is restricted to the cotyledon (Figure 2.13CD). In contrast, JIM5 appears slightly lower in 7 DPA *hms-1* compared to WT seed sections (Figure 2.13EF). In 10 DPA *hms-1* and WT sections the JIM7 binding is similarly distributed in the cotyledon and radical (Figure 2.14CD). JIM5 signal appears slightly lower in the *hms1-1* embryo as compared to WT (Figure 2.14EF). Taken together, the differences observed in the labelling of embryo by JIM5 and JIM7 is consistent with an increase in the DM specific to the *hms-1* 7 DPA embryos.

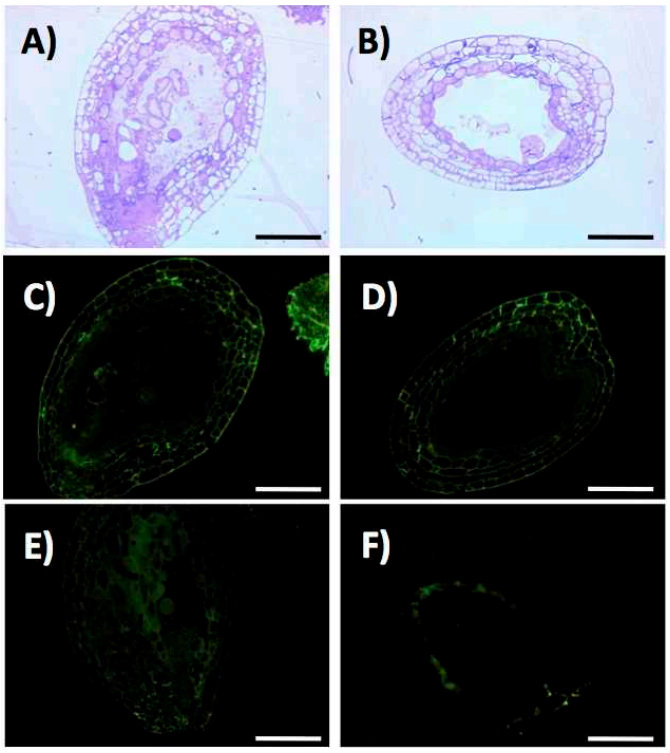

Figure 2.12: The binding of JIM5 and JIM7 antibody to 4 DPA seed sections.
(A) to (B) Sections stained with Toluene Blue. (C) to (D) Sections immuno-labeled with the antibody JIM7. (E) to (F) Sections immuno-labeled with the antibody JIM5. WT in (A), (C), (E) and *hms-1* in (B), (D), (F). Bar = 100 μm

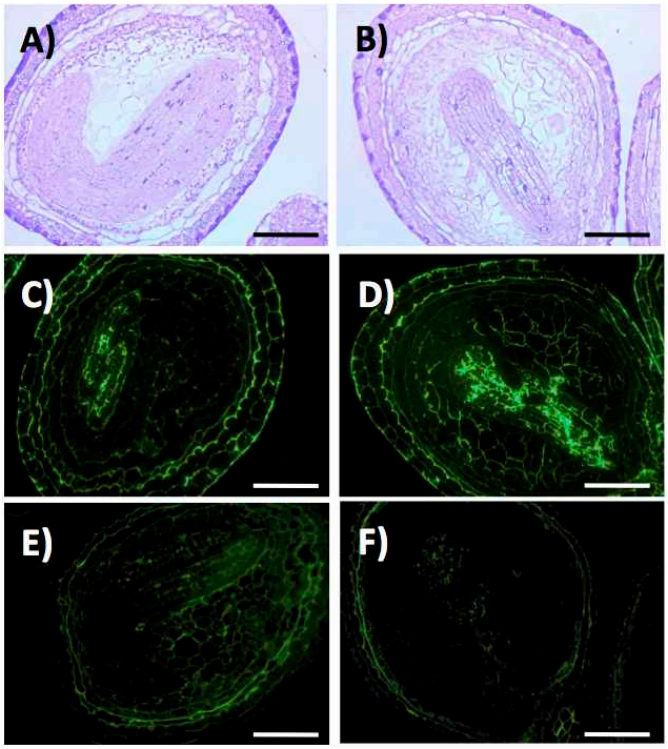

Figure 2.13: The binding of JIM5 and JIM7 antibody to 7 DPA seed sections.
(A) to (B) Sections stained with Toluene Blue. (C) to (D) Sections immuno-labeled with the antibody JIM7. (E) to (F) Sections immuno-labeled with the antibody JIM5. WT in (A), (C), (E) and *hms-1* in (B), (D), (F). Bar = 100 μm

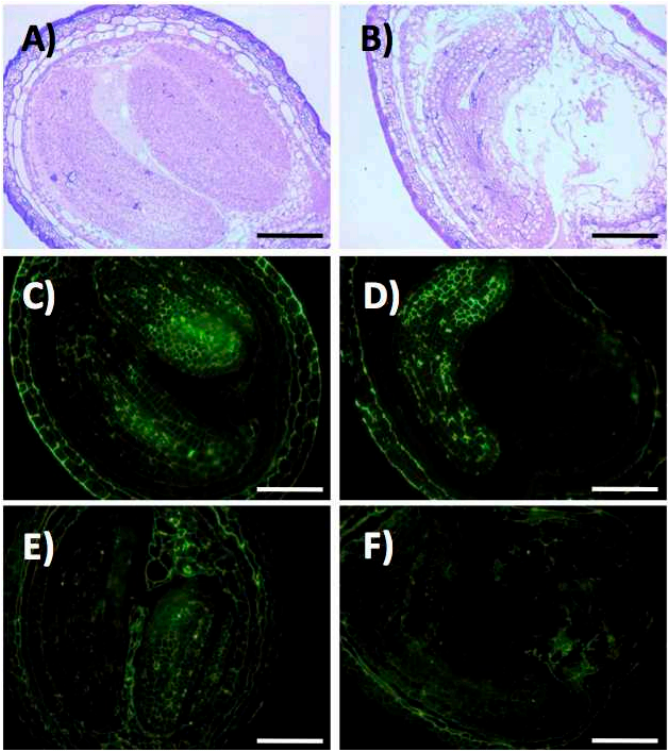

Figure 2.14: The binding of JIM5 and JIM7 antibody to 10 DPA seed sections.
(A) to (B) Sections stained with Toluene Blue. (C) to (D) Sections immuno-labeled with the antibody JIM7. (E) to (F) Sections immuno-labeled with the antibody JIM5. WT in (A), (C), (E) and *hms-1* in (B), (D), (F). Bar = 100 μm

2.3.12 Additional PME(s) may acts prior to HMS in the embryo cell wall

Ectopic expression of PMEI5 driven by the 35S promoter has been shown to produce larger seeds with a bigger embryo and faster germination rate (**Müller** and *al*., 2013). In order to verify if PMEI is impacting HMS, I crossed a PMEI5 OE line with the *hms-1* mutant to generate an *hms-1*/PMEI5 OE line. The resultant *hms-1*/PMEI5 OE had seeds that look similar to PMEI5 OE with a bigger embryo and the same DM (Figure 2.16). This suggests that PMEI5 does not act through HMS and therefore must act through one or more additional PMEs.

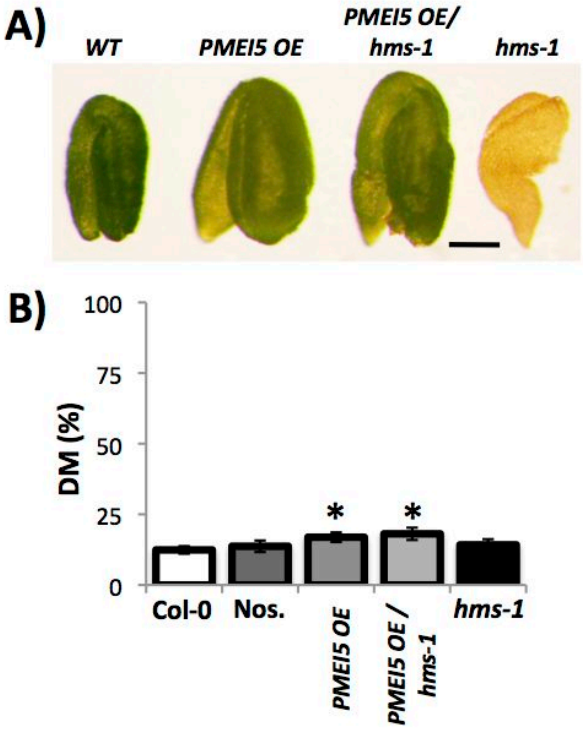

Figure 2.15: PMEI5 OE suppresses the *hms-1* mutant phenotype.
(A) Dissected mature embryos of the genotypes WT, PMEI5 OE, PMEI5 OE/*hms-1,* and *hms-1*. Bar = 100 μm (B) Biochemical determination of the % methyl-esters of galacturonic acid in mature seed comparing WT, *hms-1*, PMEI5 OE, resultant cross between PMEI5 OE and *hms-1*. Values represent the mean ± SE of 4 replicates. Asterisks indicate significant difference using a Students t-test with a Bonferroni correction ($P < 0.05$).

2.3.13 HMS causes the softening of plant tissues

PME may strengthen or loosen the cell wall depending on the pattern of demethyl esterification. In an effort to assess the consequence of the lack of PME activity in *hms-1* on the rigidity of the tissue, we first performed Atom force Microscopy (AFM). The embryo morphology and tissues characteristics were not appropriate for this AFM technique (Appendix D). As an alternative, I performed a Dynamic Mechanical Analysis (DMA) and calculated the percentage seed deformation. The resultant average of seed percentage deformation is reduced in the *hms-1* mutant in comparison to WT and the

hms-1 plants transformed with *pHMS:HMS* (Figure 2.17). This result is consistent with the hypothesis that normal HMS activity promotes a loosening of seed tissue wall and that in its absence (*hms-1*) the tissues are more rigid and resistant to deformation.

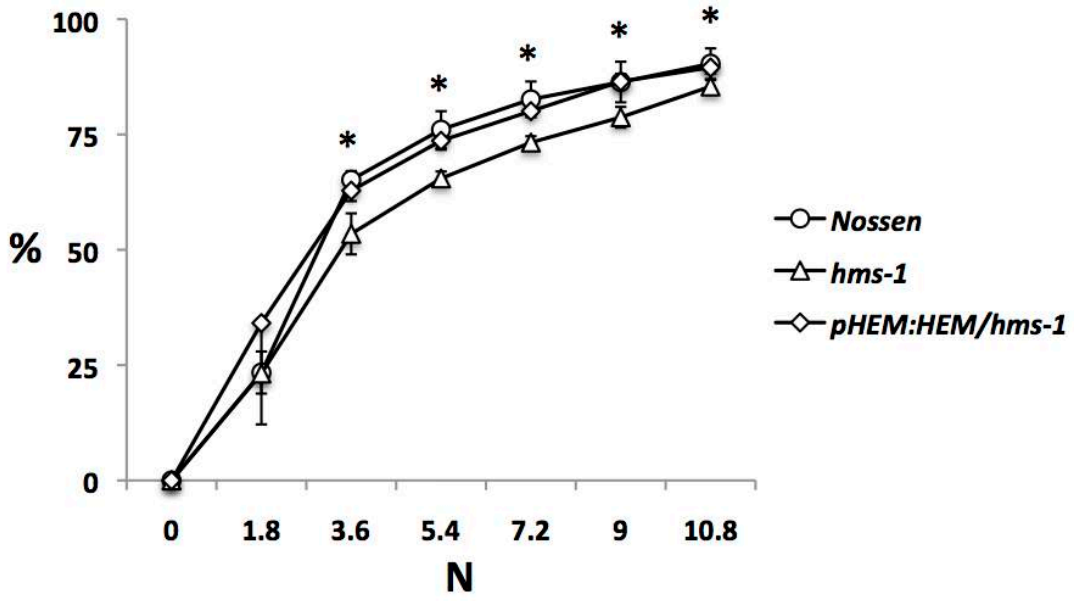

Figure 2.16: Seed deformation induced by increasing amounts of force.
Average deformation in % of the total seed length comparing WT, *hms-1* and *hms-1* transformed with *pHMS:HMS* construct. Values represent the mean ± SE of 10 replicates. Asterisks indicate significant difference using a Students t-test with a Bonferroni correction ($P < 0.05$).

2.4 Discussion

2.4.1 HMS encodes a PME

The annotation for predicted PME genes in *A. thaliana* was assigned by sequence homology (The Arabidopsis Genome initiative, 2000). My research has generated several lines of evidence that support this annotation. First, there is a strong correlation between HMS function and PME activity in 7 DPA seed extracts. The loss of HMS function (in *hms-1*) resulted in a decrease in PME activity (Fig. 2. 10). Further, an increase in HMS

expression (*pUBQ1:HMS*) caused an increase in PME activity (Fig. 2.11). These results demonstrate that HMS is needed for WT PME activity in seeds. Second, HMS activity is correlated with the level of detectable DM in the seed as observed by direct measurement (Figs. 2.10, 2.11) and the binding of HG specific antibodies that are sensitive to the DM (Figs. 2.12, 2.13, 2.14). Finally, as expected for a PME, my data support the idea that HMS is localized in the apoplast (Fig. 2.9). These results support the hypothesis that HMS is an active PME.

2.4.2 HMS plays an important role in embryo growth

HMS plays a profound role in embryo morphogenesis. After 4 DPA, *hms-1* embryos developed more slowly than WT, reaching at most, the bent cotyledon stage (Figs. 2.2, 2.3 2.7). The dry mature seed is wrinkled and weighs considerable less than WT. These changes in morphogenesis could be due to poor growth. Indeed, cells in the embryo were generally smaller in size and failed to accumulate the normal amount of storage compound (Figs. 2.7, 2.8). Taken together, these results suggest that HMS functions to promote normal cell growth. One important function of PMEs is to promote or inhibit cell wall expansion and elongation by loosening or stiffening the cell wall (Liu et al., 2013; Pilling et al., 2004; Al-Qsous et al., 2004; Moustacas et al., 1991). Since *HMS* encodes a PME, I conclude that HMS removes methyl groups in a non-blockwise manner allowing for cell wall loosening at the stage when cell expansion is needed to complete morphogenesis and make room for storage compound deposition (Figure 2.17, see below). In support of this hypothesis, PME induced changes in DM are known to impact the mechanical properties of cell wall (Peaucelle et al., 2011) and here I demonstrated that *hms-1* seeds exhibit a lower seed percentage deformation, which suggests a higher rigidity. The change in seed rigidity observed in this study may be the consequence of the stronger cell walls.

Examples of *A. thaliana* PME mutants causing developmental defects (Jiang et al., 2005; Francis et al., 2006; Rockel et al., 2008; Tian et al., 2006; Guenin et al., 2011; Hongo et al., 2012) are rare. Furthermore, few PMEs have been shown to loosen the cell

wall in *A. thaliana* and physiological evidence for the involvement of PME in cell wall expansion is scarce (Peaucelle et al., 2011; Moustacas et al., 1991; Al-Qsous et al, 2004). The identification of *hms-1* with a seed embryo phenotype represents a novel function for PMEs in development. My hypothesis for HMS function, outlined above, predicts that an increase in HMS activity in the embryo (eg. *pUBQ1:HMS*) should increase the loosening of the cell wall producing a general increase in cell sizes. However, the ectopic expression of *HMS* in the plants transformed with *pUBQ1:HMS* resulted in smaller plants with smaller cells (Figure 2.11).

2.4.3 The role of HMS in the seed coat is unclear

The initial goal of my thesis research was to identify and characterize *PME* genes involved in seed mucilage modification in order to determine the effect of HG methylation on seed mucilage properties. Genes annotated as encoding PMEs expressed in the seed coat were identified and insertion mutants for each gene were screened for mucilage phenotypes. *At1g23200* (*HMS*) was selected on the basis of its high seed coat expression at 7 DPA and the mucilage extrusion defects of the *hms-1* mutant. However, I have shown that the mucilage extrusion defects are a secondary effect of the loss of HMS function in the embryo. The *hms-1* seed coats alone have no obvious defects in differentiation or mucilage extrusion (Figs. 2.4 and 2.6) or the degree of HG methylation (Figs. 2.12, 2.13, 2.14). The strong expression of *HMS* in the seed coat suggests that HMS has a role in that tissue, but if so either the role is subtle, my phenotypic assays have not been the correct ones or the role is masked by redundancy. Because there are at least 7 genes expressed in the seed coat it is possible that one or more are redundant with HMS.

2.4.4 PMEs present in the seed, other than HMS, act to limit the growth of the embryo

OE PMEI5 plants have bigger seeds with bigger embryos (Chap III: **Müller** et al., 2013), a phenotype contrasting that of *hms-1*. This suggests that PMEI5 inhibits PMEs

that strengthen the cell wall rather than loosening it as hypothesized for HMS. The fact that *OE PMEI5* is able to suppress the *hms-1* phenotype (Figure 2.15) indicates that HMS activity is only necessary if other PMEs have acted previously to strengthen the cell walls in the embryo. Thus, cell wall strength in the embryo must be balanced through space and time, at least in part, through the use of different PME activities with opposing roles (Fig. 2.17).

2.4.5 A model for cell wall loosening during embryogenesis

The evidence accumulated in this chapter support that PMEs (including HMS) are active in the seed with different modes of action: blockwise and non blockwise. I demonstrated this by showing that (1) the absence of HMS results in seed with defects in embryo cell expansion and a higher mechanical strength supporting a role for HMS in non-blockwise activity and, (2) the inhibition of unknown PME(s) by *OE PMEI5* results in bigger seeds (Chapter III; **Müller** et al., 2013) supporting a blockwise activity and (3) PMEI OE acts independently of HMS. A model integrating all of this information is represented in Figure 2.17.

In this model, early in development unknown PME(s) act blockwise causing the strengthening of the cell wall needed to limit cell expansion. Later in development, around 7 DPA, HMS acts in a non-blockwise fashion causing embryo cell wall loosening to accommodate cell expansion. The loss of cell wall loosening in *hms-1* results in a stiffer cell wall and the loss of cell wall stiffening in OE PMEI5 results in a looser cell wall. When both PME activities (loosening and stiffening) are lost in *hms-1*/OE PMEI5, the highly methyl esterified wall is looser.

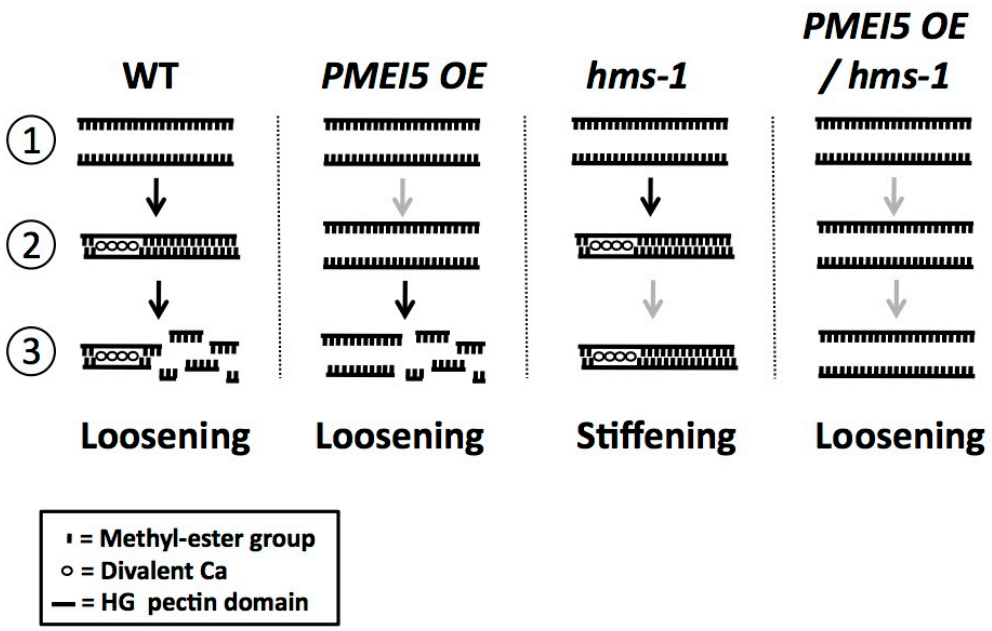

Figure 2.17: Model for PME-induced cell wall modification in *A. thaliana* embryo.

In WT under normal conditions the **1)** newly synthesize highly methyl esterified homogalacturonan (HG) pectin is **2)** demethyl esterified by PME(s) acting blockwise resulting in a tightening of the cell wall prior to **3)** the action of HMS PME acting individually on the HG pectin to loosen the cell wall and support embryo cell wall extension. In PMEI5 OE the highly methyl esterified pectin is not demethyl esterified blockwise and is made even looser after the action of HMS promoting embryo cell wall expansion. In the *hms-1* mutant, PMEs acting blockwise tighten the cell wall but the lack of subsequent cell wall loosening prevents cell expansion in the embryo. In PMEI5 OE / *hms-1,* the newly synthesize highly methyl esterified homogalacturonan is not demethyl esterified and remains loose, promoting embryo cell wall expansion.

Chapter 3: Demethyl esterification of pectins plays a role in seed germination

3.1 Introduction

A significant numbers of genes encoding pectin-modifying enzymes and associated regulators show significant differential regulation during the first 24 h of *A. thaliana* seed germination (Nakabayashi et al., 2005). The mechanical restraint imposed by the seed tissues surrounding the radicle is one potential factor that governs the completion of germination. According to the "mechanical restraint" hypothesis, the growth potential of the radicle must exceed the mechanical resistance of the surrounding living seed tissues (e.g. the endosperm, perisperm, or megagametophyte, depending on the seed type) to permit the completion of germination (Bewley, 1997a; Müller et al., 2006). Enzymes involved in cell wall loosening, including xyloglucanase endotransglycosylase, endo-β-mannanase and expansins were shown to be involved in tissue weakening and increasing the growth potential of the embryo (Wu et al., 1994; Chen et al., 2002; Chen and Bradford, 2000; Nonogaki et al., 2000; Sanchez and de Miguel, 1997; Downie et al., 1997).

PMEs and PMEIs are encoded by large gene families, with over 60 members in *A. thaliana* (Jolie et al, 2010). Very little is known about the role of PMEs in the germination of angiosperm seeds, although one study has characterized their role in dormancy breakage and germination of conifer seeds (Ren and Kermode, 2000). Co-expression of different PMEs in seed tissues suggests functional redundancy. Individual PMEIs interact with a number of different PMEs, often even across species boundaries (Giovane et al., 2004). In this chapter we attempted to verify if the degree of pectin methyl esterification affects germination by determining if (1) PME activity is differentially regulated during seed germination in *A. thaliana*, (2) the degree of pectin methyl esterification of the cell walls of seed tissues is correlated with the rate of germination, and (3) changing to the degree of pectin methyl esterification through overexpression (OE) of a *PMEI* would alter seed germination.

3.2 Materials and methods

3.2.1 PME activity assays

The *A. thaliana* tissue was ground in liquid nitrogen and 100µL extraction buffer (100 mM Tris-HCl, pH 7.5, 500 mM NaCl containing protease inhibitor cocktail composed of 100 mM phenylmethylsulfonyl fluoride, 2 mM bestatin, 0.3 mM pepstatin A, and 0.3 mM trans-Epoxysuccinyl-L-leucylamido(4-guanidino)butane E-64 [ABMGood; www.abmgood.com]) was added. Extracts were then mixed at 4°C for 30 min and centrifuged at 11,500g at 4°C for 20 min. Fresh supernatants were used immediately for all enzyme assays. A coupled enzymatic assay was performed as described by Grsic-Rausch and Rausch (2004) using a spectrophotometric plate reader (SpectraMax M2e; Molecular Devices; www.moleculardevices.com). A Student's t-test of the data sets was run in Graphpad Prism 6.0 (www.graphpad.com). Dr. Kerstin **Müller** and Gabriel Levesque-Tremblay performed the PME activity assays.

3.2.2 RNA extraction and cDNA synthesis

A. thaliana tissues were ground in liquid nitrogen, and total RNA was extracted as as per Chang et al. (1993) with the following modifications: after the addition of buffer (2% hexadecyl trimethylammonium bromide, 2% polyvinylpyrrolidone [molecular weight = 40,000], 100mM Tris-HCl, pH 8.0, 25mM EDTA, pH 8.0, 2M NaCl, and 2% b-mercaptoethanol), the extracts were kept at 65°C for 10 min. All chloroform-isoamylalcohol extractions were repeated once. RNA was treated with DNAse-I (Fermentas; www.thermoscientificbio.com/fermentas/) to remove remaining genomic DNA, and the quantity and purity of the RNA were determined with a Nanodrop spectrophotometer (ND-2000C; Thermo Scientific; www.thermoscientific.com). One microgram of RNA was reverse transcribed using the EasyScript Plus kit (ABMGood; www. abmgood.com) with a mixture of random hexamers and oligo(dT) primers. cDNA from four biological replicate RNA samples was used for quantitative reverse transcription (qRT)-PCR. Dr. Kerstin **Müller** performed the RNA extraction and cDNA

synthesis.

3.2.3 qRT-PCR

qRT-PCR was run in 15μL reactions on an ABI7900HT machine (Applied Biosystems; www.appliedbiosystems.com) using PerfeCTa Sybr Green Supermix with ROX (Quanta Biosciences; www.quantabio.com). Primers were designed with the primer3 (Rozen and Skaletsky, 2000) tool in Geneious 4.8.5 and based on sequence AY327264 from the NCBI (forward primer 59-TTGCGATAACGCAGTCAAAAATG-39 and reverse primer 59 GAAGTCCAAGTTCCCAAGCTG- 39). Actin7 (ACT7) and Elongation Factor1α (EF1α) were used as reference genes. The reaction mixture consisted of 150 ng of cDNA (RNA equivalent), 7.5 mL of Supermix, and 140 nM of each primer. The mix was subjected to a temperature regime of 3 min at 95°C and 40 cycles of 15 s at 95°C and 1 min at 60°C. A dissociation curve was run after each quantitative PCR to validate that only one product had been amplified in each well. The efficiency (E) of the primer pairs was calculated as the average of the efficiencies of the individual reactions by using raw fluorescence data with the publicly available PCR Miner tool (http://www.miner.ewindup.info/ version2; Zhao and Fernald, 2005). The efficiency was then used to calculate transcript abundance for the individual samples as (1 + E) ^ (2CT) as described by Graeber et al. (2011). No-template controls were included for each primer pair to check for contamination of the reaction solutions, and no-reverse transcription controls were used to check for genomic DNA contamination in the RNA. Dr. Kerstin **Müller** performed the (qRT)-PCR experiments.

3.2.4 Generation of transgenic *A. thaliana* lines

The open reading frame of *At2g31430* was amplified from genomic *A. thaliana* DNA using 31430_fw primer (59 GGGGACAAGTTTGTACAAAAAAGCAGGCTTGatggccacaatgctaataaaccac- 39) and 31430_rv primer (59 GGGGACCACTTTGTACAAGAAAGCTGGGTCttaggtcacaagcttgttgaaaataag- 39),

including Gateway (Invitrogen; www.invitrogen.com) attB1 and attB2 sites, respectively. The PCR product was then inserted into the pDONR207 donor plasmid, sequenced, and recombined with the binary destination vector pB2GW7 (Karimi et al., 2002). *A. thaliana* plants were transformed by the floral dip method (Clough and Bent, 1998). The transgenic progeny were selected by spraying BASTA (120 mg L21) on seedlings grown in soil. Experiments were conducted on the T1 and T2 generations, as later generations were characterized by gene silencing that generally led to loss of phenotypes over about four to five generations. A total of five selections were performed on T1 seedlings at different times, yielding 10 to 25 independent transgenic lines per selection, all of which displayed the described phenotypes. Dr. Sebastian Bartels generated the transgenic *A. thaliana* lines.

3.2.5 Germination testing

A. thaliana plants (WT ecotype Col-0 and lines overexpressing the *PMEI5* gene [At2g31430]) were grown in soil in pots maintained in a growth chamber at 22°C with a 16 h photoperiod (long days). Mature dry seeds were either used immediately for germination testing ("fresh seeds") or were monitored for their germination after first undergoing after-ripening at room temperature for 3 months. For germination tests, seeds were surface sterilized 2 min with 70% ethanol, washed with 100% ethanol, and air-dried. Three sets of 50 seeds were sown on one-half strength Murashige and Skoog medium (pH 6.5) solidified with 1% agar. Germination was scored with a Zeiss dissection microscope. Seeds in which the endosperm was visible through a crack in the testa were considered to have reached testa rupture; seeds in which the radicle tip had emerged through the endosperm were considered to have reached endosperm rupture. The effects of ABA on germination were also determined. For these studies, (6)-ABA (Sigma; www.sigmaaldrich.com) at various concentrations was added to the germination medium. Dr. Kerstin **Müller** performed the germination assays.

3.2.6 Immunofluorescence studies and histological examination

Seeds at 35 h after imbibition were prepared for high-pressure freezing, freeze substitution, resin embedding, and sectioning as per Rensing et al. (2002). Two percent (w/v) osmium tetroxide and 8% (v/v) dimethoxypropane in acetone were used for general histological examination of sections, and 0.25% (v/v) glutaraldehyde and 2% (w/v) uranyl acetate in 8% (v/v) dimethoxypropane in acetone were used for immunolabelling. The samples were embedded in Spurr's resin (Spurr, 1969), and sections (0.5 mm) were stained with toluidine blue for general examination. For immunolabelling, the samples were embedded in LR White (London Resin; www.2spi.com), and sections were incubated in a blocking solution (1% bovine serum albumin [Sigma] in 20 mM Tris, 500 mM NaCl, and 0.2% Tween 20). After rinsing in buffer (20 mM Tris, 500 mM NaCl, and 0.2% Tween 20), the sections were incubated in the primary antibodies JIM7, JIM5, and 2F4 (Knox et al., 1990; 1:10 dilutions; Plant Probes; www.plantprobes.net). Following incubation in the secondary antibody (Alexa Fluor 488 goat anti-rat IgG [Invitrogen A11006], used at a dilution of 1:100 for JIM5 and JIM7; Alexa Fluor 488 goat anti-mouse IgG [Invitrogen A11001], used at a dilution of 1:100 for 2F4; www.invitrogen.com), the sections were examined via epifluorescence using a DMR light microscope (Leica Microsystems; www.leica.com). Gabriel Levesque-Tremblay performed the immunofluorescence studies and histological examination.

3.2.7 Quantification of methyl esters in seed cell walls

Seeds (100–120) of *PMEI* OE and WT plants were imbibed for 2 h at 22°C in petri dishes containing filter paper and water. The seeds were then ground in liquid nitrogen, and 200 mL of methanol was added. The ground seed materials were extracted four times with a 1:1 (v/v) methanol:chloroform mixture, the extracted residue was washed once with acetone, and dried overnight at room temperature. The weight of the dried cell wall materials was determined, and 0.5 to 1.0 mg was washed with 2 mL water. To release the methyl esters, the cell wall materials were incubated for 1 h at room temperature with 100 mL of 0.5M NaOH. After neutralization with 50 mL of 1M HCl,

the samples were centrifuged at 2,000g for 10 min. Fifty microliters of the supernatant was used to quantify the methanol released during saponification (Klavons and Bennett, 1986). In brief, the released methanol was oxidized for 15 min at room temperature on a shaker using 0.03 units of alcohol oxidase (Sigma-Aldrich; www. sigmaaldrich.com) in 50 mL 20mM phosphate buffer, pH 7.5. The resultant extract was then developed for 15 min at 60°C in 20mM acetyl acetone, 50mM acetic acid, and 2M ammonium acetate. Absorbance was measured at 412 nm using a Spectramax M2e microplate reader (Molecular Devices; www. moleculardevices.com) and compared with a standard curve generated with a methanol dilution series. A Student's t test of the data sets was evaluated in Graphpad Prism 6.0 (www.graphpad.com). Environmental SEM (eSEM) images were taken with a Quanta 250 FEG environmental scanning microscope (FEI; www.fei.com). An accelerating voltage of 10 kV was used for all images; the stage was cooled to approximately 3°C for all samples, and a disk of wetted filter paper was used to keep the samples hydrated. The relative humidity was maintained at 80% to 100% during imaging. Dr. Kerstin **Müller** performed the Quantification of methyl esters in seed cell walls and Dr. Alexandra Wormit performed the eSEM.

3.2.8 Cell wall composition analysis

Water-soluble mucilage was extracted from 6 to 8 mg of seeds by shaking in 1 mL of distilled water for 2 h at 37°C. The remaining pellets were ground in a ball mill (Retsch; www.retsch.de) to a fine powder, and seed cell wall material was prepared by washing with 1 mL of 70% (v/v) ethanol, three times with 1 mL of chloroform:methanol (1:1), and twice with acetone before drying. Starch was removed from the pellet by incubation with alpha-amylase and amyloglucosidase overnight before hydrolysis to monosaccharides. Hydrolysis was performed by incubation with 2 M trifluoracetic acid for 1 h at 121°C. The content of uronic acids was determined by the m-hydroxybiphenyl colorimetric uronic acid assay (Blumenkrantz and Asboe-Hansen, 1973). The content of cell wall monosaccharides was determined by gas chromatography-mass spectrometry analysis of the respective alditol acetates, as described previously (Foster et al., 2010). Dr. Karin Weitbrecht performed the cell wall composition analysis.

3.2.9 Seed mucilage and morphology examination

Seeds were slowly shaken in water for 45 min, so that the mucilage could fully develop. Seeds were then washed once with water, and stained with 0.05 % (w/v) ruthenium red for 30 min. The staining solution contained either water, 50 mM EDTA, or 50 mM $CaCl_2$, as indicated. Following a second wash, the seeds were photographed with a AxioPlan 2 microscope. For **SEM,** dried *A. thaliana* seeds were mounted on stubs and coated with gold-palladium alloy using the Hummer VI sputtering system (Anatech). The prepared samples were observed with a Hitachi S-800 scanning electron microscope and images were captured with Evex Nano Analysis digital imaging system. Gabriel Levesque-Tremblay performed the Ruthenium red staining for seeds mucilage examination and the SEM for morphology examination.

3.3 Results

3.3.1 PME activities change during different phases of *A. thaliana* seed germination

Dr. Kerstin **Müller** sought to determine the temporal pattern of PME activity during the different stages of germination of WT *A. thaliana* seeds (Figure 3.1). PME activities increased before and shortly after seed coat (testa) rupture and decreased once endosperm rupture commenced and phase III set in.

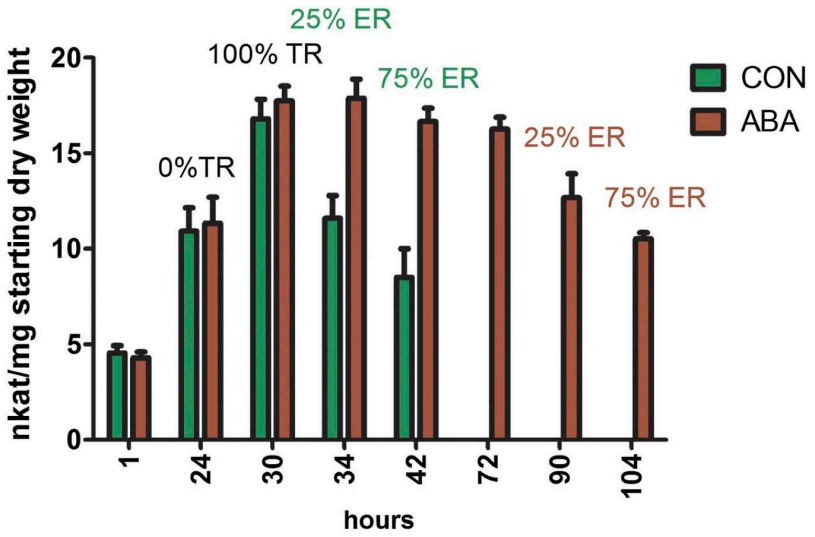

Figure 3.1: PME activities during germination of *A. thaliana* WT seeds in the absence and presence of 1 mM ABA.

Control (CON) green bars and ABA brown bars). Data represent averages 6 SE of four biological replicates of about 100 seeds each. Seeds were weighed before imbibition, and the activity shown is relative to the starting seed weight. The percentages over the bars list the proportions of seeds that had achieved testa rupture (TR) and endosperm rupture (ER). Note that both control seeds and ABA-treated seeds have reached 100% testa rupture at 32 h. Control seeds proceed to endosperm rupture, while ABA-treated seeds remain at the testa rupture stage for several days. Values represent the mean ± SE of 4 replicates. This figure was made by Dr. Kerstin **Müller** and was reprinted with the permission of the ASPB.

In order to determine whether the increase in PME activities over the first 24 to 30 h of imbibition is connected to the event of testa rupture or is associated with the plateau in water uptake associated with phase II of germination, the effects of ABA were determined by Dr. Kerstin **Müller**, as this hormone specifically prolongs phase II of germination by delaying endosperm rupture without affecting the timing of testa rupture (Müller et al., 2006; Weitbrecht et al., 2011). ABA significantly extended the period associated with higher PME activities in the seeds (e.g. in the period between 30 and 72 h; Figure 1). The patterns mimicked those found in untreated seeds in that the activities declined once endosperm rupture was reached. Thus, we conclude that high PME activity

is a feature of phase II of *A. thaliana* seed germination both in the presence and in the absence of exogenous ABA, and might be linked to the ABA-mediated delay in endosperm rupture and prolonged plateau phase of water uptake.

3.3.2 *PMEI5* is a novel PMEI expressed in seeds, buds, and mature flowers

Dr. Kerstin **Müller** chose a transgenic OE approach to determine whether changes in PME activities, and thus the degree of cell wall pectin methyl esterification, would affect seed germination. Dr. Sebastian Bartels generated *A. thaliana* lines overexpressing *At2g31430*, a gene encoding a PMEI that was denoted *PMEI5* (the fifth *PMEI* with a confirmed function in *A. thaliana*; Wolf et al., 2012). PMEI5 is predicted to encode a protein of 179 amino acids with a PMEI domain (pfam PF04043) spanning almost the entire protein. Two complementary DNA (cDNA) sequences are available at the National Center for Biotechnology Information (NCBI; AY327264 and AY327265). The latter shows retention of the one intron; translation of the transcripts would lead to a truncated protein due to a premature stop codon.

Before embarking on our *PMEI5* OE work, Dr. Kerstin **Müller** examined expression of the *PMEI5* gene during different stages of the *A. thaliana* life cycle based on the NCBI sequence AY327264 that yields the full-length protein. Transcripts encoding the full-length *PMEI5* were barely detectable in seedlings, rosette leaves, roots of 20-d-old seedlings, and immature siliques (Figure 3.2). Mature dry seeds and 24-h imbibed seeds showed moderate *PMEI5* expression; the highest expression occurred in flower buds, particularly in mature flowers.

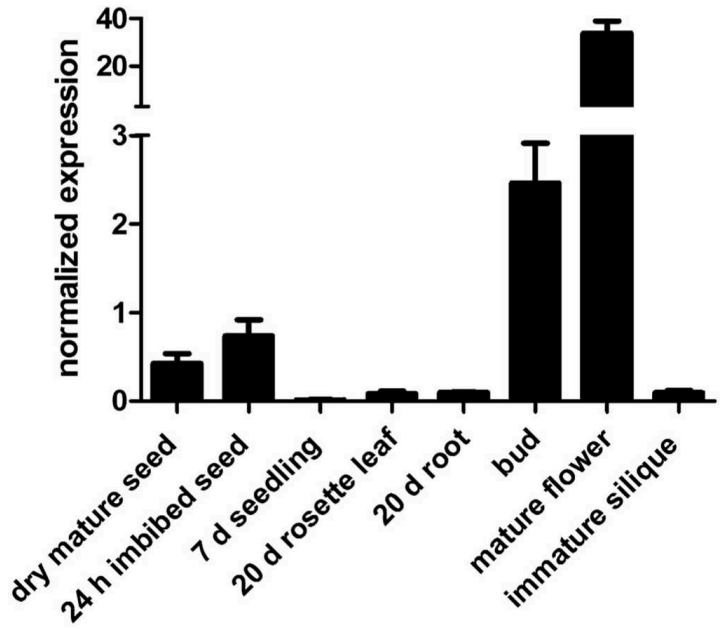

Figure 3.2: Transcript abundance of *PMEI5* in different organs and at different life cycle stages of *A. thaliana* as determined by qRT-PCR.
Transcript levels were normalized to the mean of two reference genes, EF1α and ACT7. Values represent the mean ± SE of 6 replicates. This figure was made by Dr. Kerstin **Müller** and was reprinted with the permission of the ASPB.

3.3.3 OE of *PMEI5* reduces PME activities of seeds and leads to an increased degree of cell wall pectin methyl esterification

Dr Sebastian Bartels overexpressed the *PMEI5* gene by placing its full-length coding sequence under the control of a cauliflower mosaic virus 35S promoter. Several independent transgenic lines were obtained (see "Materials and Methods"), and five lines were examined for their *PMEI5* transcript levels and for PME activity. *PMEI5* transcripts in the OE lines were 10- to 50-fold higher in leaves (Figure 3.3A) than in the WT untransformed controls. PME activities were significantly reduced in seeds ($P < 0.005$) and seedlings ($P < 0.02$), as well as in vegetative tissues of adult plants (e.g. in leaves and stems; $P < 0.02$; Figure 3.3B). An *in situ* effect of the PMEI was confirmed by the incubation of protein extracts derived from the WT plants with extracts from *PMEI* OE plants. This resulted in an average reduction in PME activity of 30.3% ± 5.1%. After

undergoing extensive methyl esterification in the Golgi complex, HGs are secreted into the cell wall and subsequently demethyl esterified by PMEs (Zhang and Staehelin, 1992; Sterling et al., 2006). Inhibition of PME activity through OE of the *PMEI*, therefore, was expected to lead to a marked increase in the degree of pectin methyl esterification in both the vegetative tissues of the plants and in seeds.

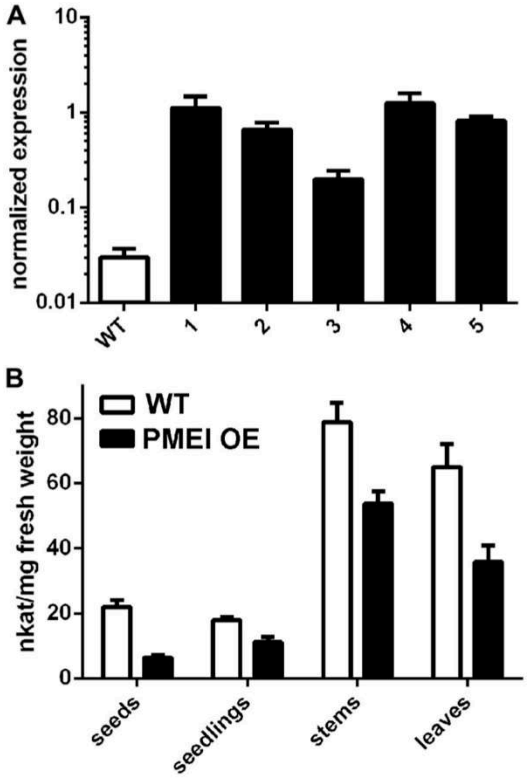

Figure 3.3: Effect of *PMEI5* OE on *PMEI5* transcript levels and PME activity.
(A) Transcript abundance of *PMEI5* in the leaves of WT plants and in the leaves of five independent *PMEI* OE lines (1–5) as determined by qRT-PCR. Transcript levels were normalized to the mean of two reference genes, *EF1*α and *ACT7*. (B) PME activities in different tissues of adult *A. thaliana* plants and in seeds and seedlings. The leaves and stems were of plants harvested 24 d after sowing. The seeds were sampled after 16 h of imbibition (i.e. during phase II of germination), and seedlings were 5 d post germination. WT or non-transgenic controls. The data in B are based on average PME activities determined from five WT lines and five *PMEI5* OE lines that represented independent insertions 6 ± SE. This figure was made by Dr. Kerstin **Müller** and was reprinted with the permission of the ASPB.

To examine if the effect of the overexpression on cell walls modification was specific to the process of pectin demethyl esterification, water-soluble and trifluoracetic acid fractions of seed cell walls were examined by Dr. Alexandra Wormit and Dr. Bjoern Usadel. Indeed, an analysis of *PMEI* OE seed cell walls after the non-adherent mucilage was removed showed no statistically significant difference in their neutral sugar and uronic acid composition from that of WT seeds (Figure 3.4A). However, Dr. Kerstin **Müller** quantified a higher methanol content in the cell wall fraction of seed from *PMEI* OE as compared with WT (Figure 3.4B), which is indicative of a greater predominance of cell wall methyl esters associated with *PMEI5* OE. The calculation for the determination of methanol in this experiment may be influenced by the subtle increase in the average of uronic acid. Nevertheless, the PMEI OE mature seeds have higher methanol content using another protocol (Figure 2.15B).

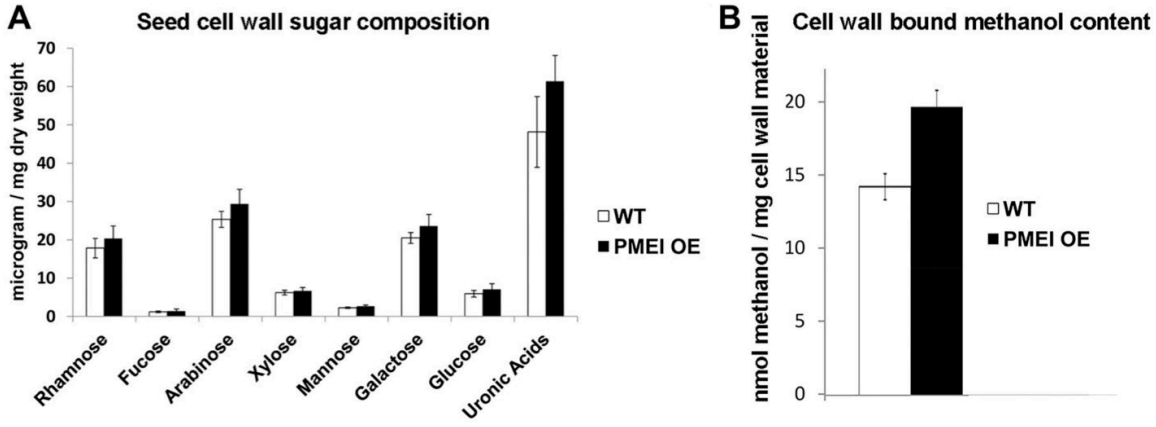

Figure 3.4: Cell wall sugars and degree of methyl esterification.
(A) Sugar composition of cell walls of WT and *PMEI* OE seeds (2 h after imbibition). The data are based on averages of five replicates ± SE. (B) Estimated methyl ester content as based on methanol associated with saponified cell wall materials. The data are based on averages of three replicates ± SE. This figure was made by Dr. Kerstin **Müller**, Dr. Alexandra Wormit, Dr. Bjoern Usadel and reprinted with the permission of the ASPB.

To investigate the DM of cell wall pectins, I analyzed WT and *PMEI* OE seeds at phase II of germination by immunofluorescence, in which they were challenged with

different antibodies specific for HGs of differing degrees and patterns of methyl esterification. These included a JIM7 antibody, which is believed to binds exclusively to highly methyl esterified HGs possessing dense stretches of methyl esters, and JIM5, which recognizes pectins with lower degrees of methyl esterification and more sporadic methyl esters. In addition the 2F4 antibody was employed, which recognizes homogalacturonan stretches that are largely demethyl esterified and cross-linked by calcium bridges (Willats et al., 2000). As expected from the reduced PME activity of the *PMEI* OE lines, the most dramatic differences were observed with the JIM7 antibody, whose signal was much greater in the cell walls of *PMEI5* OE seeds as compared with to WT seeds (Figure 5AB). This was pronounced in all parts of the embryo and to a slightly lesser extent in the endosperm; no differences were evident in the testa. While the signal was generally quite weak, the presence of JIM5 epitopes was more evident in the *PMEI5* OE embryos (but less abundant in the testa) as compared with that of WT seeds (Figure 5CD). The 2F4 antibody bound most tenaciously to the endosperm cells in all samples (Figure 5EF) and revealed some localized differences in binding in the OE versus WT seeds. Thus, the inhibition of PME activity by OE of *PMEI5* appears to have resulted in a more dense methyl esterification of cell wall HG in the embryo and endosperm.

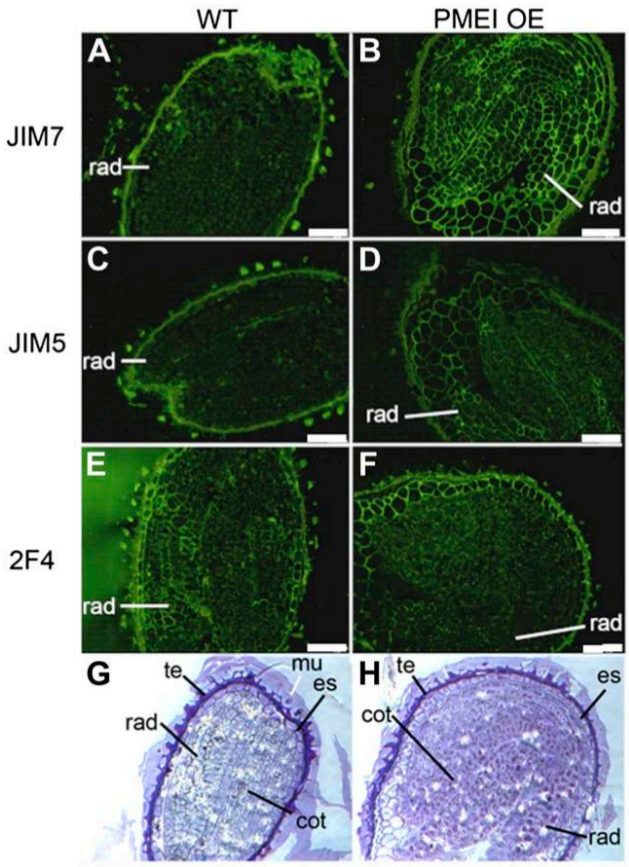

Figure 3.5: Effects of *PMEI5* OE on cell size and the degree of pectin methyl esterification of the embryo, endosperm, and testa.

(A) to (F) Immunolabeling of representative sections derived from *PMEI* OE and WT seeds with the JIM7 antibody in (A) and (B), JIM5 antibody in (C) and (D), and 2F4 antibody in (E) and (F). (G) and (H) are staining of sections. All images were taken at the same magnification for the WT and *PMEI* OE. Note that the cells of *PMEI* OE seeds are larger. cot, Cotyledons; es, endosperm; mu, mucilage; rad, radical; te, testa. Bars = 65 mm. This figure was made by Gabriel Levesque-Tremblay and reprinted with the permission of the ASPB.

3.3.4 PME inhibition leads to faster seed germination and a lowered sensitivity of seeds to the inhibitory effects of ABA on germination

One key characteristic of the *PMEI5* OE lines was that their rate of seed germination was significantly faster than that exhibited by WT seeds, as measured by Dr.

Kerstin **Müller**; this was the case for both testa rupture and endosperm rupture (Figure 3.6A). Both fresh and after-ripened seeds of the OE lines exhibited faster germination, showing that the effect of the resultant cell wall modifications is not mediated through reduced dormancy. Germination on medium containing 1 mM ABA led to a prolonged phase II and higher PME activities in WT seeds throughout phase II (Figure 3.1). The OE seeds showed a reduced sensitivity to ABA with respect to a delay of endosperm rupture (Figure 3.6B). To more closely examine the delay of endosperm rupture in response to ABA, Dr. Kerstin **Müller** compared the times required to reach 50% endosperm rupture of the OE and WT seed populations as a function of the concentration of exogenous ABA (0.1–2 mM). She found that with increasing ABA concentrations, the average delay of endosperm rupture within the population is less pronounced for the *PMEI5* OE seeds than for the WT seeds (data not shown). Thus, the OE seeds exhibited a greater speed of completion of germination relative to the WT seeds as the ABA concentration was increased in this assays. While this is indicative of a lowered ABA sensitivity of the OE seeds, we recognize the limitations of these exogenous ABA studies.

Dr Kerstin **Müller** assayed PME activities in the OE lines to see if there were any changes in PME activities during phase II of the germination process, despite the presence of the inhibitor in OE lines. Unlike the PME activities of WT seeds (Figure 3.1), the PME activities of the OE lines (while reduced relative to the WT seeds) were maintained at a low level throughout germination, and exogenous ABA had little effect on the low steady state levels (Figure 3.6C). The faster germination and apparent decline in sensitivity to ABA of the OE seeds was thus associated with both the reduction of PME activities as well as a loss of differential regulation of PME activities during germination.

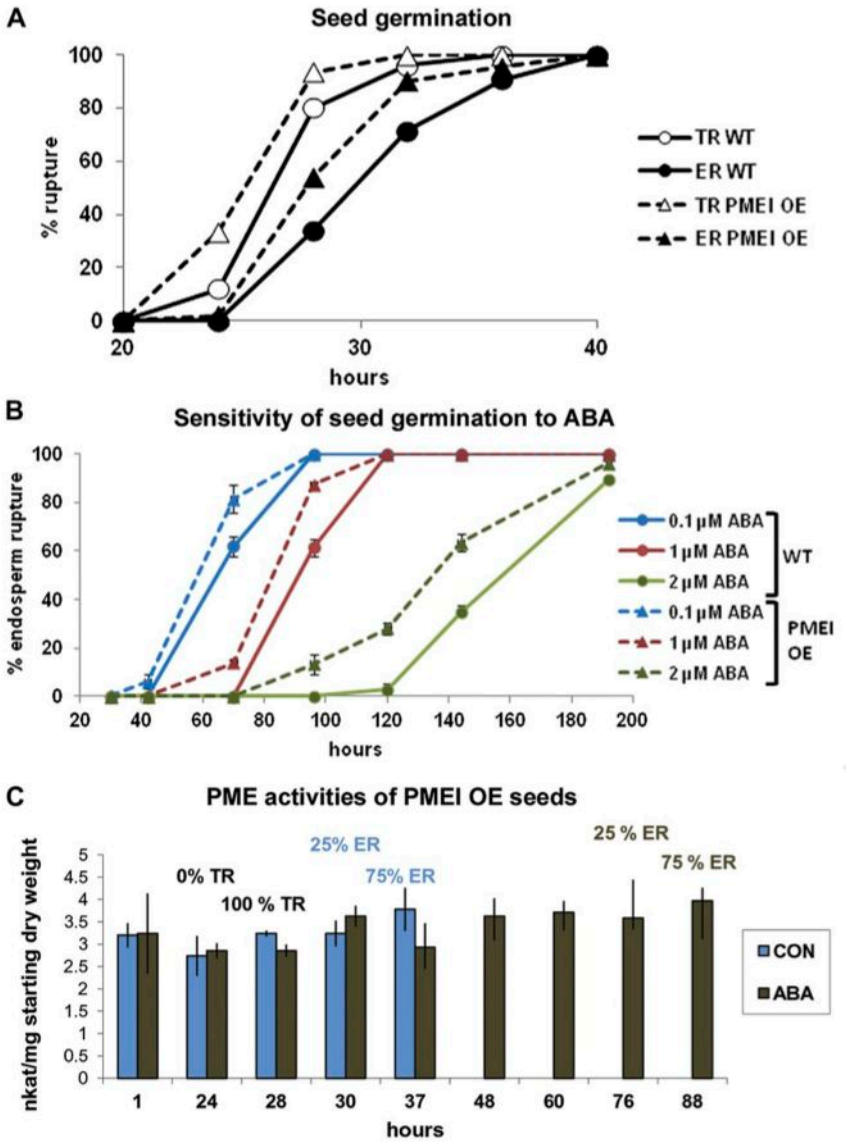

Figure 3.6: Effects of *PMEI5* OE on seed germination characteristics.

(A) Testa rupture (TR) and endosperm rupture (ER) in seeds of the *PMEI5* OE lines as compared with the WT. Data represent averages 6 SE of three replicates of 50 seeds each. (B) Effects of different concentrations of ABA on the germination (endosperm rupture) of *PMEI5* OE lines versus the WT. Data represent averages 6 SE of three replicates of 50 seeds each. (C) PME activities of protein extracts derived from *PMEI5* OE lines during germination in the absence control (CON; blue bars), and presence of 1 µM ABA (ABA; gray bars). Data are based on averages 6 ± SE of four biological replicates of about 100 seeds each. Seeds were weighed before imbibition, and the activity shown is relative to the starting seed weight. The percentages over the bars list

the proportion of seeds that had achieved testa rupture and endosperm rupture. This figure was made by Dr. Kerstin **Müller** and Gabriel Levesque-Tremblay and reprinted with the permission of the ASPB.

To examine the process of testa rupture and endosperm rupture in more detail, Dr. Kerstin **Müller** examined WT and *PMEI5* OE seeds by light microscopy (Figure 3.7A) and Dr. Karin Weitbrecht examined WT and PMEI5 OE seeds by environmental SEM (Figure 3.7B). Testa rupture in the PMEI OE seeds occurred in a morphologically similar fashion to that found for the WT seeds (data shown only for WT seeds; Figure 3.7). In both cases, cell separation causes testa rupture, and the outlines of the cells constituting the testa were clearly visible. Thus, any abnormal rupture of the testa does not accompany the faster germination of the *PMEI5* OE seeds. The endosperm appeared to stretch more extensively over the radicle in the PMEI OE seeds during phase II; a residual collar-like structure appeared around the radicle after endosperm rupture (Figure 3.7). This collar like structure was composed of endosperm cells and was particularly evident in the eSEM images; the rupture point of the endosperm was unaffected.

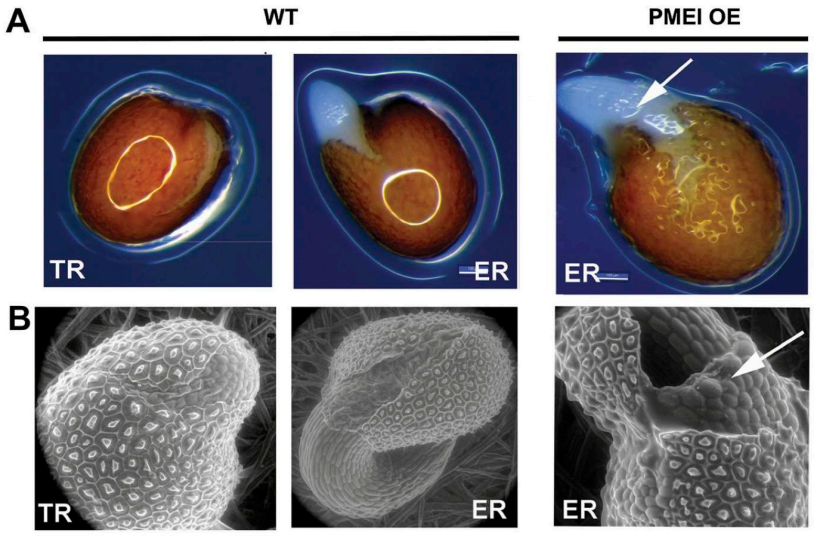

Figure 3.7: Testa rupture and endosperm rupture of WT and *PMEI5* OE seeds.
(A) Light microscopy images of WT and *PMEI5* OE seeds. (B) eSEM images. Arrows show how the endosperm of *PMEI* OE seeds is stretched more extensively and retained as a collar-like structure of cells that clings to the radicle after endosperm rupture. Note

the clear rupture lines of the testa shown for WT seeds in (B). Testa rupture (TR) and endosperm rupture (ER). This figure was made by Dr. Karin Weitbrecht and reprinted with the permission of the ASPB.

In order to see if these changes in testa morphology were also accompanied by changes in the mucilage that is secreted upon imbibition, I stained imbibed seeds with ruthenium red (Figure 3.8). There were no obvious differences in the mucilage volume or density when the seeds were stained with solutions containing water or other agents. The other agents included EDTA, which chelates calcium ions of the cell wall and thereby destroys calcium bridges, thereby extending the mucilage volume, and $CaCl_2$, which contracts the mucilage due to the formation of more extensive calcium bridges. A comparison of the two sets of seeds (OE and wild type) stained in the presence of these agents clearly showed that they exhibited similar mucilage profiles (Figure 3.8).

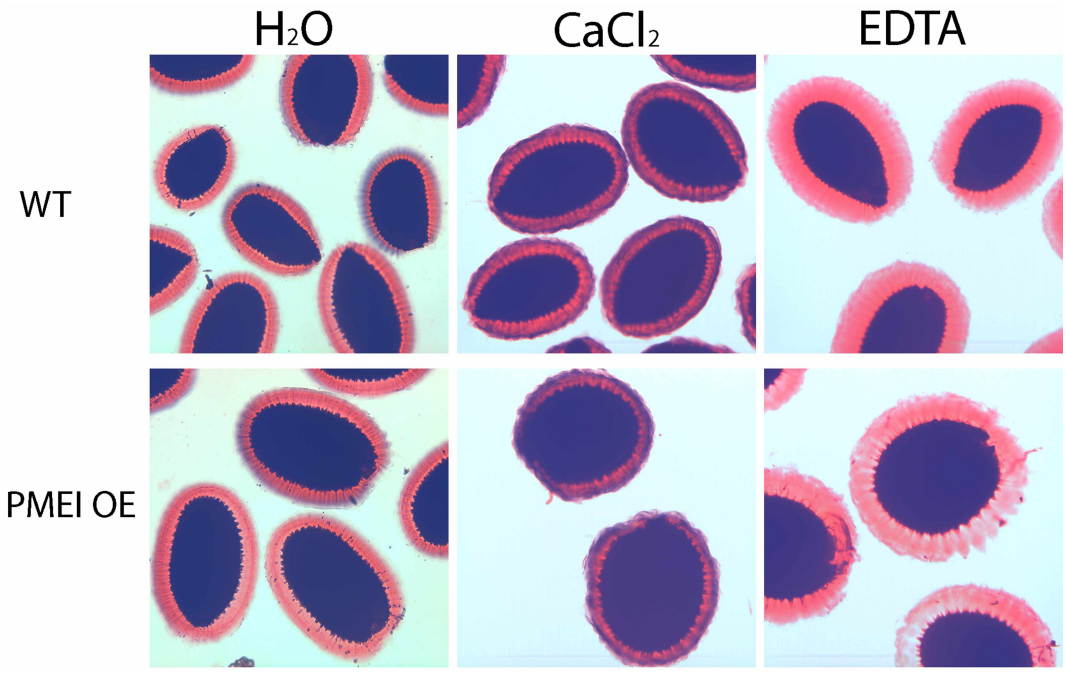

Figure 3.8: Ruthenium red staining of seeds to examine the mucilage associated with WT seeds and with *PMEI5* OE seeds.

The staining medium (water, EDTA, or $CaCl_2$) is indicated. No differences were observed between WT and *PMEI5* OE seeds with regard to mucilage volume under any of the staining conditions. This figure was made by Gabriel Levesque-Tremblay and

reprinted with the permission of the ASPB.

Another feature of the *PMEI5* OE seeds that was evident was that they were larger in size. Dr. Kerstin **Müller** and I, therefore, measured the cell size. Larger cells made up the testa, endosperm, and embryo of the *PMEI5* OE seeds as compared with WT seeds (Figures 3.5 and 3.9B). In accordance with the larger cell size, but similar cell numbers, both dry and imbibed seeds of the *PMEI5* OE lines were larger and heavier than dry and imbibed WT seeds, respectively (Figure 3.9C). This change could be due to the altered cell wall properties or to the fact that *PMEI* OE plants showed a marked reduction of seed production, with often only one or two seeds per silique. This could perhaps be due to greater resource allocation from the parent plant (because of the lower seed number). In any event, I showed that the siliques of *PMEI* OE plants are shortened and wrinkled (Figure 3.9A).

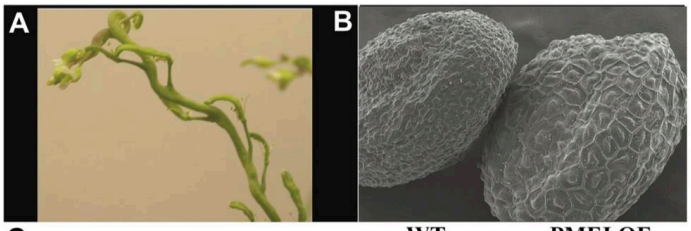

C	WT	PMEI OE
Seeds		
Dry seed length (µm)	356 +/- 31	464 +/- 20
Imbibed seed length (µm)	421 +/- 25	529 +/- 32
Dry seed width (µm)	232 +/- 14	324 +/- 24
Imbibed seed width (µm)	301 +/- 22	424 +/- 27
Dry seed weight (mg/150 seeds)	2.5 +/- 0.1	2.9 +/- 0.2
Imbibed seed weight (mg/150 seeds)	10.6 +/- 0.5	14.0 +/- 1.1
Siliques		
Silique length (mm)	14.4 +/- 0.9	9.6 +/- 0.4

Figure 3.9: Morphological phenotypes of *PMEI5* OE seeds and siliques.
(A) Siliques of *PMEI5* OE plants are wrinkled and shorter than those of WT plants. Also note the twisted growth of the stem. (B) eSEM image of dry seeds of the WT (left) and *PMEI5* OE (right). Note the larger size of *PMEI5* OE testa cells. (C) Quantitative differences between the characteristics of seeds, siliques, and plant growth of WT and

PMEI5 OE lines. Values represent the mean ± SE of 6 replicates. This figure was made by Dr. Kerstin **Müller** and Gabriel Levesque-Tremblay and reprinted with the permission of the ASPB.

In relation to the causes of the lowered seed numbers per silique, reciprocal hand crosses with WT plants and even between two *PMEI5* OE parents generated by Dr. Kerstin **Müller** demonstrated that this was not exclusively due to defective pollen (e.g. with an inability to fertilize the egg cell) or a mechanical problem with the silique shape, as the artificial transfer of the pollen led to a significant increase in seed numbers. Hand crosses between *PMEI5* OE parents led to 30 ± 2 seeds per silique, *PMEI5* OE pollen on WT stigma (*PMEI5* OE × WT) developed 36 ± 2 seeds per silique, and WT × *PMEI5* OE generated 44 ± 3 seeds per silique. These seed numbers are still below that characteristic of the WT (56 ± 5 seeds per silique). A closer visual examination of the reproductive organs of the *PMEI5* OE lines showed that filament elongation is likely not sufficiently coordinated with style elongation, as the anthers often seemed too short for the pollen to reach the stigma.

3.4 Discussion

Functional redundancy within the large PME family is problematic for determining the effects of changes in the degree of cell wall pectin methyl esterification on plant development and morphology by using a PME gene knockout strategy. Dr. Sebastian Bartels circumvented this problem by expressing the PME inhibitor *PMEI5* ectopically. The inhibitory activity of PMEI5 on PME activity was evident in the transgenic lines, and we were able to show that there was changes (increases) in the degree of pectin methyl esterification in the seed tissues of the *PMEI5* OE lines compared to WT. Five *PMEI*s have been functionally characterized in *A. thaliana* to date. *PMEI1* and *PMEI2* (Wolf et al., 2003) are highly expressed in flowers, and *PMEI1* expression is specific to pollen. The expression of *PMEI3* is particularly high in the apical meristem (Peaucelle et al., 2008), while *PMEI6* is expressed in the seed coat (Saez Aguayo et al., 2013). *PMEI4* is up-regulated during growth acceleration in skotomorphic

hypocotyls (Pelletier et al., 2010). *PMEI5* is not represented on the most commonly used microarray chips; thus, no prior information was available about its expression patterns. Dr. Kerstin **Müller** found that *PMEI5* is most highly expressed in flowers, and showed that its spatial expression is similar to that of *PMEI1* and *PMEI2*. We confirmed the information from NCBI that some cDNAs of *PMEI5* show intron retention. In wheat, regulation of the *PMEI* genes themselves is mediated, in part, by intron retention; processed and unprocessed transcripts of two *PMEI* genes accumulate in several organs of wheat, but anthers contain exclusively mature transcripts. *PMEI3* of wheat lacks introns, and its transcript accumulates mainly in stem internodes (Rocchi et al., 2012).

PMEs show differential expression during different stages of the *A. thaliana* life cycle (Electronic Fluorescent Pictograph browser [http://www.bar.utoronto.ca/efp/ cgi bin/efpWeb.cgi]; Winter et al., 2007). The phenotypes affected by *PMEI5* OE are likely indicative of this inhibitor interacting with a number of different PMEs, similar to the findings of others in which *PMEIs* show cross-species and even cross-family interactions (Giovane et al., 2004). Pelletier et al. (2010) overexpressed the *PMEI3* gene in *A. thaliana* to study the role of pectin methyl esterification in dark-induced hypocotyl elongation. Interestingly, they did not observe several of the morphological phenotypes evident in our *PMEI5* OE line, including the looping stem growth (Figure 3.9A). This demonstrates that individual PMEIs may have selective effects despite interacting with several PMEs.

3.4.1 PME activity plays a role in *A. thaliana* seed germination

Biochemical changes in the cell wall that manifest in loosening in seed micropylar tissues are an important aspect of germination. In order for a seed to complete germination, the growth potential of the radicle must be greater than the resistance of the tissues enveloping it (Bewley, 1997b; Müller et al., 2006). Hydrolase-mediated changes in the mechanical properties of the cell walls, particularly in the radicle itself (to promote its growth potential) and in the seed micropylar tissues surrounding the radicle tip (to promote mechanical weakening), are thus crucial to this process. These extensibility

changes obviously must be subject to strict spatial and temporal control. Expansins and xyloglucan endotransglucosylases are expressed in the endosperm cap of germinating tomato seeds (Chen et al., 2002), and differential regulation of the expression and activity of the hydrolases β-1,3-glucanase and β-1,4-mannanase in the endosperm accompanies seed germination in tobacco (Leubner-Metzger et al., 1995) and tomato (Nonogaki et al., 2000), respectively. OE of a β-1,3-glucanase gene in tobacco has been shown to alter dormancy, but does not affect the germination process *per se* (Leubner- Metzger, 2002).

In this study, we identified a role for PME activity in seed germination and found a significant effect of PME inhibition on increasing the rate of germination; dormancy was unaffected. PME activities increased in WT seeds over the first 24 to 30 h of germination, a period associated with several metabolic changes (e.g. the translation of newly transcribed mRNAs, mitochondrial repair and biogenesis, and the mobilization of soluble sugars to prepare the seed for the completion of germination) and testa rupture (Weitbrecht et al., 2011). The activities declined thereafter, during the period associated with the completion of germination (endosperm rupture and radicle protrusion). As noted in the introduction, higher PME activity (and thus cell wall pectin demethyl esterification) influences cell wall biomechanical properties. The proposed mechanisms of PME action in these processes can be summarized as follows: (1) creating an acidic environment within the cell wall as a result of de-esterification of pectins, thus promoting cell wall extension or growth, perhaps through the modulation of expansins (see above) (2) facilitating the hydrolysis of polygalacturonic chains by polygalacturonases (Wakabayashi et al., 2003), and (3) promoting the formation of calcium cross linkages (through demethylation of pectins) that ultimately change the state of the pectin matrix by generating free carboxyl groups that are able to bind Ca^{2+} (Micheli, 2001; Peaucelle et al., 2012). In yellow cedar (*Callitropsis nootkatensis*) seeds, the micropylar megagametophyte loses mechanical strength following a dormancy-breaking treatment, and during germination, the cells of the megagametophyte in the area immediately surrounding the radicle exhibit a loss of their internal structure, which would represent significant weakening to allow radicle emergence (Ren and Kermode, 1999). Concurrently, the embryo exhibits increased turgor and a reduced sensitivity to low

osmotic potentials; both the weakening and strengthening processes are positively associated with PME activities (Ren and Kermode, 2000).

Thus, decreasing the extent of cell wall pectin demethyl esterification (e.g. through PME inhibition) could lead to either enhanced or reduced elongation growth, implying an increased or decreased wall extensibility, respectively. For example, reduced elongation is the case for the growth of hypocotyls and pollen tubes (Bosch and Hepler, 2005; Derbyshire et al., 2007; Pelletier et al., 2010). We speculate that PME inhibition led to faster endosperm rupture and completion of germination by improving the capacity of the radicle to break through this tissue; this improved growth potential of the embryo could be related to an increased rate of water uptake. Accordingly, the reduced PME activities associated with seeds of the overexpressing lines could have made their cell walls more permeable to water and more extensible, possibly through altering the ability of cell wall homogalacturonans to form Ca^{2+} bridges, a process requiring blockwise demethyl esterification. Indirect evidence in support of this comes from a study by Rautengarten et al. (2008), in which increased PME activity in a subtilase-deficient mutant, *atsbt1.7*, was associated with a decrease in germination capability under water-limiting conditions induced by polyethylene glycol. It is possible that the mechanical resistance of the micropylar endosperm was also altered; our morphological studies (Figure 3.7) indicate that this is the case. Changes in mechanical resistance could be caused directly by the increased pectin methyl-esterification changing the biophysical properties of the cell wall. It is also possible that the faster radicle emergence of the OE seeds is due to the larger size of cells of the *PMEI* OE seeds; thus, cell size-related changes in cell wall mechanical properties may be operative. The cell wall in these cells may lack blockwise demethyl esterification by PME which would lead to looser cell walls and higher rates of cell wall extension. In any case, the endosperm cells may be weakened in relation to the opposing force of the growing radicle.

Wolf et al. (2012) recently demonstrated a link between altered cell wall pectin methyl esterification and BR signaling. They demonstrated the up-regulation of BR signalling pathways as a result of the inhibition of pectin methyl esterase activity induced

via genetic and pharmacological means, including *PMEI5* OE. The authors propose that this up-regulation of the BR pathway is likely the result of a feedback ("compensatory") mechanism that the plant uses to restore cell wall homeostasis. In this way, the potential for catastrophic changes in cell wall integrity can be avoided. It is possible that the faster germination of *PMEI* OE seeds in our study is due to this up-regulation of BR signalling, as these pathways can act to promote *A. thaliana* seed germination (Steber and McCourt, 2001).

Microarray data certainly support the contention that changes in the pectin matrix occur during germination; transcripts encoding a large number of pectin-modifying enzymes change during germination phases I and II, and the regulation of these genes appears to be highly complex (Nakabayashi et al., 2005). PME activity increases in a tissue-specific manner during seed dormancy release and germination of yellow cedar seeds (Ren and Kermode, 2000), where pectin is the predominant polysaccharide in the cell walls of the megagametophyte (Ren and Kermode, 1999). In the seeds of this highly dormant conifer species, the addition of ABA to intact seeds after dormancy breakage suppresses the activity of two PME isoforms (Ren and Kermode, 2000).

3.4.2 Increased cell wall pectin methyl esterification leads to an apparent reduced sensitivity of seed germination to ABA

In seeds of several species, ABA specifically delays endosperm rupture without having a major effect on the timing of testa rupture (Müller et al., 2006). In *A. thaliana* WT seeds, the delay in the onset of endosperm rupture caused by exogenous ABA was associated with a prolonged period of higher PME activities. It is still unclear how the increase in the duration of phase II is brought about by the presence of ABA. In WT seeds, PME activities peaked in phase II of seed germination; ABA prolongs the period of high PME activities, such that they do not decline until just around the onset of endosperm rupture. As with the control seeds, in the ABA-treated seeds, the PME activities were suppressed once 75% of the seeds had reached endosperm rupture. Thus, changes in the cell wall pectin characteristics might play a role in the mechanism by

which ABA delays endosperm rupture. In *A. thaliana* seeds, ABA leads to a delay in endosperm weakening (Müller et al., 2006), which is part of the process that allows the radicle to emerge through this tissue. In accordance with the hypothesis that PME activity contributes to ABA inhibition of endosperm rupture, ABA delayed the endosperm rupture of *PMEI5* OE seeds to a lesser degree than that of WT seeds. More information is needed to support the contention that ABA specifically delays endosperm rupture via changes in cell wall pectin characteristics. While my collaborator and I did not address any role of endogenous ABA, this factor has been linked to cell wall composition changes. For example, leaves of the ABA-deficient *sitiens* mutant of tomato have lower levels of GalUA in their cell walls and are less susceptible to degradation by pectinases than those of the WT leaves (Curvers et al., 2010). The authors conclude that the GalUA residues within the cell walls of the *sitiens* leaf cells, while lower in amount, have a higher degree of pectin methyl esterification, which in turn renders them more resistant to pectinolysis. While this effect is on cell wall composition and therefore differs from our study, it is interesting that endogenous ABA can influence cell wall properties.

Chapter 4: Conclusions and future direction

4.1 Conclusion

Cell walls are diverse in their composition and this diversity is necessary to support a variety of cellular functions and physiological activities. One essential activity is to reproduce: to generate viable progeny that are contained in the seeds that ultimately germinate to create the next generation. Seed development and germination require complex cell wall modifications to accommodate cell division, elongation and differentiation. Little is known about the specific cell wall-related enzymes involved in seed development, despite the identification of several key cell wall-related Carbohydrate Active enZymes (CAZy). *PMEs* and their proteinaceous inhibitor, *PMEI,* form two large families of genes in this database.

In my Ph.D. research project, I focused on two major objectives:

1. Identify and characterize a PME involved in seed mucilage structure and function by screening T-DNA and transposon insertional mutants for mucilage defects. Characterize the function of the *PME* gene(s) related to the phenotype(s) using cytological and biochemical methods.
2. Verify if the degree of pectin methyl-esterification affects germination by manipulating the amount of PMEI in the seed.

To address these objectives I used a *PME* and a *PMEI* from *A. thaliana* to study the changes in methyl esterification occurring during seed development and germination. Research described in chapter 2 and 3 demonstrate that the regulation of the HGs pectin methyl esterification is important for seed development and germination.

4.1.1 *HMS* is involved in seed development

Previously the transcripts of a few *PMEs* were found in the siliques, seeds and seed coat (Louvet et al., 2006; Wolf and al., 2010). However, only one, *At1g23200*

(*HMS*) was shown to display specific expression during the mid-silique developmental stage (Louvet et al., 2006). However *HMS* expression is highly specific to 7 DPA in the seed coat when mucilage is secreted in the apoplast. *HMS* is also expressed in the embryo at 7 DPA where cell expansion occurs (Goldberg and al., 1994; Western et al., 2000; Le and al., 2010). I showed that the mucilage phenotype in the *hms-1* mutant is the indirect cause of a defect in embryo development. I also showed that in the presence of the normal level of *HMS*, the rigidity of seed material is decreases, which supports the idea that the concept that *HMS* is required for normal embryo morphogenesis, rigidity of seed material, embryo cell size, HG methylation and pectin methyl esterase activity. I conclude that HMS is needed to remove methyl groups from HG to permit the loosening of the cell walls of the embryo and subsequent cell expansion during accumulation of storage reserves. This is in agreement with another study, in which PME activity has been shown lead to the loosening of the cell wall necessary for organogenesis and growth (Peaucelle et al., 2011).

4.1.2 Pectin methyl esterification affects germination

Biochemical changes in the cell wall that cause cell wall loosening of seed tissues are an important aspect of germination. Evidence for PME expression and involvement in seed germination were found in yellow cedar (Ren and Kermode, 2000). In this study, we identified a role for PME activity in seed germination and found a significant effect of PME inhibition on increasing the rate of germination. ABA was also shown to delay endosperm rupture (Müller et al., 2006). Dr Kerstin **Müller** and I collaborated to demonstrate that this delay is associated with a prolonged period of higher PME activity in *A. thaliana*. The prolonged PME activity is likely to sustain the strengthening of the cell wall in the seed tissues, thereby delaying the endosperm rupture and embryo cell wall extension necessary for the radicule to protrude. In this study we showed that an increase in DM in OE *PMEI5* plants was correlated with a faster germination rate. The *PMEI5* OE plants produced larger seeds with a larger embryo. This may be the effect of the inhibition of PME(s) acting blockwise during development, which stimulates cell wall loosening and extension in the seed tissues. We acknowledge that the phenotypes we

observe in *PMEI* OE may also, or alternatively, be due to the activation of BR signalling pathways. Nevertheless, it is clear that PME(s) is involved in the normal completion of germination.

4.2 Future directions

One interesting conclusion from both projects of my thesis is that there are probably PMEs with different modes of action in the seed. For example, we showed that OE *PMEI5* acts on PME independently of HMS in the seeds, suggesting that PMEI5 influence different PMEs. In addition, the phenotypes of OE *PMEI5* and *hms-1* result in different phenotypes (bigger and smaller embryo cells, respectively) even though both genotypes are expected to decrease PME activity, again suggesting that they work on PMEs with very different modes of action. The identification of the PME inhibited by OE PMEI5 is needed. Identification of the PME expressed in the embryo and the use of T-DNA or transposon mutant lines may help answer this question.

4.2.1 Seed development

In my research I showed that *HMS* is highly expressed in the seed coat during mucilage biosynthesis and secretion, at around 7 DPA. However, we also demonstrated that the seed coat mucilage defect was an indirect consequence of a defect in embryo development. This does not rule out the possibility that HMS impacts mucilage directly, because the activity of PMEs encoded by other genes may be redundant with *HMS*. A future follow-up study should attempt to generate double and triple mutant analysis with the 7 PMEs isolated for their specific expression in the seed coat. Also, proteomic analysis of the mucilage is needed to identify potential proteins in this compartment. I suggest extracting the mucilage and purifying the protein component by SDS-PAGE and using mass spectroscopy to identify the proteins.

We hypothesize that HMS is involved in the loosening of the embryo cell wall, which ultimately facilitates growth. We also hypothesized that other PMEs act blockwise

in the embryo. It would be interesting to investigate other PMEs expressed in the embryo and their relative importance in these tissues using reverse genetics. If other PME(s) act blockwise in the embryo, they may be responsible for restraining growth. Mutations in such PME(s) may increase cell expansion and consequently lead to a bigger seed. This would be in accordance with our model and add support to our hypothesis. One important tool missing in the study of PME function is the lack of purified enzymes with well-define patterns of action (blockwise or non-blockwise). Having a PME that acts blockwise (strengthening cell wall) and non-blockwise (loosening the cell wall) would help test the physiological role of these two types of demethyl esterification. One experiment that could be done using such enzymes would be to apply them to various tissues or cell wall material (e.g. mucilage) to observe their effect.

4.2.2 Regulation of HGs methyl esterification in germination

As far as germination is concerned, in this study, the lines over-expressing *PMEI5* exhibited a higher degree of cell wall pectin methyl esterification, and the seeds completed germination faster. We would need to conduct studies on the resultant changes in the mechanical strength of the different seed tissues (especially those of the micropylar endosperm and radicle) to determine the precise effects of the PME inhibition on cell wall extensibility of these tissues. However, these experiments are very difficult to perform in *A. thaliana* seed tissues. In this study, we mainly analyzed and discussed the seed related phenotype of OE *PMEI5* plants. A study of potential defects in other tissues, such as the stem and the internodes, may help unravel important physiological roles for PME and PMEI. In our study, OE *PMEI5* did not affect testa rupture. Little is known about the mechanism and enzymatic involvement in testa rupture during germination. PMEs that promote the loosening or strengthening of the cell walls in the testa may be involved in this process and their identification may help toward a better understanding of the mechanism of testa rupture.

Bibliography

Albramoff, M.D., Magalhaes, P.J., Ram, S.J. (2004) Image processing with ImageJ. Biophonetics Int. 11, 36-42.

Al-Qsous, S., Carpentier, E., Klein-Eude, D., Burel, C., Mareck, A., Dauchel, H., Gomord, V., Balangé, A.P. (2004) Identification and isolation of a pectin methylesterase isoform that could be involved in flax cell wall stiffening. Planta. 219(2): 369-378.

An, S.H., Sohn, K.H., Choi, H.W., Hwang, I.S., Lee, S.C., Hwang, B.K. (2008) Pepper pectin methylesterase inhibitor protein CaPMEI1 is required for antifungal activity, basal disease resistance and abiotic stress tolerance. Planta. 228(1); 61-78.

Atmodjo, M.A., Sakuragi, Y., Zhu, X., Burrell, A.J., Mohanty, S.S., Atwood, J.A. 3rd, Orlando, R., Scheller, H.V., Mohnen, D. (2011) Galacturonosyltransferase (GAUT)1 and GAUT7 are the core of a plant cell wall pectin biosynthetic homogalacturonan : galacturonosyltransferase complex. Proc Natl Acad Sci U S A. 108(50): 20225-20230.

Balestrieri, C., Castaldo, D., Giovane, A., Quagliuolo, L., Servillo, L. (1990) A glycoprotein inhibitor of pectin methylesterase in kiwi fruit (*Actinidia chinensis*). Eur. J. Biochem., 193(1), 183–187.

Barrôco, R.M., Van Poucke, K., Bergervoet, J.H., De Veylder, L., Groot, S.P., Inzé, D., Engler, G. (2005) The role of the cell cycle machinery in resumption of postembryonic development. Plant Physiol. 137(1): 127-140.

Baud, S., Boutin, J.P., Miquel, M., Lepiniec, L., Rochat, C. (2002) An integrated overview of seed development in *Arabidopsis thaliana* ecotype WS. Plant Physiol. Biochem. 40, 151–160.

Bewley, J.D. (1997a) Seed germination and dormancy. Plant Cell 9, 1055–1066.

Bewley, J.D. (1997b) Breaking down the walls: a role for endo-b-mannanase in release from seed dormancy? Trends Plant Sci. 2, 464–469.

Blumenkrantz, N., Asboe-Hansen, G. (1973) New method for quantitative determination of uronic acids. Anal. Biochem. 54, 484–489.

Bordenave, M., Goldberg, R. (1993) Purification and characterization of pectin methylesterases from mung bean hypocotyl cell walls. Phytochemistry 33, 999-1003.

Bosch, M., Hepler, P.K. (2005) Pectin methylesterases and pectin dynamics in pollen tubes. Plant Cell. 17, 3219–3226.

Bourgault, R., Bewley, J.D. (2002) Variation in its C-terminal amino acids determines whether endo-beta-mannanase is active or inactive in ripening tomato fruits of different cultivars. Plant Physiol. 130(3), 1254-1262.

Bouton, S., Leboeuf, E., Mouille, G., Leydecker, M.T., Talbotec, J., Granier, F., Lahaye, M., Höfte, H., Truong, H.N. (2002) QUASIMODO1 encodes a putative membrane-bound glycosyltransferase required for normal pectin synthesis and cell adhesion in *Arabidopsis*. Plant Cell. 14(10): 2577-2590.

Brummell, D.A., Dal Cin,V., Crisosto, C.H., Labavitch, J.M. (2004) Cell wall metabolism during maturation, ripening and senescence of peach fruit. J. Exp. Bot. 55(405), 2029-2039.

Buchanan, B.B., Gruissem, W., Jones, R.L. editors. (2000) Biochemistry & molecular biology of plants. John Wiley & Sons.

Caffall, K.H., Mohnen, D. (2009). The structure, function, and biosynthesis of plant cell wall pectic polysaccharides. Carbohydr Res 344(14), 1879-1900.

Caffall, K.H., Pattathil, S., Phillips, S.E., Hahn, M.G., Mohnen, D. (2009) *Arabidopsis thaliana* T-DNA Mutants Implicate *GAUT* Genes in the Biosynthesis of Pectin and Xylan in Cell Walls and Seed Testa. Mol. Plant. 5, 1000-1014.

Camardella, L., Carratore, V., Ciardiello, M.A., Servillo, L., Balestrieri. C., Giovane, A. (2000) Kiwi protein inhibitor of pectin methylesterase amino-acid sequence and structural importance of two disulfide bridges. Eur. J. Biochem. 267(14), 4561-4565.

Cannon, M.C., Terneus, K., Hall, Q., Tan, L., Wang, Y., Wegenhart, B.L., Chen, L., Lamport, D.T., Chen, Y., Kieliszewski, M.J. (2008) Self-assembly of the plant cell wall requires an extensin scaffold. Proc. Natl. Acad. Sci. USA. 105(6), 2226-2231.

Cătălin, V., Gillian, H.D., Jonathan, S.G., Kerstin, K., Yeen, T.H., Alan, G., Graham, D., Tamara, L.W., Mark, E., George, W.H. (2013) FLYING SAUCER 1 is a transmembrane RING E3 ubiquitin ligase that controls the degree of pectin methylesterification in *Arabidopsis* seed mucilage. Plant Cell. 25, 944-959.

Catoire, L., Pierron, M., Morvan, C., du Penhoat, C.H., Goldberg, R. (1998) Investigation of the action patterns of pectinmethylesterase isoforms through kinetic analyses and NMR spectroscopy. Implications in cell wall expansion. J. Biol. Chem. 273, 33150-33156.

Chang S, Puryear J, Cairney J (1993) A simple and efficient method for isolating. RNA from pine trees. Plant Mol. Biol. Rep. 11, 113–116.

Chen, F., Bradford, K.J. (2000) Expression of an expansin is associated with endosperm weakening during tomato seed germination. Plant Physiol. 124, 1265–1274.

Chen, F., Nonogaki, H., Bradford, K.J. (2002) A gibberellin-regulated xyloglucan endotransglycosylase gene is expressed in the endosperm cap during tomato seed germination. J. Exp. Bot. 53, 215–223.

Chen, M.H., Citovsky, V. (2003) Systemic movement of a tobamovirus requires host cell pectin methylesterase. Plant J. 35, 386–392.

Chen, M.H., Sheng, J., Hind, G., Handa, A.K., Citovsky, V. (2000) Interaction between the tobacco mosaic virus movement protein and host cell pectin methylesterases is required for viral cell-to-cell movement. EMBO J. 19(5), 913-920.

Clough, S.J., Bent, A.F. (1998) Floral dip: a simplified method for *Agrobacterium*-mediated transformation of *Arabidopsis thaliana*. Plant J. 16, 735–743.

Clouse, S.D., Sasse, J.M. (1998) BRASSINOSTEROIDS: essential regulators of plant growth and development. Annu. Rev. Plant Physiol. Plant Mol. Biol. 49, 427–451.

Cosgrove, D.J. (2005) Growth of the plant cell wall. Nat. Rev. Mol. Cell Biol. 6(11), 850-861.

Cosgrove, D.J., Jarvis, M.C. (2012) Comparative structure and biomechanics of plant primary and secondary cell walls. Frontiers in Plant Science. 3(204), 1-6.

Coutinho, P.M., Stam, M., Blanc, E., Henrissat, B. (2003) Why are there so many carbohydrate-active enzyme-related genes in plants? Trends Plant Sci. 12, 563-565.

Curvers, K., Seifi, H., Mouille, G., de Rycke, R., Asselbergh, B., Van Hecke, A., Vanderschaeghe, D., Höfte, H., Callewaert, N., Van Breusegem, F., Höfte, M. (2010) Abscisic acid deficiency causes changes in cuticle permeability and pectin composition that influence tomato resistance to *Botrytis cinerea*. Plant Physiol. 154, 847–860.

Dean, G.H., Cao, Y., Xiang, D., Provart, N.J., Ramsey, L., Ahad, A., White, R., Selvaraj, G., Datla, R. and Haughn, G. (2011) Analysis of gene expression patterns during seed coat development in *Arabidopsis*. Mol. Plant. 4, 1074-1091.

Dean, G.H, Zheng, H., Tewari, J., Huang, J., Young, D.S., Hwang, Y.T., Western, T.L., Carpita, N.C., McCann, M.C., Mansfield, S.D., Haughn, G.W. (2007) The *Arabidopsis* MUM2 gene encodes a beta-galactosidase required for the production of seed coat mucilage with correct hydration properties. Plant Cell. 19, 4007-4021.

DeBono, A.G. (2011) The role and behavior of Arabidopsis thaliana lipid transfer proteins during cuticular wax deposition. Dissertation, University of British Columbia.

Dedeurwaerder, S., Menu-Bouaouiche, L., Mareck, A., Lerouge, P., Guerineau, F. (2009) Activity of an atypical *Arabidopsis thaliana* pectin methylesterase. Planta. 229, 311-321.

Dekkers, B.J., Pearce, S., van Bolderen-Veldkamp, R.P., Marshall, A., Widera, P., Gilbert, J., Drost, H.G., Bassel, G.W., Müller, K., King, J.R., Wood, A.T., Grosse, I., Quint, M., Krasnogor, N., Leubner-Metzger, G., Holdsworth, M.J., Bentsink, L. (2013) Transcriptional dynamics of two seed compartments with opposing roles in *Arabidopsis* seed germination. Plant Physiol. 163(1), 205–215

De-la-Pena, C., Badri, D.V., Vivanco, J.M. (2008) Novel role for pectin methylesterase in *Arabidopsis*: A new function showing ribosome-inactivating protein (RIP) activity. Biochim. Biophys. Acta. 1780, 773-783.

Denes, J.M., Baron, A., Renard, C.M., Pean, C., Drilleau, J.F. (2000) Different action patterns for apple pectin methylesterase at pH 7.0 and 4.5. Carbohydr. Res. 327, 385-393.

Derbyshire, P., McCann, M.C., Roberts, K. (2007) Restricted cell elongation in Arabidopsis hypocotyls is associated with a reduced average pectin esterification level. BMC Plant Biol. 7, 31.

Di Matteo, A., Giovane, A., Raiola, A., Camardella, L., Bonivento, D., De Lorenzo, G., Cervone, F., Bellincampi, D., Tsernoglou, D. (2005) Structural basis for the interaction between pectin methylesterase and a specific inhibitor protein. Plant Cell. 3, 849-858.

Dorokhov, Y.L., Skurat, E.V., Frolova, O.Y., Gasanova, T.V., Ivanov, P.A., Ravin, N.V., Skryabin, K.G., Mäkinen, K.M., Klimyuk, V.I., Gleba, Y.Y., Atabekov, J.G. (2006) Role of the leader sequence in tobacco pectin methylesterase secretion. FEBS Lett. 580(13), 3329–3334.

Downie, B., Dirk, L.M., Hadfield, K.A., Wilkins, T.A., Bennett, A.B., Bradford, K.J. (1998) A gel diffusion assay for quantification of pectin methylesterase activity.

Anal. Biochem. 264(2), 149-157.

Downie, B., Hilhorst, H.W.M., Bewley, J.D. (1997) Endo-b-mannanase activity during dormancy alleviation and germination of white spruce (*Picea glauca*) seeds. Plant Physiol. 101, 405–415.

Esau, K. Editor. (1977) Anatomy of seed plants. John Wiley and Sons, New York.

Flego, D., Marits, R., Eriksson, A.R., Koiv, V., Karlsson, M.B., Heikinheimo, R., Palva E.T. (2000) A two-component regulatory system, pehR-pehS, controls endopolygalacturonase production and virulence in the plant pathogen *Erwinia carotovora* subsp. *carotovora*. Mol. Plant Microbe Interact. 13(4), 447–455.

Focks, N., Benning, C. (1998) wrinkled1: a novel, low-seed-oil mutant of *Arabidopsis* with a deficiency in the seed-specific regulation of carbohydrate metabolism. Plant Physiol. 118, 91–101.

Foster, C.E., Martin, T.M., Pauly, M. (2010) Comprehensive compositional analysis of plant cell walls (lignocellulosic biomass). Part II. Carbohydrates. J. Vis. Exp. 37, e1745.

Francis, K.E., Lam, S.Y., Copenhaver, G.P. (2006) Separation of Arabidopsis pollen tetrads is regulated by QUARTET1, a pectin methylesterase gene. Plant Physiol. 142(3):1004-1013.

Fry, S.C. (2004) Primary cell wall metabolism: tracking the careers of wall polymers in living plant cells. New phytol. 161, 641-675.

Gimeno-Gilles, C., Lelièvre, E., Viau, L., Malik-Ghulam, M., Ricoult, C., Niebel, A., Leduc, N., Limami, A.M. (2009) ABA-mediated inhibition of germination is related to the inhibition of genes encoding cell-wall biosynthetic and architecture:

modifying enzymes and structural proteins in Medicago truncatula embryo axis. Mol Plant. 2(1):108-119.

Giovane, A., Servillo, L., Balestrieri, C., Raiola, A., D'Avino, R., Tamburrini, M., Ciardiello, M.A. Camardella, L. (2004). Pectin methylesterase inhibitor. Biochim. Biophys. Acta 1696(2), 245-252.

Goldberg R.B., de Paiva, G., Yadegari R. (1994) Plant embryogenesis: Zygote to seed. Science 266: 605-614

Goldberg, R., Morvan, C., Jauneau, A., Jarvis, M.C. (1996) Methyl-esterification, de-esterification and gellation of pectins in the primary cell wall, in pectin and pectinase, Progress in Biotechnology. 14, 151-172.

Goldberg, R., Pierron, M., Bordenave, M., Breton, C., Morvan, C., Du Penhoat, C.H. (2001) Control of Mung bean pectinmethylesterase isoform activities. Influence of pH and carboxyl group distribution along the pectic chains. J. Biol. Chem. 276, 8841–8847.

Gomez, L.D., Baud, S., Gilday, A., Li, Y., Graham, I.A. (2006) Delayed embryo development in the *Arabidopsis* TREHALOSE-6-PHOSPHATE SYNTHASE 1 mutant is associated with altered cell wall structure, decreased cell division and starch accumulation. Plant J. 46, 69–84.

Gomez, L.D., Gilday, A., Feil, R., Lunn, J.E., Graham, I.A. (2010) AtTPS1-mediated trehalose 6-phosphate synthesis is essential for embryogenic and vegetative growth and responsiveness to ABA in germinating seeds and stomatal guard cells. Plant J. 64, 1–13.

Goubet, F., Barton, C.J., Mortimer, J.C., Yu, X., Zhang, Z., Miles, G.P., Richens, J.,

Liepman, A.H., Seffen, K., Dupree, P. (2009) Cell wall glucomannan in *Arabidopsis* is synthesised by CSLA glycosyltransferases, and influences the progression of embryogenesis. Plant J. 60, 527–538.

Graeber, K., Linkies, A., Wood, A.T.A., Leubner-Metzger, G. (2011) A guideline to family-wide comparative state-of-the-art quantitative RT-PCR analysis exemplified with a Brassicaceae cross-species seed germination case study. Plant Cell. 23, 2045–2063.

Griesbeck, O., Baird, G.S., Campbell, R.E., Zacharias, D.A., Tsien, R.Y. (2001) Reducing the environmental sensitivity of yellow fluorescent protein. J. Biol. CHMS 276, 29188–29194.

Grsic-Rausch, S., Rausch, T. (2004) A coupled spectrophotometric enzyme assay for the determination of pectin methylesterase activity and its inhibition by proteinaceous inhibitors. Anal. Biochem. 333, 14–18.

Guénin S, Mareck A, Rayon C, Lamour R, Assoumou Ndong Y, Domon JM, Sénéchal F, Fournet F, Jamet E, Canut H, Percoco G, Mouille G, Rolland A, Rustérucci C, Guerineau F, Van Wuytswinkel O, Gillet F, Driouich A, Lerouge P, Gutierrez L, Pelloux J. (2011) Identification of pectin methylesterase 3 as a basic pectin methylesterase isoform involved in adventitious rooting in *Arabidopsis thaliana*. New Phytol. 192(1), 114-126.

Haughn., G., Chaudhury, A. (2005) Genetic analysis of seed coat development in *Arabidopsis*. Trends Plant Sci. 10(10), 472-477.

Hayashi, T., Kaida, R. (2011) Functions of xyloglucan in plant cells. Mol. Plant. 4(1), 17-24.

Hongo, S., Sato, K., Yokoyama, R., Nishitani, K. (2012) Demethylesterification of the primary wall by PECTIN METHYLESTERASE35 provides mechanical support to the *Arabidopsis* stem. Plant Cell. 24(6), 2624-2634.

Hothorn, M., Wolf, S., Aloy, P., Greiner, S., Scheffzek, K. (2004) Structural insights into the target specificity of plant invertase and pectin methylesterase inhibitory proteins. Plant Cell 16, 3437-3447.

Irifune, K., Nishida, T., Egawa, H., Nagatanim, A. (2004) Pectin methylesterase inhibitor cDNA from kiwi fruit. Plant Cell Rep. 23(5): 333-338.

Ito, T., Motohashi, R., Kuromori, T., Mizukado, S., Sakurai, T., Kanahara, H., Seki, M., Shinozaki, K. (2002) A new resource of locally transposed dissociation elements for screening gene-knockout lines *in silico* on the *Arabidopsis* genome. Plant Physiol. 129, 1695-1699.

Jarvis, M.C., Apperley, D.C. (1995) Chain conformation in concentrated pectic gels: Evidence from 13C NMR. Carbohydr. Res. 275, 131-145.

Jenkins, J., Mayans, O., Smith. D., Worboys, K., Pickersgill, R.W. (2001) Three-dimensional structure of Erwinia chrysanthemi pectin methylesterase reveals a novel esterase active site. J Mol Biol. 305(4): 951-960.

Jiang, L., Yang, S.L., Xie, L.F., Puah, C.S., Zhang, X.Q., Yang, W.C., Sundaresan, V., Ye, D. (2005) VANGUARD1 encodes a pectin methylesterase that enhances pollen tube growth in the *Arabidopsis* style and transmitting tract. Plant Cell. 2, 584-596.

Johansson, K., El-Ahmad, M., Friemann, R., Jornvall, H., Markovic, O and Eklund, H. (2002) Crystal structure of plant pectin methylesterase. FEBS Lett. 514, 243-249.

Jolie, R.P., Duvetter, T., Van Loey, A.M., Hendrickx, M.E. (2010) Pectin methylesterase and its proteinaceous inhibitor: a review. Carbohydr. Res. 345(18), 2583-2595.

Juge, N. (2006) Plant protein inhibitors of cell wall degrading enzymes. Trends Plant Sci. 7, 359-367.

Karimi, M., Inzé, D., Depicker, A. (2002) Gateway vectors for *Agrobacterium* mediated plant transformation. Trends Plant Sci. 7, 193–195.

Keegstra K. (2010) Plant cell walls. Plant Physiol. 154(2): 483-486.

Keegstra, K., Talmadge, K.W., Talmadge, K.W., Bauer, W.D. Albersheim, P. (1973) The structure of plant cell walls: III. A model of the walls of suspension-cultured sycamore cells based on the interconnections of the macromolecular components. Plant Physiol. 51, 188-197.

Klavons, J.A., Bennett, R.D. (1986). Determination of methanol using alcohol oxidase and its application to methyl ester content of pectins. J. Agric. Food Chem. 34, 597–599.

Knox, J.P. (2008) Revealing the structural and functional diversity of plant cell walls. Curr. Opin. Plant Biol. 11, 308–313.

Knox, J.P., Linstead, P.J., King, J., Cooper, C., Roberts, K. (1990) Pectin esterification is spatially regulated both within cell walls and between developing tissues of root apices. Planta. 181, 512–521.

Kunst, L., Taylor, D.C., Underhill, E.W. (1992) Fatty acid elongation in developing seeds of *Arabidopsis thaliana*. Plant Physiol. Biochem. 30, 425–434.

Kuromori. T., Hirayama, T., Kiyosue, Y., Takabe, H., Mizukado, S., Sakurai, T., Akiyama, K., Kamiya, A., Ito, T., Shinozaki. K. (2004) A collection of 11800 single-copy Ds transposon insertion lines in *Arabidopsis*. Plant J. 37, 897-905.

Kuromori, T., Wada, T., Kamiya, A., Yuguchi, M., Yokouchi, T., Imura, Y., Takabe, H., Sakurai, T., Akiyama, K., Hirayama, T., Okada, K., Shinozaki, K. (2006) A trial of phenome analysis using 4000 Ds-insertional mutants in gene-coding regions of *Arabidopsis*. Plant J. 47, 640-651.

Lau, J.M., McNeil, M., Darvill, A.G., Albersheim, P. (1985) Structure of the backbone of rhamnogalacturonan I, a pectic polysaccharide in the primary cell walls of plants. Carbohydr. Res. 137, 111-125.

Le, B.H., Cheng, C., Bui, A.Q., Wagmaister, J.A., Henry, K.F., Pelletier, J., Kwong, L., Belmonte, M., Kirkbride, R., Horvath, S., Drews, G.N., Fischer, R.L., Okamuro, J.K., Harada, J.J., Goldberg, R.B. (2010) Global analysis of gene activity during Arabidopsis seed development and identification of seed-specific transcription factors. Proc Natl Acad Sci U S A. 107(18): 8063-8070.

Leubner-Metzger, G. (2002) Seed after-ripening and over-expression of class I b-1,3-glucanase confer maternal effects on tobacco testa rupture and dormancy release. Planta. 215, 959–968.

Leubner-Metzger, G., Fründt, C., Vögeli-Lange, R., Meins, F.Jr. (1995) Class I b-1,3-glucanases in the endosperm of tobacco during germination. Plant Physiol. 109, 751–759.

Liners, F., Letesson, J., Didembourg, C. Van Cutsem, P. (1989) Monoclonal antibodies against pectin: Recognition of a conformation induced by calcium. Plant Physiol. 91, 1419-1424.

Linkies, A., Graber, K., Knight, C., Leubner-Metzger, G. (2010) The evolution of seeds. New Phytologist. 186, 817–831.

Lionetti, V., Cervone, F., Bellincampi, D. (2012) Methyl esterification of pectin plays a role during plant-pathogen interactions and affects plant resistance to diseases. Plant Physiol. 169, 1623-1630.

Lionetti, V., Francocci, F., Ferrari, S., Volpi, C., Bellincampi, D., Galletti, R., D'Ovidio, R., De Lorenzo, G., Cervone, F. (2010) Engineering the cell wall by reducing de-methyl-esterified homogalacturonan improves saccharification of plant tissues for bioconversion. Proc. Natl. Acad. Sci. USA 107(2), 616–21.

Lionetti, V., Raiola, A., Camardella, L., Giovane, A., Obel, N., Pauly, M., Favaron, F., Cervone, F., Bellincampi, D. (2007) Overexpression of pectin methylesterase inhibitors in *Arabidopsis* restricts fungal infection by *Botrytis cinerea*. Plant Physiol. 143(4), 1871–1880.

Liu, P.P., Koizuka, N., Homrichhausen, T.M., Hewitt, J.R., Martin, R.C., Nonogaki, H. (2005) Large-scale screening of *Arabidopsis* enhancer-trap lines for seed germination-associated genes. Plant J. 41, 936–944

Louvet, R., Cavel, E., Gutierrez, L., Guenin, S., Roger, D., Gillet, F., Guerineau, F., Pelloux, J. (2006) Comprehensive expression profiling of the pectin methylesterase gene family during silique development in *Arabidopsis thaliana*. Planta. 224, 782-791.

Macquet, A., Ralet, M.C., Kronenberger, J., Marion-Poll, A., North, H.M. (2007) *In situ*, chemical and macromolecular study of the composition of Arabidopsis thaliana seed coat mucilage. Plant Cell Physiol. 48(7): 984-999.

Manz., B., Müller., K., Kucera, B., Volke, F., Leubner-Metzger, G. (2005) Water uptake and distribution in germinating tobacco seeds investigated *in vivo* by nuclear magnetic resonance imaging. Plant Physiol. 138, 1538–1551

Markovic, O., Kohn, R. (1984) Mode of pectin deesterification by trichoderma reesei pectinesterase. Experientia. 40, 842-843.

McQueen-Mason, S., Cosgrove, D.J. (1994) Disruption of hydrogen bonding between plant cell wall polymers by proteins that induce wall extension. Proc. Natl. Acad. Sci. 91, 6574–6578.

Micheli, F. (2001) Pectin methylesterases: Cell wall enzymes with important roles in plant physiology. Trends Plant Sci. 6, 414-419.

Micheli, F., Sundberg, B., Goldberg, R., Richard, L. (2000) Radial distribution pattern of pectin methylesterases across the cambial region of hybrid aspen at activity and dormancy. Plant Physiol. 124(1), 191-199.

Minic, Z., Jamet, E., San-Clemente, H., Pelletier, S., Renou, J.P., Rihouey, C., Okinyo, D.P., Proux, C., Lerouge, P., Jouanin, L. (2009) Transcriptomic analysis of Arabidopsis developing stems: a close-up on cell wall genes. BMC Plant Biol. 16(9): 1-6.

Mohnen, D. (1999) Biosynthesis of pectins and galactomannans. In Baron, D., & Nakanishi, K. (Editors), Comprehensive natural products chemistry. Amstersam: Elsevier Science.

Mouille, G., Ralet, M.C., Cavelier, C., Eland, C., Effroy, D., Hematy, K., McCartney, L., Truong, H.N., Gaudon, V., Thibault, J.F., Marchant, A., Hofte, H. (2007) Homogalacturonan synthesis in *Arabidopsis thaliana* requires a

golgi-localized protein with a putative methyltransferase domain. Plant J. 50, 605-614.

Moustacas, A.M., Nari, J., Borel, M., Noat, G., Ricard, J. (1991) Pectin methylesterase, metal ions and plant cell-wall extension. The role of metal ions in plant cell-wall extension. Biochem J. 279, 351-354.

Müller, K., Levesque-Tremblay, G., Bartels, S., Weitbrecht, K., Wormit, A., Usadel, B., Haughn, G., Kermode, A.R. (2013) Demethylesterification of cell wall pectins in *Arabidopsis* plays a role in seed germination. Plant Physiol. 161(1): 305-316.

Müller K, Tintelnot S, Leubner-Metzger G (2006) Endosperm-limited *Brassicaceae* seed germination: abscisic acid inhibits embryo-induced endosperm weakening of Lepidium sativum (cress) and endosperm rupture of cress and *Arabidopsis thaliana*. Plant Cell Physiol. 47, 864–877.

Nakabayashi, K., Okamoto, M., Koshiba, T., Kamiya, Y., Nambara, E. (2005) Genome-wide profiling of stored mRNA in *Arabidopsis thaliana* seed germination: epigenetic and genetic regulation of transcription in seed. Plant J. 41, 697–709.

Nakamura, A., Furuta, H., Maeda, H., Takao, T., Nagamatsu, Y. (2002) Structural studies by stepwise enzymatic degradation of the main backbone of soybean soluble polysaccharides consisting of galacturonan and rhamnogalacturonan. Biosci. Biotechnol. Biochem. 66, 1301-1313.

Narsai, R., Law, S.R., Carrie, C., Xu, L., Whelan, J. (2011) In-depth temporal transcriptome profiling reveals a crucial developmental switch with roles for RNA processing and organelle metabolism that are essential for germination in *Arabidopsis*. Plant Physiol. 157(3), 342-362.

Nielsen, K., Boston, R.S. (2001) RIBOSOME-INACTIVATING PROTEINS: A plant perspective. Annu. Rev. Plant Physiol. Plant Mol. Biol. 52, 785-816.

Nonogaki, H., Gee, O.H., Bradford, K.J. (2000) A germination-specific endob-mannanase gene is expressed in the micropylar endosperm cap of tomato seeds. Plant Physiol. 123, 1235–1246.

Obroucheva, N.V., Antipova, O.V. (1997) Physiology of the initiation of seed germination. Russian Journal of Plant Physiology. 44, 250–264.

Ohto, M.A., Floyd, S.K., Fischer, R.L., Goldberg, R.B. and Harada, J.J. (2009) Effects of APETALA2 on embryo, endosperm, and seed coat development determine seed size in *Arabidopsis*. Sex Plant Reprod. 22, 277-289.

O'Neill, M.A., Ishii, T., Albersheim, P., Darvill, A.G. (2004) Rhamnogalacturonan II: structure and function of a borate cross-linked cell wall pectic polysaccharide. Annu. Rev. Plant Biol. 55, 109-39.

Peaucelle A, Braybrook SA, Höfte H (2012) Cell wall mechanics and growth control in plants: the role of pectins revisited. Front. Plant Sci. 3, 121.

Peaucelle, A., Louvet, R., Johansen, J.N., Höfte, H., Laufs, P., Pelloux, J., Mouille, G. (2008) *Arabidopsis* phyllotaxis is controlled by the methyl-esterification status of cell-wall pectins. Curr. Biol. 18(24), 1943-1948.

Peaucelle, A., Louvet, R., Johansen, J.N., Salsac, F., Morin, H., Fournet, F., Belcram, K., Gillet, F., Höfte, H., Laufs, P., Mouille, G., Pelloux, J. (2011) The transcription factor BELLRINGER modulates phyllotaxis by regulating the expression of a pectin methylesterase in *Arabidopsis*. Development. 138(21), 4733-4741.

Pelletier. S., Van Orden, J., Wolf, S., Vissenberg, K., Delacourt, J., Ndong, Y.A., Pelloux, J., Bischoff, V., Urbain, A., Mouille, G., Lemonnier, G., Renou, J.P., Höfte, H. (2010) A role for pectin de-methylesterification in a developmentally regulated growth acceleration in dark-grown *Arabidopsis* hypocotyls. New Phytol. 188(3), 726-739.

Pelloux, J., Rusterucci, C., and Mellerowicz, E.J. (2007) New insights into pectin methylesterase structure and function. Trends Plant Sci. 6, 267-277.

Phan, T.D., Bo, W., West, G., Lycett, G.W., Tucker, G.A. (2007) Silencing of the major salt-dependent isoform of pectinesterase in tomato alters fruit softening. Plant Physiol. 144(4), 1960-1967.

Pilling, J., Willmitzer, L., Bücking, H., Fisahn, J. (2004) Inhibition of a ubiquitously expressed pectin methyl esterase in *Solanum tuberosum L.* affects plant growth, leaf growth polarity, and ion partitioning. Planta. 219(1): 32-40.

Pina. C., Pinto, F., Feijó, J.A., Becker, J.D. (2005) Gene family analysis of the Arabidopsis pollen transcriptome reveals biological implications for cell growth, division control, and gene expression regulation. Plant Physiol. 2005 138(2): 744-756.

Pinzón-Latorre, D., Deyholos, M.K. (2013) Characterization and transcript profiling of the pectin methylesterase (PME) and pectin methylesterase inhibitor (PMEI) gene families in flax (*Linum usitatissimum*). BMC Genomics. 14(1), 742.

Qu. T., Liu, R., Wang, W., An, L., Chen, T., Liu, G., Zhao, Z. (2011) Brassinosteroids regulate pectin methylesterase activity and *AtPME41* expression in *Arabidopsis* under chilling stress. Cryobiology. 63(2), 111-117**.**

Raiola, A., Camardella, L., Giovane, A., Mattei, B., De Lorenzo, G., Cervone, F., Bellincampi, D. (2004) Two *Arabidopsis thaliana* genes encode functional pectin methylesterase inhibitors. FEBS Lett. 557, 199–203.

Raiola, A., Lionetti, V., Elmaghraby, I., Immerzeel, P., Mellerowicz, E.J., Salvi, G., Cervone, F., Bellincampi, D. (2011) Pectin methylesterase is induced in *Arabidopsis* upon infection and is necessary for a successful colonization by necrotrophic pathogens. Mol. Plant Microbe Interact. 24(4), 432-440.

Rautengarten, C., Usadel, B., Neumetzler, L., Hartmann, J., Büssis, D., Altmann, T. (2008) A subtilisin-like serine protease essential for mucilage release from *Arabidopsis* seed coats. Plant J. 54(3), 466-480

Ren, C., Kermode, A.R. (1999) Analyses to determine the role of the megagametophyte and other seed tissues in dormancy maintenance of yellow cedar (*Chamaecyparis nootkatensis*) seeds: morphological, cellular and physiological changes following moist chilling and during germination. J. Exp. Bot. 50, 1403–1419.

Ren, C., Kermode, A.R. (2000) An increase in pectin methyl esterase activity accompanies dormancy breakage and germination of yellow cedar seeds. Plant Physiol. 124, 231–242.

Rensing, K.H., Samuels, A.L., Savidge, R.A. (2002) Ultrastructure of vascular cambial cell cytokinesis in pine seedlings preserved by cryofixation and substitution. Protoplasma. 220, 39–49.

Ridley, B., O'Neill, M.A., Mohnen, D. (2001) Pectins: Structure, biosynthesis, and oligogalacturonide-related signaling. Phytochemistry. 57, 929-967.

Rocchi, V., Janni, M., Bellincampi, D., Giardina, T., D'Ovidio, R. (2012) Intron retention regulates the expression of pectin methyl esterase inhibitor (Pmei) genes during wheat growth and development. Plant. Biol. (Stuttg). 14, 365–373.

Röckel, N., Wolf, S., Kost, B., Rausch, T., Greiner, S. (2008) Elaborate spatial patterning of cell-wall PME and PMEI at the pollen tube tip involves PMEI endocytosis, and reflects the distribution of esterified and de-esterified pectins. Plant J. 53(1): 133-143.

Rozen, S., Skaletsky, H.J. (2000) Primer3 on the WWW for general users and for biologist programmers. In S Krawetz, S Misener, eds, Bioinformatics Methods and Protocols: Methods in Molecular Biology. Humana Press, Totowa, NJ, 365–386.

Ruben, P.J., Duvetter, T., Van Loey, A.M., Hendrickx, M.E. (2010) Pectin methylesterase and its proteinaceous inhibitor: a review. Carbohydrate Res. 345, 2583-2595.

Rustérucci, C., Guerineau, F., Van Wuytswinkel, O., Gillet, F., Driouich, A., Lerouge, P., Gutierrez, L., Pelloux, J. (2011) Identification of pectin methylesterase 3 as a basic pectin methylesterase isoform involved in adventitious rooting in *Arabidopsis thaliana*. New Phytol. 192(1), 114-126.

Ruuska, S.A., Girke, T., Benning, C., Ohlrogge, J.B. (2002) Contrapuntal networks of gene expression during Arabidopsis seed filling. Plant Cell. 14(6): 1191-1206.

Saez-Aguayo, S., Ralet, M.C., Berger, A., Botran, L., Ropartz, D., Marion-Poll, A., North, H.M. (2013) PECTIN METHYLESTERASE INHIBITOR6 promotes *Arabidopsis* mucilage release by limiting methylesterification of homogalacturonan in seed coat epidermal cells. Plant Cell. 25(1), 308-323.

Sanchez, R.A., de Miguel, L. (1997) Phytochrome promotion of mannandegrading enzymes in the micropylar endosperm of *Datura ferox* L. seeds and its relationship with germination. J. Exp. Bot. 37, 1574–1580.

Schmohl, N., Pilling, J., Fisahn, J., Horst, W.J. (2000) Pectin methylesterase modulates aluminium sensitivity in *Zea mays* and *solanum tuberosum*. Plant Physiol. 109, 419-427.

Schopfer, P. (2006) Biomechanics of plant growth. Am J Bot. 93(10): 1415-1425.

Scognamiglio, M.A., Ciardiello, M.A., Tamburrini, M., Carratore, V., Rausch, T.L., Camardella, L. (2003) The plant invertase inhibitor shares structural properties and disulfide bridges arrangement with the pectin methylesterase inhibitor. J. Protein Chem. *22*, 363-369.

Siedlecka, A., Wiklund, S., Péronne, M.A., Micheli, F., Lesniewska, J., Sethson, I., Edlund, U., Richard, L., Sundberg, B., Mellerowicz, E.J. (2008) Pectin methyl esterase inhibits intrusive and symplastic cell growth in developing wood cells of *Populus*. Plant Physiol. 146(2), 554-565.

Sliwinska, E., Bassel, G.W., Bewley, J.D. (2009) Germination of Arabidopsis thaliana seeds is not completed as a result of elongation of the radicle but of the adjacent transition zone and lower hypocotyl. J Exp Bot. 60(12): 3587-3594.

Somerville, C., Bauer, S., Brininstool, G., Facette, M., Hamann, T., Milne, J., Osborne, E., Paredez, A., Persson, S., Raab, T., Vorwerk, S., and Youngs, H. (2004) Toward a systems approach to understanding plant cell walls. Science. 306, 2206–2211.

Staehelin, L.A., Moore, I. (1995) The plant golgi apparatus: Structure, functional organization and trafficking mechanisms. Annu. Rev. Plant Physiol. Plant Mol. Biol. 46, 261-288.

Steber, C.M., McCourt, P. (2001) A role for brassinosteroids in germination in *Arabidopsis*. Plant Physiol. 125, 763–769.

Sterling, J.D., Atmodjo, M.A., Inwood, S.E., Kumar Kolli, V.S., Quigley, H.F., Hahn, M.G., Mohnen, D. (2006) Functional identification of an *Arabidopsis* pectin biosynthetic homogalacturonan galacturonosyltransferase. Proc. Natl. Acad. Sci. USA. 103, 5236-5241.

Sterling, J.D., Quigley, H.F., Orellana, A., Mohnen, D. (2001) The catalytic site of the pectin biosynthetic enzyme alpha-1,4-galacturonosyltransferase is located in the lumen of the Golgi. Plant Physiol. 127, 360-371.

Sun, X., Shantharaj, D., Kang, X., Ni, M. (2010) Transcriptional and hormonal signaling control of *Arabidopsis* seed development. Curr. Opin. Plant Biol. 13, 611–620.

Talmadge, K.W., Keegstra, K., Bauer, W.D, Albersheim, P. (1973) The structure of plant cell walls: the macromolecular components of the walls of suspension-cultured sycamore cells with a detailed analysis of the pectic polysaccharides. Plant Physiol. 51, 158-173.

Tan. L., Eberhard, S., Pattathil, S., Warder, C., Glushka, J., Yuan, C., Hao, Z., Zhu, X., Avci, U., Miller, J.S., Baldwin, D., Pham, C., Orlando, R., Darvill, A., Hahn, M.G., Kieliszewski, M.J, Mohnen, D. (2013) An *Arabidopsis* cell wall proteoglycan consists of pectin and arabinoxylan covalently linked to an arabinogalactan protein. Plant Cell. 25(1), 270-287.

The Arabidopsis Genome initiative (2000) Analysis of the genome sequence of the flowering plant *Arabidopsis thaliana*. Nature. 408, 796-815.

Tian, G.W., Chen, M.H., Zaltsman, A., Citovsky, V. (2006) Pollen-specific pectin methylesterase involved in pollen tube growth. Ev. Biol. 294, 83-91.

van den Hoogen, B.M., van Weeren, P.R., Lopes-Cardozo, M., van Golde, L.M., Barneveld, A., van de Lest, C.H. (1998) A microtiter plate assay for the determination of uronic acids. Anal Biochem. 257(2): 107-111.

Voiniciuc, C., Dean, G.H., Griffiths, J.S., Kirchsteiger, K., Hwang, Y.T., Gillett, A., Dow., G., Western, T.L., Estelle, M., Haughn, G.W. (2013) Flying saucer1 is a transmembrane RING E3 ubiquitin ligase that regulates the degree of pectin methylesterification in Arabidopsis seed mucilage. Plant Cell. 25(3):944-59.

Wakabayashi, K., Hoson, T., Huber, D.J. (2003) Methyl de-esterification as a major factor regulating the extent of pectin depolymerization during fruit ripening: a comparison of the action of avocado (*Persea americana*) and tomato (*Lycopersicon esculentum*) polygalacturonases. J. Plant Physiol. 160, 667–673.

Wang, M., Yuan, D., Gao, W., Li, Y., Tan, J., Zhang, X. (2013) A comparative genome analysis of PME and PMEI families reveals the evolution of pectin metabolism in plant cell walls. PLoS One. 8(8), 1-12.

Weber, M., Deinlein, U., Fischer, S., Rogowski, M., Geimer, S., Tenhaken, R., Clemens, S. (2013) A mutation in the *Arabidopsis thaliana* cell wall biosynthesis gene pectin methylesterase 3 as well as its aberrant expression cause hypersensitivity specifically to Zn. Plant J. 76(1), 151-64.

Weitbrecht, K., Müller, K., Leubner-Metzger, G. (2011) First off the mark: early seed germination. J. Exp. Bot. 62, 3289–3309.

Western, T.L., Burn, J., Tan, W.L., Skinner, D.J., Martin-McCaffrey, L., Moffattm, B.A., Haughn, G.W. (2001). Isolation and characterization of mutants defective in seed coat mucilage secretory cell development in *Arabidopsis*. Plant Physiol. 127, 998-1011.

Western, T.L., Skinner, D.J., Haughn, G.W. (2000) Differentiation of Mucilage Secretory Cells of the Arabidopsis Seed Coat. Plant Physiol. 122(2), 345–355.

Western, T.L., Young, D.S., Dean, G.H., Tan, W.L., Samuels, A.L., Haughn, G.W. (2004) MUCILAGE-MODIFIED4 encodes a putative pectin biosynthetic enzyme developmentally regulated by APETALA2, TRANSPARENT TESTA GLABRA1, and GLABRA2 in the *Arabidopsis* seed coat. Plant Physiol. 134, 296-306.

Willats, W.T.G., Limberg, G., Bucholt, H.C., Van Alebeek, G.-J., Benen J., Christensen, T.M.I.E., Visser, J., Voragen, A., Mikkelsen, J.D., Knox, J.P., (2000) Analysis of pectic epitopes recognized by conventional and phage display monoclonal antibodies using defined oligosaccharides, polysaccharides and enzymatic degradation. Carbohydrate Research, 327, 309-320.

Willats, W.T.G., McCartney, L. Knox J.P. (2001) *In-situ* analysis of pectic polysaccharides in seed mucilage and at the root surface of *Arabidopsis thaliana*. Planta, 213, 37-44.

Winter, D., Vinegar, B., Nahal, H., Ammar, R., Wilson, G.V., Provart, N.J. (2007) An "Electronic Fluorescent Pictograph" browser for exploring and analyzing large-scale biological data sets. PLoS ONE. 2, e718.

Wolf. S., Grsic-Rausch. S., Rausch, T., Greiner, S. (2003) Identification of pollen-expressed pectin methylesterase inhibitors in *Arabidopsis*. FEBS Lett. 555, 551–555.

Wolf, S., Mouille, G., Pelloux, J. (2009) Homogalacturonan methyl-esterification and plant development. Mol. Plant. 5, 851-860.

Wolf, S., Mravec, J., Greiner, S., Mouille, G., Höfte, H. (2012) Plant cell wall homeostasis is mediated by brassinosteroid feedback signaling. Curr. Biol. 22(18), 1732-1737.

Wu, Y., Spollen, W.G., Sharp, R.E., Hetherington, P.R., Fry, S.C. (1994) Root growth maintenance at low water potentials: increased activity of xyloglucan endotransglycosylase and its possible regulation by abscisic acid. Plant Physiol. 106, 607–615.

Yoneda, A., Ito, T., Higaki, T., Kutsuna, N., Saito, T., Ishimizu, T., Osada, H., Hasezawa, S., Matsui, M., Demura, T. (2010) Cobtorin target analysis reveals that pectin functions in the deposition of cellulose microfibrils in parallel with cortical microtubules. Plant J. 64(4), 657-67.

York, W.S., Kumar Kolli, V.S., Orlando, R., Albersheim, P., Darvill, A.G. (1996) The structures of arabinoxyloglucans produced by solanaceous plants. Carbohydr. Res. 285, 99-128.

Yu, X., Li, L., Zola, J., Aluru, M., Ye, H., Foudree, A., Guo, H., Anderson, S., Aluru, S., Liu, P., Rodermel, S., Yin, Y. (2011) A brassinosteroid transcriptional network revealed by genome-wide identification of BESI target genes in *Arabidopsis thaliana*. Plant J. 65(4), 634-646.

Zablackis, E., Huang, J., Muller, B., Darvill, A.G., Albersheim, P. (1995) Characterization of the cell-wall polysaccharides of *Arabidopsis thaliana* leaves. Plant Physiol. 107, 1129-1138.

Zhao, S., Fernald, R.D. (2005) Comprehensive algorithm for quantitative realtime polymerase chain reaction. J. Comput. Biol. 12, 1047–1064.

Zhang, G.F., Staehelin, L.A. (1992) Functional compartmentation of the golgi apparatus of plant cells: immunocytochemical analysis of high-pressure frozen- and freeze substituted sycamore maple suspension culture cells. Plant Physiol. 99, 1070-1083.

Zhong, J., Ren, Y., Yu, M., Ma, T., Zhang, X., Zhao, J. (2011) Roles of arabinogalactan proteins in cotyledon formation and cell wall deposition during embryo developmentof *Arabidopsis*. Protoplasma. 248, 551–563.

Appendix A – Whole seed mucilage immunolabeling

Introduction

The gene *HMS* is specifically up-regulated in the seed coat at 7 DPA, which corresponds to the timing and location of mucilage biosynthesis and secretion. The *hms-1* x wt F1 complement the *hms-1* phenotype supporting that the *hms-1* embryo phenotype indirectly causes most if not all of the observable mucilage extrusion phenotype. Nevertheless, a subtle mucilage phenotype may be visible using whole seed mucilage immunolabeling.

Methodology:

Whole seed immunolabeling was conducted according to Harpaz-Saad et al., 2011. JIM5 and JIM7 (CarboSource) primary antibodies were used with Goat-anti-rat secondary antibody conjugated to Alexafluor488 (Molecular Probes, Invitrogen). The 2F4 (PlantProbes) primary antibody was used with Goat-anti-mouse secondary antibody conjugated with Alexafluor488 (Molecular Probes, Invitrogen). Seeds were imaged using a 488-nm laser (antibody fluorescence) and 561-nm laser (seed intrinsic fluorescence, background) on a Zeiss 510 Meta laser scanning confocal microscope (Carl Zeiss) or a Perkin-Elmer Ultraview VoX spinning disk confocal system. All confocal micrographs were processed with ImageJ (Abramoff et al., 2004). Images containing signals from multiple optical stacks were rendered using the Z-project maximum intensity method. The Degree of methyl esterification was calculated as a percentage molar ratio of methanol released after cell wall saponification (Lionetti et al., 2007) to uronic acids measured using the m-hydroxydiphenyl assay (van den Hoogen et al., 1998). Mucilage was extracted by vigorously shaking seeds in 50 mM EDTA for 1 h.

Results and discussion

The *hms-1* embryo phenotype indirectly causes most if not all of the observable mucilage extrusion phenotype. I also examined the role of the seed coat and embryo in determining differences in the degree of methyl esterification of mucilage between wild type and *hms-1*. Mature hydrated seeds of wild type, *hms-1*, *hms-1* x wt F1, and *hms-1* transformed with *pHMS:HMS* were immunolabelled with three different anti-HG antibodies including JIM5, JIM7 and 2F4. JIM7 binds to heavily (35 to 81%) methylesterified HG (Knox et al., 1990), and JIM5 binds partially (up to 40%) methylesterified HG (Vandenbosch et al., 1989). 2F4 is an antibody that specifically binds unesterified blocks of HG cross-linked by Ca2+ ions (Liners et al., 1989). JIM5 and JIM7 recognize partially overlapping domains within seed mucilage and both labeled smaller and irregular regions in *hms-1* as compared to WT seeds (A, B, E, F). 2F4 only labeled primary cell wall material in wild-type seeds and labeling is lower in *hms-1* seeds as compare to WT (I, J). When the *hms-1* mutant was used as the female parent in a cross with WT, the F1 seeds have a seed coat that is homozygous for *hms-1* and an embryo that is heterozygous. The labeling of the F1 seed mucilage using JIM5, JIM7 and 2F4 is comparable to that of WT (C, G, K) supporting the hypothesis that differences in labeling of *hms-1* versus wild type is due to loss of HMS function in the embryo. Similar results were obtained for the *pHMS:HMS* transformed *hms-1* seeds (D,H,L).

To further exclude the possibility that alterations in methyl esterification of *hms-1* seed mucilage, the degree of methyl esterification was determined using biochemical assays. Compared to wild type, a higher degree of methyl esterification was observed in *hms-1* but not in the hms-1 x wild type F1 or the *pHMS:HMS* transformed *hms-1* seed mucilage (M). These data support the hypothesis that the observed change in the degree of methylesterification of *hms-1* relative to wild type is due to loss of HMS function in the embryo.

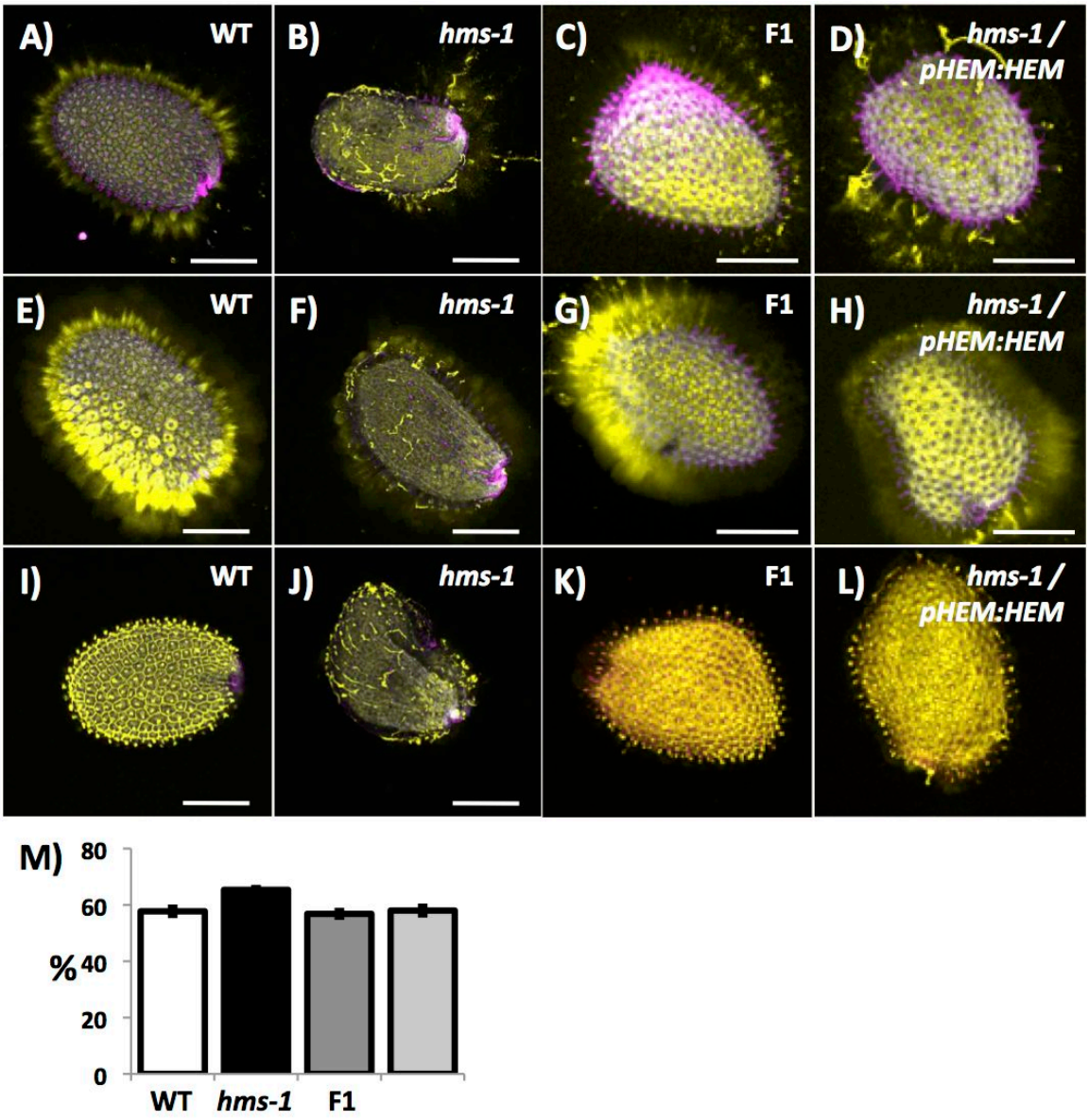

Figure 1: Immunolabeling and biochemical analysis to determine the degree of pectin methyl esterification in seed mucilage.

(A) to (D) JIM5 immunolabeling (yellow) of highly unesterified HG and seed intrinsic fluorescence (magenta). (E) to (H) JIM7 immunolabeling (yellow) of lowly unesterified HG and seed intrinsic fluorescence (magenta). (I) to (L) 2F4 immunolabeling (yellow) of unesterified HG bond to Ca^{2+} and seed intrinsic fluorescence (magenta). WT seed in (A), (E), (I). *hms-1* seed in (B), (F), (G). F1 seed in (C), (G), (K). hms-1 / pHMS:HMS seed in (D), (H), (L). (M) Biochemical determination of degree of methylesterification in mucilage. Asterisks indicate significant difference using a Students t-test with a Bonferroni correction ($P < 0.05$). Values represent the mean ± SE of 4 replicates.

Appendix B – Localization of YFP-HMS and HMS-YFP proteins

Introduction

The lack of complementation of *hms-1* seed phenotype by the construct pro_{HMS}*:HMS::YFP* with *YFP* fused in frame to the in C-terminus prompted us to generate another construct pro_{HMS}*:PP::YFP::HMS* with *YFP* positioned after the putative pre-pro domain. I investigated the localization of HMS using both constructs pro_{HMS}*:HMS::YFP* and pro_{HMS}*:PP::YFP::HMS*.

Methodology:

Developing 4, 7, 10 DPA pro_{HMS}*:HMS::YFP* and *pHMS:pp:YFP::HMS* seeds were mounted with water between a glass slide and a coverslip. Images were captured in darkness immediately. Imaging was performed on an Olympus FV1000 laser scanning confocal microscope using a 63× numerical aperture oil-immersion objective. All image processing was performed using Olympus Fluoview software and Velocity. All confocal micrographs were processed and measured using ImageJ (Albramoff et al., 2004).

Results and discussion

We investigated the localization of the resultant HMS-YFP and YFP-HMS proteins. Fluorescence was not observed in the pro_{HMS}*:HMS::YFP* and pro_{HMS}*:PP::YFP::HMS* plants at 4 DPA in either seed coat or embryo cells (A, D, G, J). 7 and 10 DPA pro_{HMS}*:HMS::YFP* and pro_{HMS}*:PP::YFP::HMS* plants showed YFP localization in the epidermal cell layer of the seed coat (B, C, H, I) as well as multiple cell layers of the embryo (E, F, K, L). Both protein fusions had similar temporal, spatial and intracellular localization patterns in the seed.

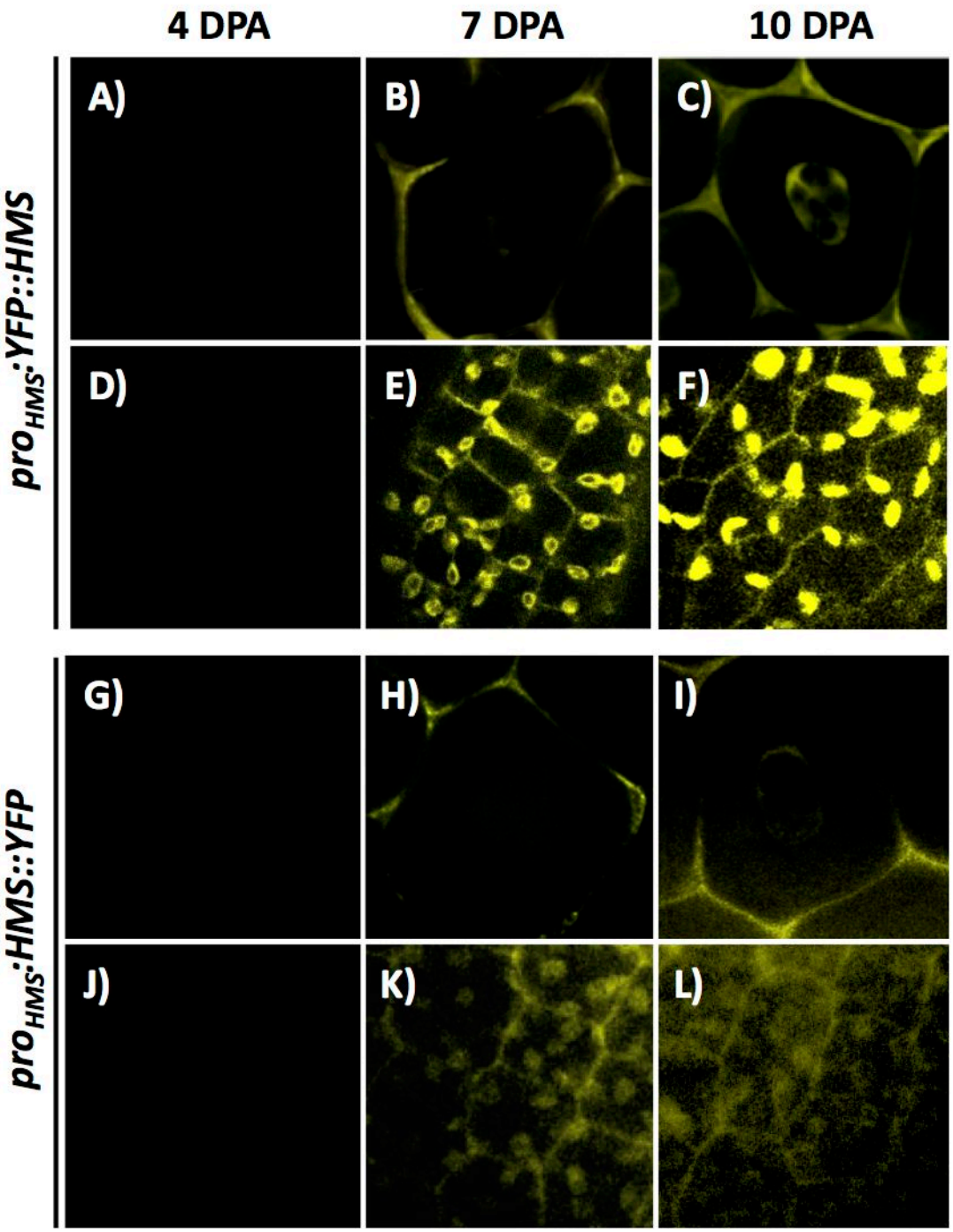

Figure 2: Localization of YFP-HMS and HMS-YFP in seed coat and embryo cells. (A) to (F) YFP signal in the plant transformed with proHMS:YFP::HMS at 4,7 and 10 DPA. (G) to (L) YFP signal in plants transformed with proHMS:HMS::YFP at 4,7 and 10 DPA. Developing seed coat epidermal cells in (A), (B), (C), (G), (H) and (I) and developing embryo cells in (D), (E), (F), (J), (K) and (L).

Appendix C – PME activity of yeast expressing HMS

Introduction

In an attempt to generate a biochemically active HMS enzyme, we transformed the yeast *Saccharomyces cerevisia* with pESC-URA-HMS and pESC-URA-ΔHMS.

Methodology:

HMS and ΔHMS were cloned into the pESC-URA yeast (Saccharomyces cerevisiae) expression vector (Agilent). Transgenic yeast cells were grown on synthetic complete (SC) selection medium (Sherman, 2002) lacking the appropriate amino acids. Individual cell lines were selected from each transgenic strain for induction of transgene expression. For immunoblot analyses, protein samples were separated on 12% SDS–PAGE gels, and detection was performed using the anti-myc antibody (Invitrogen) (1:1000) and alkaline phosphatase conjugates antibody (Sigma) (1:5000). Pectin Methyl Esterase activity was assayed using a modified version of a previously published method (Grsic-Rausch and Rausch, 2004), see chapter 2.

Results and discussion

pESC-URA-HMS contain the coding region for the full-length version of HMS including the pre-pro domain while pESC-URA-ΔHMS contain only the sequence encoding the mature enzyme after the putative pre-pro domain cleavage site (A). Immunological detection of HMS::myc and ΔHMS::myc protein fusions reveal a double band at ~60-65 kDa for HMS::myc and a single band at ~38 kDa for ΔHMS::myc (B). Yeast *Saccharomyces cerevisia* crude protein extracts transformed with pESC-URA-HMS, pESC-URA-ΔHMS or the empty vector pESC-URA had no detectable PME activity (C). By comparison, 5μL of *Arabidopsis* seed protein extract as a positive control shows significant PME activity (C).

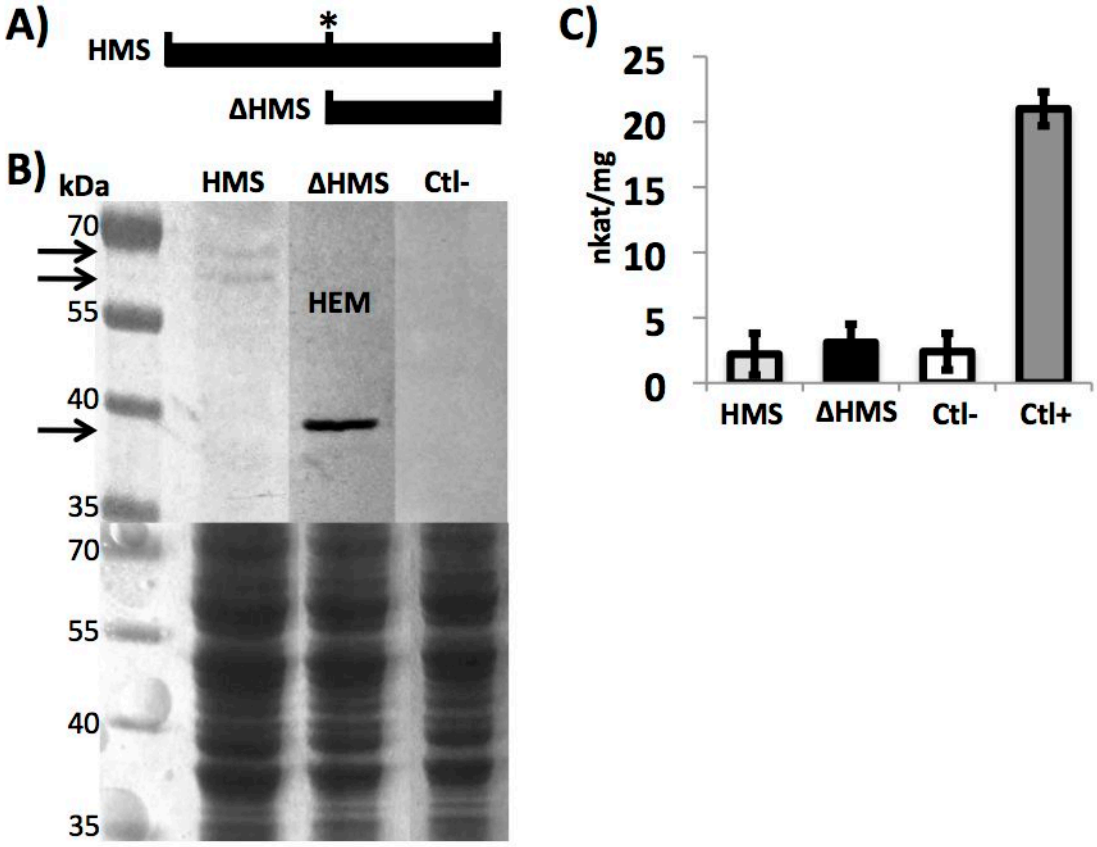

Figure 3: Immunological detection and PME activity of yeast expressing HMS and ΔHMS.

(A) PME activity of yeast transformed with a plasmid carrying either full-length HMS (HMS) or the mature HMS (ΔHMS). The putative cleavage site is marked by a *. (B) Immunological detection of HMS::myc and ΔHMS::myc. Arrows denote the predicted sizes. (C) PME activity in nkat/mg of crude protein extracts from yeast strain transformed with HMS, ΔHMS and the empty vector (Ctl-) as well as plant seed protein extracts (Ctl+). Values are means for n = 4.

Appendix D – Young's modulus (EA) from atomic force microscopy

Introduction

In a first effort to assess the consequence of the lack of PME activity in *hms-1* on the rigidity of the tissue, I performed Atomic Force Microscopy (AFM) to measure the apparent Young's modulus map.

Methodology:

The composite cell wall mechanics of the *A. thaliana* embryo was measured by mapping the apparent Young's modulus (E_A) with a MultiMode 8 Atome Force Microscope (Bruker). We used SCANASYST-AIR 70kHz probe with a spring constant of 0.40N/m (Bruker). The map shows data from successive maps of 1000 nm scan at a rate of 0.977 Hz on DMT Modulus mode with an amplitude set point of 250.00 mV. For special treatment, samples were plasmolyzed in 10% (0.55 M) mannitol prior to measurement.

Results and discussion

The map shows data from two successive maps using the same probe allowing comparisons between samples. Due to the stickiness and irregular shape of the freshly dissected embryo materials, no modulus could be measured (A, B). The plasmolysis of the tissues using a solution of mannitol prior to AFM measurements did not help improve the modulus mapping and the irregularity of the material only increased (C, D). The use of a mature dry embryo did not help decrease the stickiness and the modulus remained impossible to measure (E, F). We concluded that AFM is too sensitive for the embryo material.

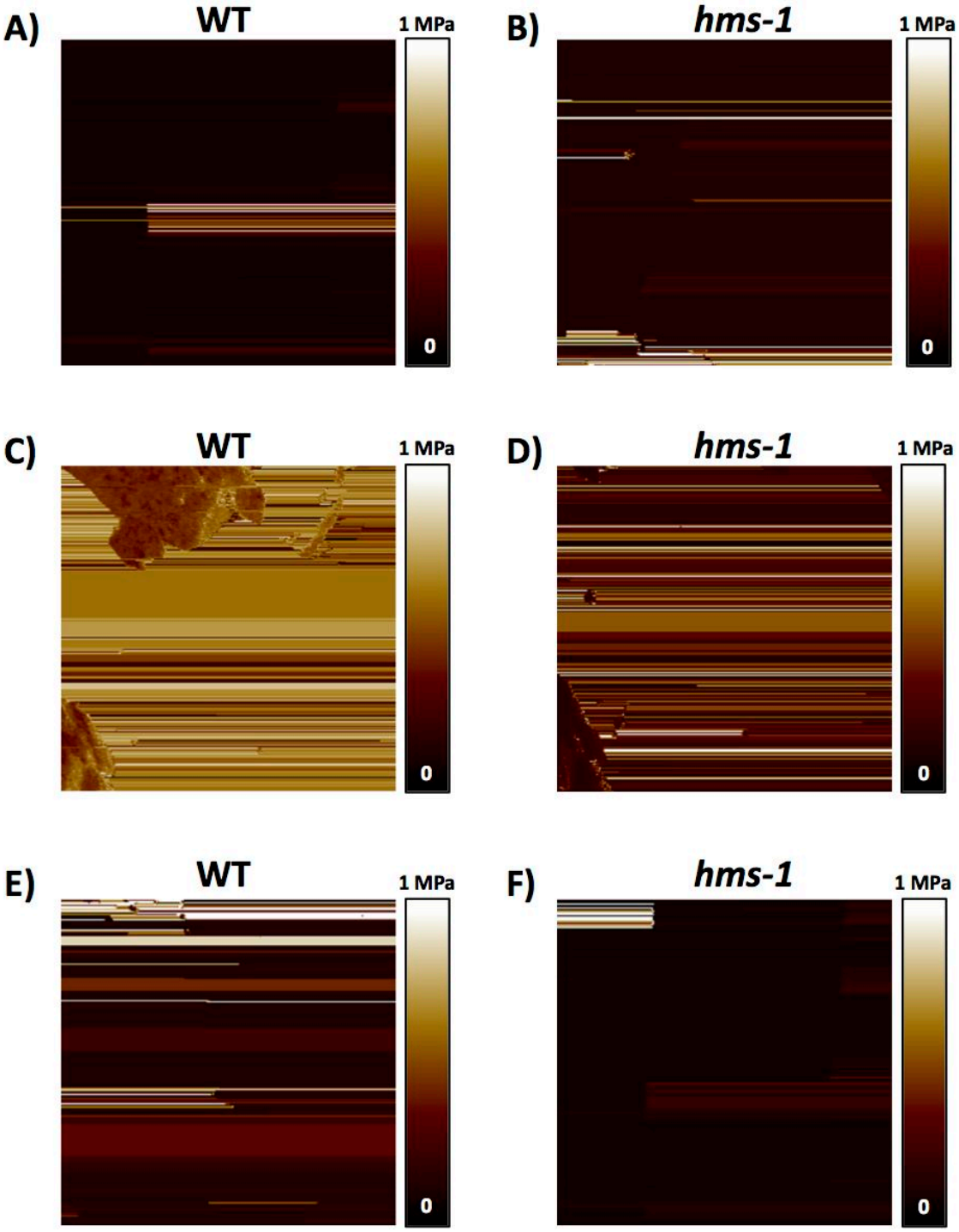

Figure 4: Representative map of the apparent Young's modulus (EA) from atomic force microscopy for WT and *hms-1* embryos.

(A,B) Untreated developing 7 DPA embryos (C,D) Developing 7 DPA embryos plasmolysed in 10% mannnitol prior to measurement (E,F) Mature dissected embryos. WT in (A), (C), (E) and *hms-1* in (B), (D), (F).